KU Leuven
Biomedical Sciences Group
Faculty of Medicine
Department of Oncology
Vesalius Research Center

THE ROLE OF PHD2 IN BREAST CANCER METASTASIS

Anna Małgorzata KUCHNIO

Jury:

Promoter: Prof. Dr Peter Carmeliet

Chair: Prof. Dr Johan Swinnen

Secretary: Prof. Dr Jean-Christophe Marine

Jury members:

Prof. Dr Gerhard Christofori

Prof. Dr Ben Wielockx

Prof. Dr. Karin Haustermans

Prof. Dr Jean-Christophe Marine

Dissertation presented in partial fulfillment of the requirements for the degree of Doctor in Biomedical Sciences

April 2015

TABLE OF CONTENTS

ACKNOWLEDGEMENTS

On the very first pages of this manuscript, I wish to acknowledge all the wonderful people who contributed in one way or another to this work and supported me throughout the past years. It is a great honor and I feel very grateful to be surrounded by colegues, friends and family like you!

First, I would like to express my gratitude towards my promotor Professor Peter Carmeliet for giving me the chance to conduct my doctoral thesis in his laboratory, and for being an invaluable mentor during the past years. Peter, thank you for encouraging my research and for the opportunity to work on several interesting and challenging projects in an extremy stimulating environment. This experience contributed to my personal and scientific development as an independent scientist.

I would like to thank Professor Mieke Dewerchin for all her scientific advices and her support in finalzing several of the research publications and for correcting my thesis manuscript. Mieke, you are always there for anyone with any scientific questions with your unconditional patience.

I would also like to thank Professor Masimiliano Mazzone for the guidance during my start as PhD student, and also for all the tips and suggestions that helped to shape the project towards its current version.

Additionaly, I am grateful to Professor Jean-Christophe Marine, Professor Karin Haustermans, Professor Gerhard Chrisotofori and Professor Ben Wielockx for dedicating time to serve as my thesis committee, and their advice and constructive comments. I also would like to thank Professor Karin Haustermans and Professor Jean-Christophe Marine for their contribution as the thesis advisory board members and their suggestions on the project during its progress.

I would like to thank our collaborators, Professor Masimiliano Mazzone

and Dr Rodrigo Leite-de-Oliveira, Professor Carmen Bartic and Andreea Ungureanu, Dr Sara Zanivan and Dr Juan Hernandez, Professor Diether Lambrechts and Dr Bernard Thienpont, Professor Agnes Noel and Professor Jean-Michael Foidart whose expertise helped to advance PHD2 breast cancer project. Morover, I would also like to thank all the other collaborators from the other projects (Professor Patrizia Agositnis and Hannelore, Professor Cedric Blanpain, Professor Barbara Susini, Professor Claudia Bagni and Rosella). Interaction with you and possibility to be involved in your projects enormously advanced my scientific development.

A big thank you to all the people from Vesalius Research Center (VRC) who have contributed in one way or another to PHD2 breast cancer project. Stijn, thank you to for all the hard work! I have really enjoyed working with you, your enthusiasm and motivation for science is enomous and contigious. I feel honoured I could guide you during your Master thesis and at the start of your PhD at VRC. I miss our chats during the long hours of mice dissection or cell isolations, the time that passed way faster thanks to the nice atmosphere and interesting talks. Even after a very long day at work, your bright smile could put anyone in a good mood. Thank you Stijn also for taking your time to read the first draft of my thesis manuscript. It has been reassuring and very helpful. Above all the hard work, thank you for your friendship! I wish you all the best of luck with your PhD project and all the happiness in your personal life.

Françoise and Henar, thank you for the guidance during my initial years of PhD. Thank you for teaching me all the basic techniques, for a great company and support. Your support and good atmosphere (with the remixes of song to “I love Gdansk”) meant a lot to me, without which my start at VRC would be less fun and definitely way more challenging.

Ulrike, thank you for your help on the project, for taking time to read my thesis and always a good word independent how busy and difficult was your day.

I hope that one day you will be able to transfer all your passion for science to your own student, leading your own lab ☺.

Michaël, thank you for choosing me as your daily supervisor. Despite, the challenging work hours we still, I think, had a great time as three musketeers. I am always happy to hear from you and other people about your progress in your PhD project and your growing confidence with every day as a young scientist. I wish you all the best with you PhD project and in your personal life.

Especially I would like to thank several wonderful people at VRC for their precious technical assistance. Ann Manderveld and An Carton for help with sectioning of all these hundreds and hundreds of tumors blocks and beautiful stainings, but more importantly for the cheerful atmosphere and big smile every day. Lucica and Kathleen thank you for help with immunoblotting. Lucica, your laugh is contiguous and will put enyone in a good mood ☺. Anneke and Ivo, I am very grateful to you for all the excellent lessons in handling mice, their dissections and in complex mouse experiments. Your instrumental help and guidance was crucial for me to reach the level of independence and experitise in animal experiments. Stefan, Kristel and Naima, thank you for the help in imaging experiments and all the good lessons and advices on the microscopy, microscopes software and image analysis. Inge, it has been pleasure to work with you during all of the projects. You are the queen of the HUVECs and no one can really compit with you in their isolations! Sabine, Kevin and Wendy, I am very grateful for your help with molecular biology work, all of these lentiviral preps preparation and all the tips and tricks for improving my technical skills in molecular cell biology techniques. Peggy, Luc, Ester, Martine, Sarah, Mahwish, Betty, Glenn, Elke, Pieter-Jan, I very appreciate your help with following my mice colonies, breeding of them and genotyping. Without your help finishing this project would be even more challenging. Katie, Leen, Christel, Gilles, Evelien thank you for the administrative support during my doctoral training. Katie, thanks

for keeping an eye on all dealines and your advices how to handle certain issues at VRC. Leen, I very appreciate your training with InDesign. Christel, thank you for the administrative assistance at my start of VRC and during my stay here. Halimah, thank you for your endless kindess and good words.

Many thanks to my office mates! Bert many thanks for help with analysis of Illumina data, for all the nice scientific and unscientific chats, jokes and for always being there to listen. Veel success met the loopende project, ik wens je het allerbeste met je doctoraat en voor de toekomst. Ellen, thank you for your kindness and generosity. You have always been there when needed, also always encouraging me to speak louder at my first year of PhD. Thanks for all the nice and supporting chats! Annelies, my ‘twin sister’, thank you for all the medical consultation, advices, prescriptions and vaccination! Good luck with the revision and your work in clinics, but overall I wish you lot of happiness in your personal life. Sandra S., thank you for your kind help in the last bit of my stay at VRC, I really appreciate it. Veel success in de laatste fase van je doctorat, just this little final push and it will be done ☺. Guy, thanks for all the scientific advises and tips on troubleshooting. Pauline, thanks for your cheerful talks and bringing fresh enthusiasm and happiness to the office. I wish you good luck with your challenging PhD project. Saar, dank u voor de heerlijke taarten elke Woensdag. No one could really resist to them! All the best with your PhD! Lena, it has been a pleasure to work with you. I wish you all the best for your stay in Belgium and a lot of success during your future career in Germany. Francesco and Ilaria, thank you for bringing the southern breeze to our office. Peter S. thanks for advices and corrections on English and also for cheerful chats. Leanne thanks for your extreme honestly, funny anegdotes and cheerfulness. Maria, thanks for all the hugs and kisses. Bart G., thanks for the help with MS experiments during CQ revision, but also for all the fun and jokes, and good advices on career choices. Cathy, Daniela, Wouter, Kristof, Bart J., Tobias many thanks for all the good time and discussion we had in our old office during my initial years at VRC.

Many thanks also to the other colleuges and friends at VRC. Brian and Sandra C., thanks for a nice working atmosphere during the looooooooong working hours during PFKFB3-project crush. Sandra, your patience, great mentoring and team working made it easier to take all the challenges at that time. Together with all the unhealthy snacks and Red Bulls that Brian was always supplying ☺ Brian, thanks for all the funny conversations, jokes and challenging nights out, usually ending in the Kult shooter bar ☺. I wish you good luck with your revision and also your future career. Inma, there are so many things I need to thank you for: teaching me a lot of basic techniques in my first years, your patience during that time, all the great technical and scientifical advices, your kindness, your good heart and always willingness to help despite the fact you had already enough of your own work. I wish you all the best for your future, both for your career and personal life. Rindert, it has always been a mystery for me how in the most stressful situation you are able to keep your inner peace and still being able to emit it to people around you. Thanks for this, talking with you always helped me out in stressful moments. I hope you will be able to keep this ability till the very end of your PhD. Veel success met je doctorat! Annachiara, you are the sweetest person (besides my Bartje) I know. We will miss you (and your gniocci) a lot when you will move back to Italy. You have to let us know when you will be planning to defend and we will come over to support you ☺. Gitte, Aleksandra, Annalisa, Pran, Annachiara, Rindert, Koen, Cisko – the party team. Thanks for taking all the initiatives and all the fun. Keep the party spirit up! Katrien, I still remember our conversation on one of the difficult days at the beginning of my PhD, there was something in it that made me stay there. Finally, after almost 6 years I made it to this moment of standing now in front of all of you and defending my PhD work. Thanks for the support and talks, your great enthusiasm for science and also fun time at the conferences. Anna-Rita, although we have been working together for a short time, I have enjoyed it a lot. Good luck in finalizing your manuscript! It is almost there ☺ Joanna (Asia) bardzo

się cieszę, że miałyśmy okazję się poznać i razem pracować. Twój entusiasm i pasja do badań naukowych są niesamowite. Mam nadzieję, że bez wzgledu na okoliczności uda Ci się to utrzymać i spełnić swoje plany. Powodzenia we wszystkim! I would like to thanks all the other current and former members of VRC, Jens, Joris, Christian, Agua, Dries, Xingwu, Jermaine, Hongling, Jacky, Karla, Philipp, Charlotte, Jonathan, Ilse, Fabio, Pawel, Veronica, Sofie, Frederik, Rodrigo, Else, Flora, Ilaria that made my life in the lab funnier, easier and nicer.

A big thanks to all the friends outside the lab: Sofie, Johan VB, Marjolein, Tom, Elise, Koen, Lies, Peter, Greet, Dirk, Ellen, David, Sarah, Terence, Patricia, Johan VM, Bea, Dries, Gerlinde, Koen, Wendy, Vincent, Brecht, Barbara, Daze, Jessy, Len, Kathleen, Pieter, Peter, Berit, Wilhem, Jelle, Katrien. Your presence and constant support helped me to get through the difficult times. Thanks for the nice dinners & drink together, trips, parties and other activities. Aleksandra & Aleks thanks for the nice dinners out and for helping me not to forget my language! Marta, Monika and Matthias, thanks for the nice weekends together and your friendship that even the distance could not challenge!

A special thanks to my family. Words cannot express how grateful I am to all of you, for all the love and support! Mamo, tato, dziekuję za wspieranie moich marzeń, wiarę że ktoraś z moich pasji ma szanse przetrwać. Wspieranie mnie na każdym etapie mojejgo życia, uczenie mnie wytrwałości, motywowanie do bycia samodzielną, odpowiedzialną za siebie i innych. Mamo, dziekuję za bycia z nami kiedykolwiek Cię potrzebowaliśmy. Marzenka, dziekuję za wiarę we mnie, za wsparcie, za bycie dla mnie przykładem jak być niezależną i dążyć do tego co chce się osiągnąć. Ostateczne skończenie tego doktoratu to jak moja mała nagroda Nobla ☺. Basiaczek, nasz maly diabełek, dziekuję zawsze za Twoje pozytwne wiadomści, rozmowy, odwiedziny, a nawet za warzywne ciasta ;-) Twoja pozytwna energia zawsze wprawia mnie w dobry humor ☺. Miejmy nadzieję, że już niedługo będę miała więcej czasu żeby Was wszystkich

odwiedzać. Karol, dziekuję za Twoją pomoc w laboratorium i wsparcie. Nasza wspólny wakacyjny czas i praca wiele dla mnie znaczyła, Twoje żarty zawsze rozpochmurniały nawet najbardziej niepogodne dni. Bardzo się cieszę, że mieliśmy okazję spędzić ten czas razem ☺

I also want to thank my family in Belgium, my parents-in-law - Marleen and Paul; Frits, Joke, Janne and Inneke for their warm, love and kindness, making me feel at home and being part of family from the very beginning I got to know you. You all have been there for me to support me on this difficult PhD track. Oma, Moeke, Oscar, Guy, Chris, Gerda, Jan, Leo, Ingrid, Marc, Olga, Katleen, Bert, Johan, Tine, Lieve, Filip, Tom, Kim, Franz, Romy, Wim, Stefanie en kindjes bedankt voor alle leuke familie feestjes, en me aan te moedigen om vlaams te leren.

At the end I would like to express appreciation to my beloved husband Bart (Bartje, Barcioszek, Peticzko, Sweety) who has been there for me at ANY time needed. Thank you for all the lunch boxes prepared every day with love, every morning hug, your lifts to and from lab at any time and at any day/night, your patience, understanding, enormous support, your sacrifices you have made on my behalf, for being a perfect assistant in the lab during the weekends, for being an amazing travel partner and taking on any challenge it came to my mind (even Kilimanjaro), your laugh that makes me smile, and your endless love. Barcioszek only with your support I could make it through these last 6 years and finally finish it ☺. Thank you so much!!!

Finally I would like to thank FWO and Kom op Tegen Kanker for supporting my research.

LIST OF ABBREVIATIONS

ANG-1	angiopoetin-1
ANG-2	angiopoietin-2
ANGPTL4	angiopoietin-like 4
ARNT	aryl hydrocarbon receptor nuclear translocator
αSMA	α-smooth muscle actin
α-KG	α-ketoglutarate
BC	breast cancer
BM	basement membrane
BMDC	bone marrow-derived cell
CAFs	cancer associated fibroblasts
cDNA	complementary DNA
Cdh2	cadherin 2, also known as N-cadherin
CK8	cytokeratin 8
CSF-1	colony-stimulating factor-1
CSFR	colony stimulating factor receptor
CTCs	circulating tumor cells
CXCR4	CXC-chemokine receptor 4
DAPI	4'-6-diamino-2phenylindole
DNA	deoxyribonucleic acid
E-cadherin	epithelial cadherin
ECs	endothelial cells
ECL	enhanced chemiluminescence
ECM	extracellular matrix
EGF	epidermal growth factor
EGFR	epidermal growth factor receptor
EGLN	egg laying defective nine homolog
ELISA	enzyme-linked immunosorbent assay
EMT	epithelial-to-mesenchymal transition
EPAS-1	endothelial PAS domain protein 1
Erk	extracellular signal-regulated kinase (Erk)
ET-1	endothelin-1
FAK	focal adhesion kinase
FAP	fibroblast activation protein
FBS	fetal bovine serum
FGFs	fibroblast growth factors
FIH	factor inhibiting HIF
FITC	fluorescein isothiocyanate
FSP1	fibroblast specific protein 1
GFP	green fluorescent protein
H&E	hematoxylin and eosin
HGF	hepatocyte growth factor
HIF	hypoxia inducible factor

HLH	helix-loop-helix
HPH	hypoxia prolyl hydroxylase
HRE	hypoxia responsive element
HRP	horseradish peroxidase
HPRT	hypoxanthine guanine phosphoribosyl transferase
ICAM-1	intercellular adhesion molecule-1
IDH	isocitrate dehydrogenase
IFP	interstitial fluid pressure
IGFs	insulin-like growth factors
ING-4	inhibitor of growth protein-4
IKK	IκB kinase
IL-2	interleukin-2
IPAS	inhibitory PAS domain protein
IκB	inhibitor of NF-κB
K_M	Michaelis constant
LN	lymph node
LOX	lysyl oxidase
LOXL	lysyl oxidase-like enzyme
LYVE-1	lymphatic endothelial hyaluronan receptor 1
MAPK	mitogen-activated protein kinase
M-CSF	macrophage colony stimulating factor
MMP	matrix metalloproteinase
MMTV	mouse mammary tumor virus
mRNA	messenger RNA
MSC	mesenchymal stem cells
N-cadherin	neural cadherin
NF-κB	nuclear factor kappa-light chain-enhancer of activated B cells
NK	natural killers, a type of cytotoxic lymphocytes
Ocln	occludin
ODD	oxygen-dependent degradation domain
2-OG	2-oxoglutarate
P4HA	prolyl-4-hydroxylases
PAS	PER-ARNT-SIM
PDGF	platelet-derived growth factor
PDGFRα	platelet-derived growth factor receptor-α
PCR	polymerase chain reaction
PFA	paraformaldehyde
PFKFB3	6-phosphfructo-2-kinase/fructose-2,6-biphosphatatase 3
PHD	prolyl hydroxylase domain-containing proteins
PI3K	phosphoinositide 3-kinase
PlGF	placental growth factor
PyMT	polyoma middle T
PHH3	phosphohistone H3
PIMO	pimonizadole
qRT-PCR	quantitative reverse transcription-PCR
RAS	rat sarcoma

RNA	ribonucleic acid
ROS	reactive oxygen species
RTKs	receptor tyrosine kinases
(R)-2-HG	*(R)*-enantiomer of 2-hydroxyglutarate
SAA3	serum amyloid A3
SDF-1	stromal derived factor-1
SDS-PAGE	sodium dodecyl sulfate polyacrylamide gel electrophoresis
SEM	standard error of the mean
TACS-3	tumor-associated collagen signature-3
TAMs	tumor-associated macrophages
TCA	tricarboxylic acid
TGF-β1	transforming growth factor-β1
Tjp1	tight junctions protein 1
uPA	urokinase type plasminogen activator
VCAM-1	vascular cell adhesion molecule-1
VEGF	vascular endothelial growth factor
VEGFR	vascular endothelial growth factor receptor
VHL	von Hippel-Lindau
Zeb	zinc finger E-box binding homeobox
ZO-1	zona occludens protein-1

SUMMARY

Breast cancer (BC) is the most frequently diagnosed cancer in women in the US and Europe, affecting one in eight women. Despite improvements in radiotherapy, cytotoxic, hormonal, and targeted therapies, BC remains the second leading cause of cancer deaths in women, exceeded only by lung cancer. Metastatic relapse is a main cause of this high mortality, and occurs up to long periods of time after the removal of the primary tumor. Understanding the mechanisms that control metastasis is therefore pivotal for the design of improved and safe breast cancer treatment regimen.

Hypoxia is a characteristic feature of most solid tumors, including BC, and is a strong stimulus of tumor cell invasion and metastasis. Hypoxia signaling regulates nearly every single step of the metastatic cascade, including epithelial-to-mesenchymal transition (EMT), intravasation, survival in the circulation, formation of the pre-metastatic niche, and growth from micro- to macro-metastatic lesions. Furthermore, hypoxic tumors display lower sensitivity to treatment, leading to poor prognosis. The hypoxia-inducible transcription factors (HIFs) mediate a variety of cellular adaptations to hypoxia. Prolyl-hydroxylases (PHD1-3) are oxygen sensors that regulate HIF levels in normoxia by targeting it for proteasomal degradation. Despite the crucial role of PHD2 as an oxygen sensor, its role in tumor growth and metastasis in general and of BC in particular, remains largely debated. Studies from our and other research teams on PHD2 in cancer yielded interesting results, highlighting different possible roles of PHD2 that may be cell-type dependent. On the one hand, the host lab demonstrated that haplodeficiency of PHD2 selectively in *endothelial cells (ECs*) reduced metastasis without affecting tumor growth, by normalizing the abnormal tumor vessels and reducing tumor cell intravasation, suggesting that PHD2 could be an anti-BC drug target. Using transplantable tumor models, others reported that

silencing of PHD2 in *cancer cells* either increased or decreased tumor growth with different underlying mechanisms. Dissection of the role of PHD2 in conditions that allow the evaluation of cell-intrinsic effects as well as the impact of bidirectional tumor / stroma cross-talk, remains strongly warranted. This is particularly relevant in light of pharmacological PHD2 blockade, which would target PHD2 in all cells inside the tumor. Furthermore, the studies mentioned above only used transplantable tumor models. The role of PHD2 in breast cancer using a clinically more relevant spontaneously arising BC model thus remains undefined.

In this study, we utilized the spontaneously arising PyMT-oncogene driven breast cancer model and intercrossed this transgenic line with mice with heterozygous gene deficiency of PHD2 ($PHD2^{+/-}$ mice; named $PyMT^{+/-}$ mice upon intercross with the the PyMT line). Tumor growth was unaffected, but metastasis and intravasation were reduced in $PyMT^{+/-}$ mice as compared to control mice (PyMT mice intercrossed with PHD2 wild type mice; named $PyMT^{+/+}$ mice). Applying genetic strategies *in vivo* and *in vitro*, we show that this reduction in metastasis and intravasation can be ascribed to two independent mechanisms. First, we show that global “genetic targeting” of PHD2 in the entire tumor in $PyMT^{+/-}$ mice induces tumor vessel normalization (a.o. tighter endothelial lining, improved pericyte coverage, better perfused), similar to selective PHD2 haplodeficiency in ECs in xenograft models. Secondly, reduction in metastasis was also attributable to reduced activation of cancer-associated fibroblasts (CAFs). As compared to $PyMT^{+/+}$ tumors, $PyMT^{+/-}$ tumors contained fewer activated CAFs, which deposited less cross-linked collagen matrix and contracted the collagen matrix less. These processes are known to induce cancer cell invasion. We showed that reduced CAF activation was independent of PHD2 level in fibroblasts, but reliant on the level of PHD2 in cancer cells.

PHD2 haplodeficiency in cancer cells lowered the release of TGF-β1 and diminished the differentiation of normal fibroblasts to activated CAFs.

Taken together, these results provide evidence that PHD2 is a potential therapeutical target; the inhibition of which can offer substantial anti-metastatic benefit. Additionally, improved vessel function in spontaneously developing tumor model by PHD2 haplodeficiency could increase chemotherapy delivery and thus provide an advantage during surgical tumor resection.

SAMENVATTING

Borstkanker is de meest voorkomende vorm van kanker bij vrouwen in de Verenigde Staten en Europa. Het treft er één op acht vrouwen. Ondanks de vooruitgang in radiotherapie, cytotoxische, hormoon -en doelgerichte therapieën, blijft borstkanker de op één na grootste doodsoorzaak bij vrouwen, na longkanker. Dit is te wijten aan de grote kans op herval vaak jaren na de behandeling van de primaire tumor. Daarom is het belangrijk om de mechanismen te begrijpen achter metastase, om veilige en meer doeltreffende behandelingen tegen kanker te ontwikkelen.

Hypoxie (zuurstoftekort) is een fenomeen dat voorkomt in de meeste vaste tumoren, waaronder ook bij borstkanker. Het beïnvloedt elke stap in het metastaseproces, van de epitheliale naar mesenchymale transitie (EMT), het binnendringen in de bloedvaten (intravasatie), het overleven in de bloedstroom, de vorming van de pre-metastatische niche, tot de groei van micro-metastatische noduli tot macrometastasen. Bovendien vermindert hypoxie in tumoren de gevoeligheid aan therapieën, wat leidt tot een slechtere prognose. De hypoxie-geïnduceerde factoren (HIFs) mediëren verschillende cellulaire aanpassingen aan hypoxie. Prolyl hydroxylasen (PHD1-3) zijn zuurstofsensors die de hoeveelheid HIFs reguleren bij een normaal zuurstofniveau (normoxie) door het stimuleren van hun proteolytische degradatie. Ondanks de cruciale rol van PHD2 als zuurstofsensor, blijft haar rol in tumorgroei en metastase, in het bijzonder bij borstkanker, omstreden. Studies van anderen alsook onze groep onthulden interessante resultaten die erop wijzen dat PHD2 verschillende rollen kan hebben, die vermoedelijk afhankelijk zijn van het celtype. Enerzijds toonde onze groep aan dat endotheelcel (EC)-specifieke haplodeficiëntie van PHD2

metastasen afremt zonder effect op tumorgroei, door tumorbloedvaten te normaliseren en zo intravasatie te verminderen. Deze resultaten geven aan dat PHD2 een mogelijk doelwit is in de strijd tegen borstkankermetastase. Andere groepen toonden in transplanteerbare tumormodellen aan dat het onderdrukken van PHD2 in tumorcellen de tumorgroei zowel kan afremmen als stimuleren, met verschillende achterliggende mechanismen. Bijgevolg is het belangrijk om de rol van PHD2 in kanker te ontwarren in een model dat zowel tumorcel-intrinsieke effecten als effecten van tumor / stroma interacties toelaat. Dit is vooral belangrijk omdat elke farmacologische PHD2-inhibitie alle cellen binnen de tumor zou treffen. Bovendien gebruikten de bovenvermelde studies enkel transplanteerbare tumormodellen. De rol van PHD2 in een klinisch meer relevant spontaan ontwikkelend borstkankermodel blijft dus nog steeds niet gedefinieerd.

In deze studie gebruikten we het spontaan ontwikkelende borstkankermodel dat geïnduceerd wordt door het PyMT-oncogen. Muizen transgeen voor dit oncogen werden gekruist met muizen met heterozygote PHD2 gen deficiëntie ($PHD2^{+/-}$ muizen; na inkruisen met de PyMT transgene lijn $PyMT^{+/-}$ muizen genoemd). Er was geen effect op tumorgroei, maar het aantal metastasen en de intravasatie waren aanzienlijk verminderd in $PyMT^{+/-}$ muizen, vergeleken met controle muizen (PyMT lijn ingekruist met PHD2 wild type muizen; verder $PyMT^{+/+}$ muizen genoemd). Gebruikmakend van genetische strategieën zowel in vivo als in vitro, toonden we aan dat deze vermindering het resultaat is van twee onafhankelijke mechanismen. Eerst toonden we aan dat de genetische onderdrukking van PHD2 in de hele tumor in $PyMT^{+/-}$ muizen tumorbloedvaten normaliseert, gelijkaardig aan endotheelcel-specifieke PHD2-onderdrukking in xenograft modellen. Ten tweede bleek de afremming van het metastaseproces mede te danken aan een verminderde activatie van kanker

geassocieerde fibroblasten (CAFs). Deze produceerden minder extracellulaire matrix en trekken de collageenmatrix minder samen. Dit zijn processen waarvan het geweten is dat ze metastasering stimuleren. We toonden aan dat de activatie van CAFs niet afhankelijk is van de hoeveelheid PHD2 in fibroblasten, maar wel van de hoeveelheid PHD2 in tumorcellen. PHD2 haplodeficiënte tumorcellen scheidden minder TGF-β1 wat de activatie van normale fibroblasten tot CAFs vermindert.

Tezamen tonen deze resultaten aan dat PHD2 een doelwit is dat bij inhibitie een aanzienlijk anti-metastatisch effect kan hebben. In dit spontane tumormodel leidt PHD2-haplodeficiëntie tot verbeterde bloedvatfunctie waardoor de chemotherapie efficiënter tot de tumor gebracht kan worden, hetgeen voordelig is voor een hieropvolgende operatieve verwijdering van de tumor.

CHAPTER I

INTRODUCTION

1. CANCER BIOLOGY

Cancer, estimated to affect on in three people during the course of their life, is the most common life-threatening disease. Normal cells strictly comply with the signals that instruct them to grow, divide and die in an orderly manner. In contrast, cancer cells are characterized by uncontrollable cell proliferation and the ability to deregulate instructing cues, eventually becoming masters of their own fate. Highly proliferative cancer cells are capable of evading growth suppressors, resisting cell death and enabling replicative immortality. They break tissue homeostasis and form tumor masses that invade adjacent tissue and eventually metastasize (Hanahan and Weinberg, 2000; Hanahan and Weinberg, 2011). The incurable nature of cancer is related to its metastatic dissemination. It has been estimated that 90% of all cancer-related deaths are caused by metastasis (Spano et al., 2012). Despite major therapeutic advances, breast cancer mortality remains the leading cause of women's mortality (Ferlay et al., 2015).

Cancer arises from normal cells through genetic and cellular alterations, which enable cancer cells to become tumorigenic and eventually malignant. Chronic proliferative capacity of cancer cells requires a sustained supply of nutrients and oxygen. To face the new metabolic needs, cancer cells promptly re-shape the tissue environment over the course of cancer progression. It is now well appreciated that heterogeneity of tumors is not only dependent on aberrant mutations in cancer cells, but also the diverse nature of their microenvironment. Most tumors are composed of cancer cells co-existing with a variety of stromal

cells: endothelial cells, pericytes, immune cells, adipocytes and cancer-associated fibroblasts (CAFs), embedded in the complex extracellular matrix (ECM) network. Along with cancer cell invasive properties, the diversity of the microenvironment (its composition, stromal cell proportion and activation states) determines the invasive and metastatic capacities of the tumor (Quail and Joyce, 2013). The contribution of some types of cells of the tumor microenvironment in the metastatic process will be discussed in more detail in section 3.

2. METASTATIC CASCADE

Metastasis is a complex, multistep biological process consisting of the following stages: Epithelial-to-Mesenchymal Transition (EMT), invasion, intravasation, survival in the circulation, organ-specific extravasation, colonization and eventually outgrowth from micro- to macro-metastasis (Figure 1).

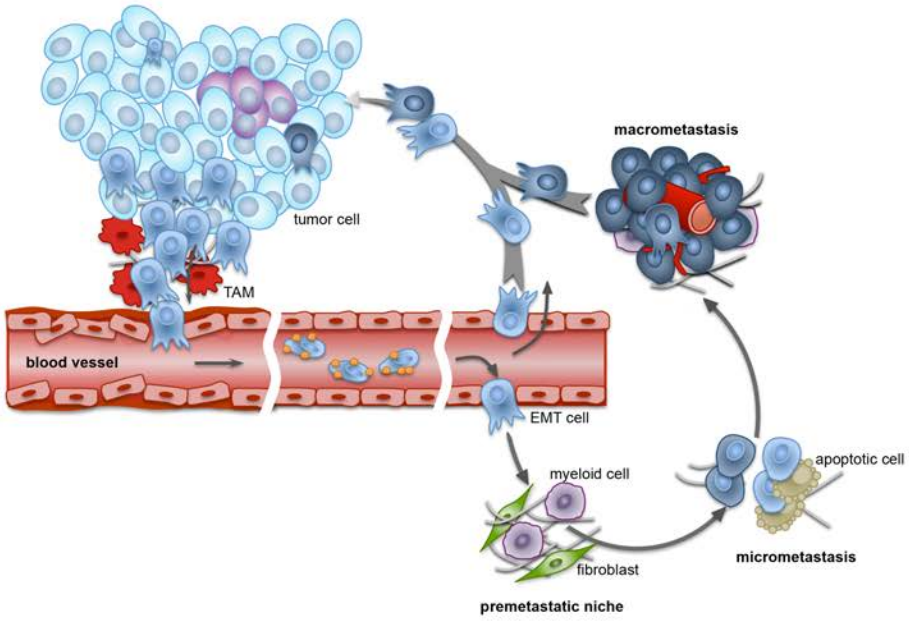

FIGURE 1: THE METASTATIC CASCADE.
Schematic representation of the different steps of the metastatic cascade. Cancer cells at the primary tumor site acquire invasive phenotype (through EMT) and are capable of escaping from the primary site alone or aided by stromal cells, after which they intravasate. In the circulation, platelets and components of the coagulation system support cancer cell survival. Cancer cells, escorted to the metastatic site, adhere to endothelial cells and extravasate. At the metastatic sites several pre-conditioned stromal cells may help to direct metastatic dissemination by creating a

niche that is permissive for cancer cell colonization, and then grow from the micro-metastases to macro-metastases. EMT, epithelial to mesenchymal transition; TAM, tumor associated macrophages. Adapted from (De Bock et al., 2011).

Successful metastasis requires bidirectional communication between cancer cells and the microenvironment at each of these steps (De Bock et al., 2011; Quail and Joyce, 2013). Moreover, hypoxia signalling plays a pivotal role in most of these steps.

2.1. LOCAL INVASION OF THE PRIMARY TUMOR

Cancer cell migration and invasion are critical parameters of metastatic spread. During this process cancer cells undergo extensive molecular and cellular adaptations that regulate cancer cell cytoskeletal dynamics and the turnover of cell-cell and cell-matrix adhesive junctions. Similar to the other steps of the metastatic cascade, reciprocal reprogramming of both cancer cells and adjacent tissue is critical, and not only enables invasion, but also determines diverse modes of dissemination (Friedl and Alexander, 2011; Yilmaz and Christofori, 2010).

In order to invade the surrounding tissue and disseminate to distant organs cancer cells must undergo epithelial-to-mesenchymal transition (EMT), an essential process also during normal embryonic development (Kalluri and Weinberg, 2009). At the cellular level, EMT involves the dissolution of adherens and tight junctions and loss of cell polarity, resulting in dissociation of individual cells from the epithelial layer of origin. This process is a consequence of molecular adaptation of cells in response to microenvironmental stimuli (i.e. hypoxia, epidermal growth factor (EGF), hepatocyte growth factor (HGF), fibroblast growth factors (FGFs) and transforming growth factor (TGF)-β1, insulin-like growth factors (IGFs), platelet-derived growth factor (PDGF)). Several of these cytokines induces expression of key EMT-associated transcription

factors (Snail-1, Snail-2, Zeb-1, Zeb-2, Twist; known repressors of E-cadherin gene expression). In addition, some of them regulate mitogen-activated protein kinase (MAPK), phosphoinositide 3-kinase (PI3K) and Wnt / β-catenin signalling's that are crucial in inducing and maintaining EMT (Tiwari et al., 2012). At the molecular level, cells undergoing EMT lose their epithelial markers, such as tight junction proteins, claudins and occludins, the adherence junction proteins (E-cadherin) and cytokeratins, and concomitantly upregulate several mesenchymal markers (N-cadherin, vimentin, fibronectin, matrix metalloproteinases, integrins α_v and β_1) (Figure 2). These molecular changes facilitate a transition from polarized epithelial cells to motile mesenchymal-like cells.

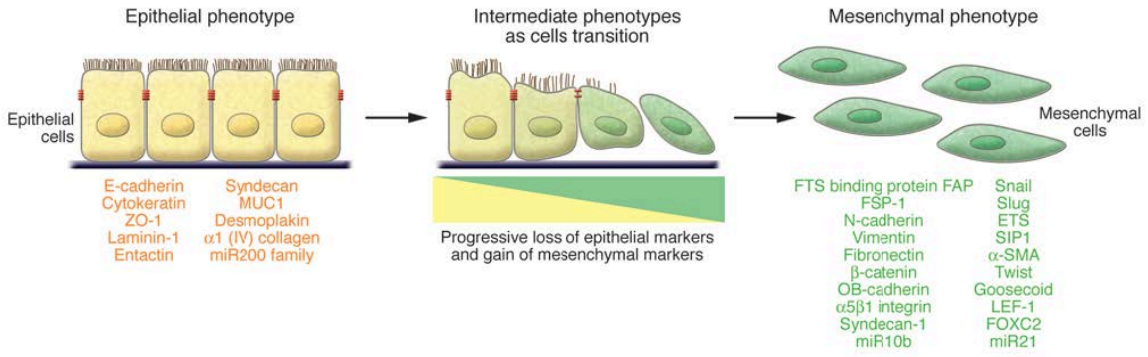

FIGURE 2: INVASIVE SWITCH: EPITHELIAL-TO-MESENCHYMAL TRANSTION (EMT).
Schematic representation of the EMT process. During EMT, cells lose their cell-cell and cell-ECM contacts and re-arrange their cytoskeleton. These cellular changes are the consequences of a transition from polarized epithelial cells (characterized by expression of epithelial-like markers, in yellow) to motile and invasive mesenchymal-like cells (identified by mesenchymal markers, in green). This molecular and cellular switch enables cancer cells to migrate, locally invade and metastasize. Adapted from (Kalluri and Weinberg, 2009).

Depending on the tumor type, multiple types of cell migration / invasion can be found to different degrees and in variable mixes. They can disseminate as individual cells or invade in solid cell strands, sheets or cluster (called 'collective migration'). While leukemias, lymphomas and most solid stormal tumors such as sarcomas disseminate as single cells, epithelial tumors (i.e. breast carcinoma, squamous cell carcinoma) use the collective migration strategy (Friedl and Wolf,

2003). Interestingly, however, recent findings highlighted, that the porosity and confinement of the ECM determines the invasion mode of mesenchymal tumor cells (fibrosarcoma and melanoma). Whereas fibrillar and highly porous ECM allows single cell dissemination, ECM of increased density induces cell-cell interaction, leader-follower cell behaviour and collective cell invasion, which relies on proteolytic degradation of the matrix (Haeger et al., 2014). These findings suggest that cancer cells acquire different invasive modes depending on ECM density; further confirming that tumor microenvironmental heterogeneity dictates molecular and phenotypic adaptations of cancer cells.

Furthermore, metastatic cancer cells, in contrast to non-metastatic ones, are able to attach to and move along collagen fibers (Wang et al., 2002). Many of these fibers are embedded in the blood vessels (Condeelis and Segall, 2003), and thus they can serve as highways for cancer cell dissemination. The invasion of cancer cells, as they move through the tumor, can be enhanced or promoted by stromal cells, such as tumor-associated macropahages (TAMs) and CAFs. Indeed, intravital microscopy revealed that breast cancer cells invade alongside TAMs (Roussos et al., 2011). This interaction occurs through a paracrine loop, in which cancer cells secrete colony-stimulating factor-1 (CSF-1) to recruit TAMs, resulting in their activation and secretion of ligands, such as EGF that in turn stimulates cancer cell motility (Figure 3) (Wyckoff et al., 2004; Wyckoff et al., 2007). Macrophages are higly plastic cell that can alter their polarization state to accommodate different physiological condtions. Clasically activated “M1” macrophages produce type I proinflammatory cytokines, participate in antigen presentation and have an anti-tumorigenic activity. Alternatively activate “M2” macrophages produce type II cytokines, promote anti-inflammatory responses and have pro-tumorgenic functions (Quail and Joyce, 2013). CAFs also contribute to a wide spectrum of secreted factors, including chemokines (CXCL12, CCL2, CCL5, CCL7, CXCL8 and CXCL14), cytokines (SDF-1, IL-6, TGF-β1) and growth factors (HGF, EGF, FGF), which stimulate the invasion of

cancer cells. Moreover, they increase angiogenesis and contribute to the recruitment of immune cells to the tumor (Cirri and Chiarugi, 2011). In addition to their paracrine signaling, CAFs exert a direct physical impact on the tumor microenvironment by modulating the ECM. CAFs not only secrete components of the ECM, but also remodel it via the secretion of proteases (matrix metalloproteases (MMPs), urokinase type plasminogen activator (uPA)) and crosslinking enzymes (lysyl oxidase (LOX), lysyl oxidase-like 2 (LOXL2)), and by direct matrix contraction (Calvo et al., 2013; Cirri and Chiarugi, 2011; Kasashima et al., 2014). Altogether, this promotes ECM stiffness and consequently increases intratumoral mechanical stress. These microenvironmental changes directly affect the malignant phenotypes and metastatic behavior of cancer cells (Kumar and Weaver, 2009).

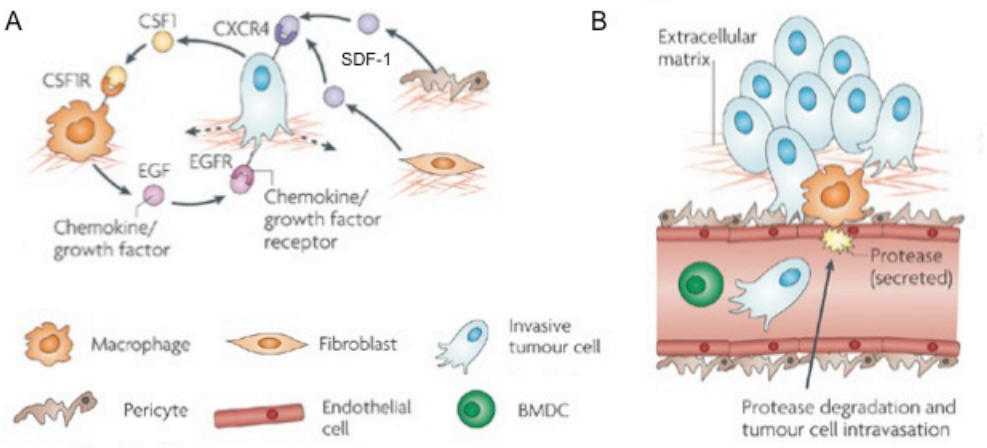

FIGURE 3: INTERACTION BETWEEN CANCER AND STROMAL CELLS - EFFECT ON INVASION AND INTRAVASATION.
A, CAFs and vascular cells, such as pericytes and ECs, secrete SDF-1 to promote the invasion of cancer cells expressing CXCR4. While cancer cells secrete CSF-1 and promote proliferation of TAMs, $CSF1R^{+}$ TAMs promote the invasion and intravasation of EGFR-expressing cancer cells by secreting EGF (Wyckoff et al., 2004). **B**, TAMs promote cancer cell intravasation through paracrine signalling, proteolytic degradation of basement membrane and dissociation of endothelial tight junctions. SDF-1, stromal derived factor-1; EGF epidermal growth factor; EGFR, EGF receptor; CSF-1 colony stimulating factor-1; CSF1R, CSF-1 receptor. Adapted from (Joyce and Pollard, 2009).

Acquiring an invasive tumor cell phenotype is a critical first step of the metastatic cascade, allowing cancer cells to egress from the primary tumor to blood or lymphatic vessels.

2.2. CANCER CELL INTRAVASATION

For successful intravasation directional migration of cancer cells towards blood vessels is required, followed by invasion through the vessel wall. This is accomplished through an adhesive interaction between cancer cells and the basement membrane (BM) of ECs and through integrin-mediated communication and proteolytic degradation of the BM (Spano et al., 2012). Most studies indicate that cancer cells actively invade and intravasate. However, it is also recognized that endothelial barrier impairment is equally important in this process (Carmeliet and Jain, 2011b; Zervantonakis et al., 2012). An impaired endothelium, with fenestrations in its lining, can enable passive cancer cell dissemination from the primary tumor to the circulation (Zervantonakis et al., 2012), as discussed in more detail in section 3.1.

Stromal cells can also assist cancer cell intravasation. Either by facilitating cancer cell motility and invasion within the primary tumor towards blood vessels (see section 2.1) or by direct physical disruption of vessels (Figure 3). Interactions between perivascular TAMs and cancer cells appear to be critical for intravasation (Wyckoff et al., 2007), suggesting that perivascular TAMs facilitate the breaching of the vascular barrier by proteolytic degradation (Figure 3B). Moreover, macrophages can also increase the permeability of the EC barrier by secreting tumor necrosis factor-α (TNF-α) (Zervantonakis et al., 2012) and locally promoting the intravasation of cancer cells.

2.3. CANCER CELL SURVIVAL IN THE CIRCULATION

Around 4 million cancer cells can be shed into the circulation every day from a gram of primary tumor (Butler and Gullino, 1975; Wong and Hynes, 2006), yet less than 0.01% of these will result in metastases (Joyce and Pollard, 2009).

Epithelial cells require a direct interaction with proximal cells or ECM for their survival, thus, in non-adherent conditions cells undergo a form of programmed cell death, known as anoikis (Frisch and Francis, 1994). Circulating cancer cells develop resistance to anoikis by several molecular mechanisms, such as upregulation of caveolin-1 (Halim et al., 2012) or by constitutive activation of downstream pro-survival signals: PI3K, Ras-Erk, NF-κB and Rho GTPase (Guadamillas et al., 2011), among others. It has also been reported that preconditioning of cancer cells in hypoxia contributed to anoikis resistance by suppressing α5 integrin (Rohwer et al., 2008) or Bim and Bmf as well as increased expression of EGFR-MAPK-extracellular signal-regulated kinase (Erk) pathway (Whelan et al., 2010).

Not only anoikis will limit the success rate of the metastatic process, but also the hostile microenvironment of the circulation. In the blood, cancer cells are confronted with many challenges, such as hemodynamic shear forces, turbulences, surveillance from and attack by immune cells, especially natural killer (NK) T cells (Gupta and Massague, 2006). To increase their chances for survival, cancer cells use platelets as a shield (Nash et al., 2002), either by binding coagulation factors on the platelets and forming an embolus aggregate that protects the cancer cell from NK cell-mediated lysis (Nieswandt et al., 1999; Palumbo et al., 2007), or through an independent mechanism related to circulating pro-thrombin (Palumbo et al., 2007). Not surprising, high platelet count is associated with decreased survival in multiple cancers (Jurasz et al., 2004). Moreover, platelets and fibrin may also promote clotting of cancer cells in small capillaries, facilitating adhesion to the endothelium and metastasis in

distant organs (Konstantopoulos and Thomas, 2009). Besides platelets, circulating cancer cells can also co-travel with stromal cells such as CAFs, which not only increase cancer cell survival in the circulation but also provides a growth advantage at the metastatic site (Duda et al., 2010).

2.4. CANCER CELL EXTRAVASATION IN DISTANT ORGANS

In order to home in on a distant tissue, circulating cancer cells must first adhere to ECs. Whereas passive entrapment might partially contribute to the metastatic seeding, active adhesion and invasion through the capillary vessel wall is necessary for establishing metastases. The process of extravasation is dependent on the type of organ-specific vascular barriers (Figure 4).

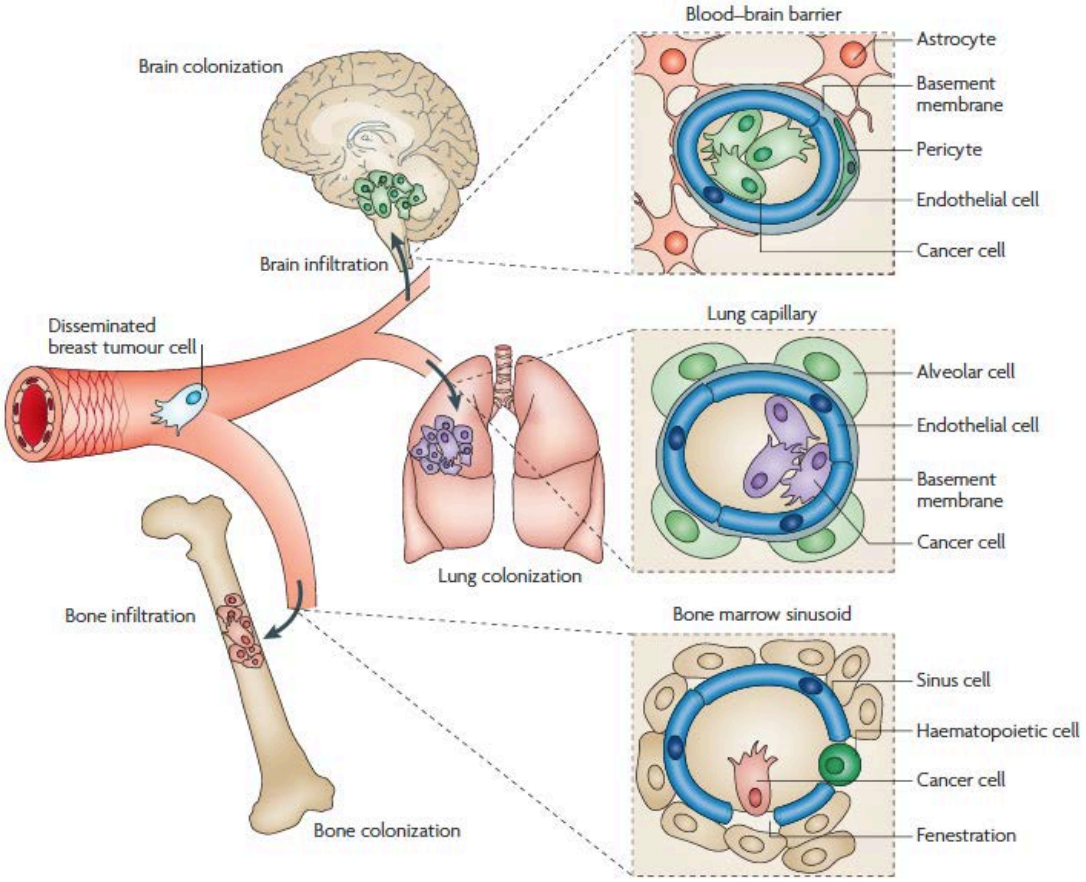

FIGURE 4: ORGAN-SPECIFIC VASCULAR BARRIERS FOR BC EXTRAVASATION.
Circulating breast cancer cells can infiltrate a distant organ they are able to survive in non-adherent conditions and breach the vessel wall at distant sites. Each of the organs, specific for

BC metastasis (brain, lung and bones), contains distinct vascular barriers for disseminating cancer cells. In the brain, the blood-brain barrier with its tightly interconnected endothelial cells and pericytes, glial cells, and a thick BM is a less-penetrable barrier for extravasation than bone marrow sinusoids with a fenestrated endothelium and lacking BM. Also, lung capillary network is well structured, consisting of a tight monolayer of EC, covered by homogenous BM and pericytes make it more challenging for cancer cells to infiltrate. BC, breast cancer; BM, basement membrane; ECs, endothelial cells. Adapted from (Nguyen et al., 2009).

Apart from the importance of structural features of capillary walls in organ-specific extravasation (see Figure 4), unique interactions between endothelial surface molecules and cancer cells are required for successful infiltration in distant organs. Indeed, *in vitro* studies of adhesion of different human prostate cancer cell lines to ECs of different origins showed that these prostate cancer cells preferentially adhere to ECs originating from the bone marrow (Lehr and Pienta, 1998; Scott et al., 2001). This is coherent with the pattern of metastatic dissemination of prostate tumors.

Hypoxia signalling can promote successful cancer cell extravasation by upregulating the expression of several adhesion molecules (E-selectin, vascular cell adhesion molecule-1 (VCAM-1), intercellular adhesion molecule-1 (ICAM-1), integrins) and carbohydrate ligands for selectins. Thus it enhances cancer cell adhesion to ECs (Koike et al., 2004). Moreover, hypoxia signaling in the primary tumor also increases the secretion of angiogenic factors (VEGF, TGF-β1, placenta growth factor (PlGF), and TNF-α) into the circulation, that can permeabilize and destabilize the vessels at the metastatic site by inducing local release of ANG-2 and proteases MMP-3 and MMP-9 (Hiratsuka et al., 2011; Huang et al., 2009). Additionally, TGF-β1 secreted by the primary BC tumor increases ANGPTL4-secretion by disseminating cancer cells. ANGPTL4 facilitates the disruption of EC cell-cell junctions in the lungs, allowing trans-endothelial passage and subsequent infiltration into the lung parenchyma of cancer cells (Padua et al., 2008). Both TGF-β1 and ANGPTL4 are upregulated by hypoxia signaling (Falanga et al., 1991; Le Jan et al., 2003). Importantly, the role of ANGPTL4 in tumor formation remains controversial. While in this (Padua

et al., 2008) and in other (Nakayama et al., 2010; Zhu et al., 2011) studies ANGPTL4 has been reported to have an oncogenic and pro-metastatic function, others suggest tumor- or angiogenesis-suppressive functions (Galaup et al., 2006; Ito et al., 2003; Li et al., 2004; Okochi-Takada et al., 2014).

2.5. CANCER CELL COLONIZATION IN DISTANT ORGANS

Metastatic colonization is a final event required for cancer cells to form metastases in distant organs. Extravasated cancer cells will follow one of three alternative paths: cell death, dormancy (the cancer cell will be able to survive in the distant organ by entering a quiescence state), or colony formation (cancer cells will proliferate and drive tumor growth by counterbalancing cell death) (Chambers et al., 2002). These fates are determined by the interaction of cancer cells with components of the target metastatic organ, such as stromal cells and the ECM. In most cases, the inability to proliferate in the new microenvironment of the target organ is the limiting factor for metastasis formation, as shown in melanoma and BC (Luzzi et al., 1998; Morris et al., 1994; Naumov et al., 2002).

Stephen Paget already recognized in 1889 that cancer cells ('the seed') will only grow when they find a compatible, hospitable tissue ('the soil') (Paget, 1889). Primary tumors can modify 'the soil' in distant organs for successful engraftment of cancer cell by secreting several factors (VEGF, PlGF, TGF-β1) that contribute to the development of a pre-metastatic niche (Figure 5).

In response to these factors inflammatory S100 chemokines and serum amyloid A3 (SAA3) are upregulated in the pre-metastatic sites, promoting the infiltration of bone marrow-derived haematopoietic cells (BMDCs) (Hiratsuka et al., 2006; Hiratsuka et al., 2008; Kaplan et al., 2005). BMDCs in turn secrete a plethora of factors (TNFα, MMP2 and MMP9, and TGF-β1) that either increase vascular permeability, remodel the ECM of the target organ, promote cancer cell

proliferation or recruit other host cells (Hiratsuka et al., 2002; Kim et al., 2009). Moreover, activated fibroblasts, possibly also originating from mesenchymal stem cells (MSCs), secrete fibronectin and LOX to modify the local ECM (Erler et al., 2009) (Figure 5A). Besides MSCs, endothelial progenitor cells are recruited to the early metastatic niche to mediate angiogenesis, enabling the switch from micro- to macro-metastasis (Gao et al., 2008; Kaplan et al., 2005) (Figure 5C).

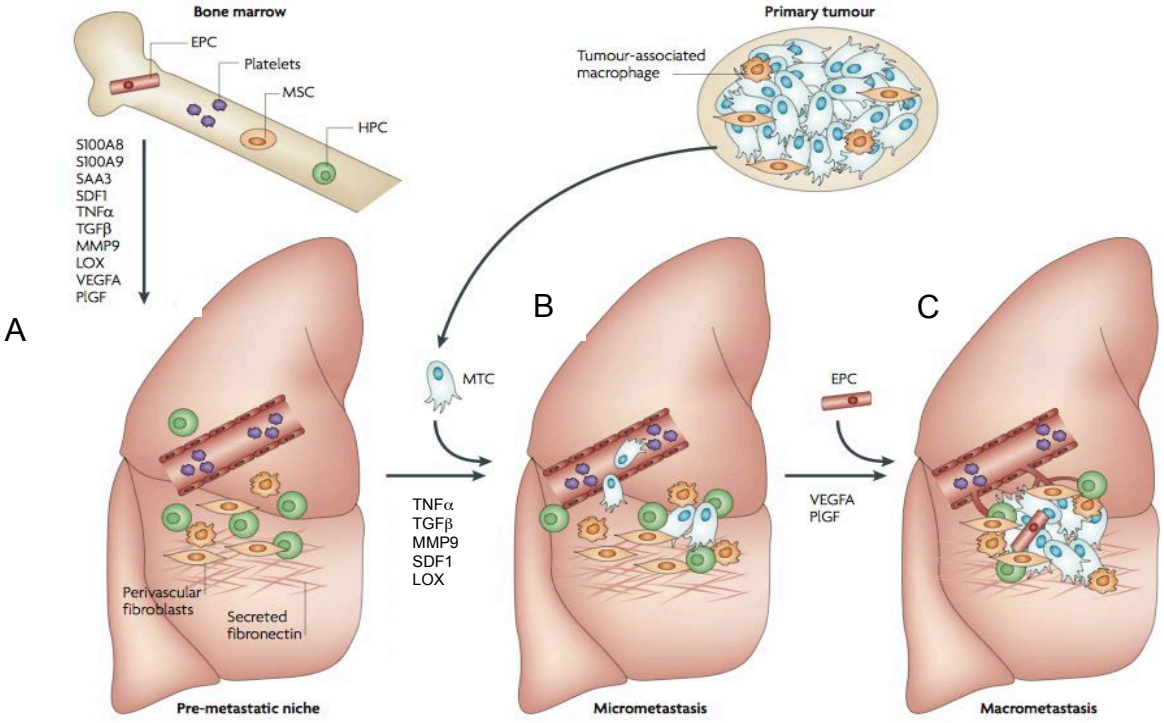

FIGURE 5: METASTATIC COLONIZATION.
This figure illustrates different steps of successful colonization: **A**, pre-metastatic niche - growth factors secreted by the primary tumor, including VEGF, PlGF and TGF-β, inflammatory S100 chemokines and SAA3 are upregulated in pre-metastatic sites leading to clustering of bone marrow-derived haematopoietic progenitor cells (HPCs) or activation of local fibroblasts that modulate the local ECM. SDF1, secreted by platelets is also chemotactic for CXCR4-positive HPCs and metastatic tumour cells (MTCs). HPCs secrete a variety of pre-metastatic factors including TNF-α, MMP9 and TGF-β. Activated fibroblasts secrete fibronectin, an important adhesion protein in the niche, and LOX, modifying the local extracellular matrix; **B**, micrometastasis – MTCs that successfully infiltrate the pre-metastatic niche of target organs will form micrometastases; **C**, macrometastasis – to supply the nutrients and oxygen, EPCs are recruited to the metastatic niche. Moreover, angiogenic tip cells provide tumor-promoting factors to facilitate switch from dormancy to proliferation. BMDCs, bone marrow-derived hematopoietic cells; CXCR4, C-X-C chemokine receptor 4, ECM, extracellular matrix; EPCs, endothelial progenitors cells; HPCs, bone marrow-derived hematopoietic cells; LOX, lysyl oxidase; MMP9, matrix metalloproteinase 9; MTCs, metastatic cancer cells; PlGF, placental growth factor; SAA3, serum amyloid A3; SDF1, stromal-derived growth factor 1; TGF-β, transforming growth factor-β;

TNF-α, tumor necrosis factor-α (VEGF, vascular endothelial growth factor A. Adapted from (Psaila and Lyden, 2009).

Hypoxia signaling can also positively regulate this step of the metastatic cascade. Hypoxia-regulated LOX is an important mediator of bone marrow cell recruitment to form the pre-metastatic niche (Erler et al., 2009). Hypoxia also induces the expression of SDF-1 and CXCR-4 (Jin et al., 2012), a signaling axis that has been reported to contribute to BC dissemination (Nguyen et al., 2009).

Cancer cells that are capable of infiltrating the target organ can remain dormant as micrometastases for a variable amount of time (up to decades). This trait of cancer cells is responsible for the untraceable nature of many malignancies. Cancer cells are dormant either because they entered a quiescent state (cellular dormancy) or because cancer cell proliferation is balanced by cell death, for example due to the lack of proper nutrient and oxygen supply by blood vessels (angiogenic dormancy) (Aguirre-Ghiso, 2007; Hedley and Chambers, 2009). These dormant cells are difficult to detect, but it is even more challenging to target them with the current therapeutic strategies (Naumov et al., 2003; Townson et al., 2009). The pre-metastatic niche and cancer stem cells, a population of cancer cells that have ability to rise to all distinct cancer cell types, significantly contribute to metastatic colonization (Giancotti, 2013; Malanchi et al., 2012), and could explain why certain patients relapse after a short time. The mechanism of metastatic outgrowth in late-relapsing patients has, however, not been completely elucidated. Indeed, a recent study of *Ghajar et al.* aimed to provide the underpinnings of it. They showed that dormancy of metastatic BC cells can be regulated by EC thrombospondin-1, but its suppressive function is overruled when angiogenesis is initiated in the metastatic organ. Sprouting vessels not only support, but accelerate metastatic growth of BC cells by secreting tumor-promoting factors (TGF-β1 and periostin (POSTN)) from the leading tip cell of the angiogenic sprouts (Ghajar et al., 2013). While this provides

additional evidence for the importance of surrounding stroma in the process of metastatic outgrowth, it does not explain the underlying mechanism regulating the reactivation of dormant cancer cells.

3. THE ROLE OF STROMAL CELLS IN TUMOR PROGRESSION AND METASTASIS

Although tumorigenesis has typically been viewed as a cancer cell – autonomous process, the contribution of stromal cells to tumor progression and metastasis has now been acknowledged (Joyce and Pollard, 2009; Quail and Joyce, 2013). The stroma consists of a diverse population of cells (ECs, smooth muscle cells, fibroblasts, immune cells) that provide structural and physiological support to the tissue. Stromal cells co-evolve with cancer cells during tumor progression and also contribute to cancer cell heterogeneity, for example by paracrine interaction. They undergo both morphological and functional transitions to create a favorable microenvironment for cancer cell growth and dissemination (Egeblad et al., 2008; Josson et al., 2010; Sung et al., 2008; Wallace et al., 2011; Weinberg, 2008). In this section I will discuss the role of some of the stromal components in tumorigenesis and metastasis relevant for this project: vascular cells and CAFs.

3.1. VASCULAR ENDOTHELIAL CELLS - ANGIOGENESIS

Tumor cell proliferation is highly dependent on oxygen and nutrient supply. At the early stages, when the tumor is still small, diffusion of oxygen (limited to a distance of 20-200 μm, depending on tissue constraints (Carmeliet and Jain, 2000; Pries and Secomb, 2014)) and other solutes (with higher maximal diffusion distance) (Pries and Secomb, 2014) suffices. However, it is generally accepted that tumors are not able to grow beyond the size of 1-2 mm in diameter without an adequate blood supply. The initiation of angiogenesis, or the ‘angiogenic

switch', has to occur to ensure exponential tumor growth (Bergers and Benjamin, 2003). It is also recognized that the 'angiogenic switch' is a rate-limiting event in carcinogenesis (Hanahan and Weinberg, 2000; Rogers et al., 2014).

Blood vessels in the tumor can develop from pre-existing capillaries or post-capillary venules by sprouting angiogenesis, intussusception (splitting of pre-existing vessel), vasculogenesis (recruitment of BMDCs and EPCs that differentiate into ECs), vessel co-option (cancer cells hijack an existing vessel) or vascular mimicry (in which cancer cells can line a vessel) (Carmeliet and Jain, 2011a). While neovascularization is the most commonly described type of angiogenesis in a variety of tumors, astrocytomas acquire their blood supply without initiating sprouting angiogenesis but by vessel co-option (Bergers and Benjamin, 2003).

Sprouting angiogenesis is initiated when cells are deprived of oxygen. In avascular areas, adaptive responses are initiated, mainly mediated by the hypoxia inducible factor-1 (HIF1) (Fraisl et al., 2009). HIF1 activates the transcription of a plethora of genes, including vascular endothelial growth factor (VEGF). VEGF is a key growth factor driving sprouting angiogenesis, both in physiological and pathological conditions. The importance of VEGF in angiogenesis has been demonstrated by genetic studies. Both haplodeficiency and overexpression of VEGF resulted in embryonic lethality between embryonic day 11 and 12 due to severe vascular defects (Carmeliet et al., 1996; Ferrara et al., 1996; Miquerol et al., 2000). The VEGF family consists of five members: VEGF-A (or simply VEGF), VEGF-B, VEGF-C, VEGF-D and PlGF (Olsson et al., 2006). These secreted, dimeric glycoproteins of approximately 40kDa ligands can bind three receptor tyrosine kinases (RTKs), VEGF receptor-1, -2, and -3 (VEGFR1-3). Binding of VEGF leads to the formation of VEGFR homodimers and heterodimers and subsequent signal transduction. The different VEGF isoforms have overlapping yet distinctive binding properties for each of their

tyrosine kinase receptors. These different properties contribute to the functional diversity of VEGF isoforms. VEGF-A, the key growth factor regulating angiogenesis, induces its angiogenic signal by binding to VEGFR-2 (also known as fetal liver kinase-1 (FLK-1) in mouse and as kinase insert domain receptor (KDR) in human). Activation of VEGFR-2 induces direct effects on ECs by promoting their proliferation, survival, vessel sprouting and permeability (Moens et al., 2014).

During sprouting angiogenesis, tip cells sprout from an existing vessel, leading the way and navigating towards the angiogenic signal. Stalk cells, trailing behind the tip cells, proliferate and extend the vascular lumen as sprouts elongate. Tip and stalk cell differentiation is tightly controlled by a feedback system of VEGF and Notch, as well as other genetic signals (De Smet et al., 2009). Recent studies from the host lab show that besides growth factors, the key glycolytic regulator 6-phosphofructo-2-kinase / fructose-2,6-bisphosphatase 3 (PFKFB3) regulates angiogenesis by controlling the balance between tip and stalk cell (De Bock et al., 2013). Phalanx cells are quiescent ECs, lining vessels once the vascular unit is established. They form a streamlined monolayer of ECs, covered by pericytes and homogenous BM (De Smet et al., 2009).

In healthy organs, blood vessels are composed of a monolayer of phalanx ECs with a smooth surface with cobblestone-morphology, interconnected by junctional molecules (VE-cadherin and claudins). They are covered by pericytes that, together with phalanx ECs, produce a BM to form a stable vascular unit (Figure 6A). In tumors however, homeostatic vessel morphogenesis is often deregulated, resulting in vessels that are abnormal in structure and shape. Abnormal tumor blood vessels are tortuous and misshapen with a highly dysfunctional, leaky and porous EC layer. Unlike normal blood vessels, they have defective BM and pericyte coverage (Carmeliet and Jain, 2011b) (Figure 6B). This abnormal structure of tumor blood vessels facilitates cancer cell

intravasation and further dissemination. The aberration of tumor blood vessels is a result of non-productive angiogenesis. Rapidly growing tumors are in constant need for oxygen and nutrients. Cancer cells try to overcome this shortage by upregulating angiogenic factors, such as vascular endothelial growth factors (VEGF), angiopoietin-2 (ANG-2), and interleukin-2 (IL-2), to attract more blood vessels. However, because of this excessive production, these angiogenic factors start to act as abnormalization factors, leading eventually to aggravated vessel disorganization, increasing intratumoral hypoxia and interstitial fluid pressure (factors positively regulating cancer cell dissemination) (Carmeliet and Jain, 2011b). Thereby, these factors fuel non-productive angiogenesis in an endless self-reinforcing loop (Figure 6B, upper right panel).

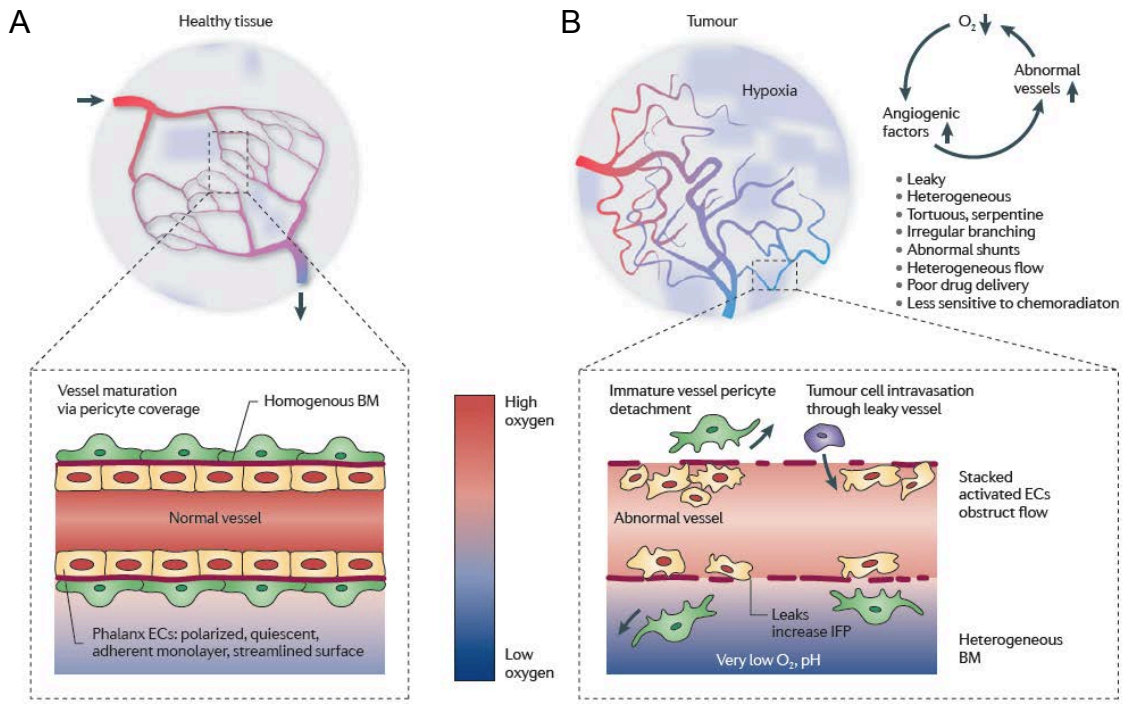

FIGURE 6: TUMOR BLOOD VESSELS ARE STRUCTURALLY AND FUNCTIONALLY ABNORMAL.
Schematic representation of structural parameters of healthy (A) and tumor (B) blood vessels. **A**, In healthy tissue, blood vessels develop a well-organized network of arteries and veins to support the need for oxygen and nutrients (upper part panel A), with a normal vessel wall and endothelium (lower part of panel A). **B**, In a rapidly growing tumor, both the vasculature (upper part of panel B), as well as the vessel wall and endothelium (lower part of panel B) are abnormal in shape and structure, resulting in increased hypoxia (represented by blue shading) and IFP. BM, basement membrane; ECs, endothelial cells; IFP, interstitial fluid pressure. Adapted from (Carmeliet and Jain, 2011b).

In addition to its crucial role as a regulator of sprouting angiogenesis, VEGF plays a critical role in promoting the permeability of tumor blood vessels, thereby further facilitating the intravasation of cancer cells (Dvorak et al., 1999). Moreover, hypoxia-induced ANG-2 destabilizes tumor blood vessels (reduces the coverage of ECs by pericytes) by antagonizing the activity of anigopoetin-1 (ANG-1) (Falcon et al., 2009).

Because of the fundamental role of angiogenesis in cancer, blocking molecules involved in angiogenesis appeared to be an attractive strategy for cancer therapies

3.1.1. ANTI-ANGIOGENIC THERAPY: SUCCESSES AND LIMITATION

Since the concept of targeting angiogenesis to starve tumors to death was introduced, more than 40 years ago (Folkman, 1971), ten anti-angiogenic drugs targeting VEGF or its receptors are approved for cancer therapy, with many more in clinical trails (Jain, 2014). Among these, the pioneers in angiogenesis inhibitors are: a ligand-trapping humanized monoclonal antibody against VEGF-A – bevacizumab (Avastin, Genentech / Roche), and two kinase inhibitors – sorafenib (Nexavar, Bayer) and sunitinib (Sutent, Pfizer) – that target tyrosine kinases (among others VEGFR-2).

Despite the encouraging intial results in pre-clinical models and clinical trials, anti-angiogenic therapy by itself failed to meet the expectations. These initial benefits, in the order of weeks to months (at best), are only transitory, because of either intrinsic resistance of tumors to these agents prior to treatment or the development of resistance after an initial response (Bergers and Hanahan, 2008; Jain, 2014). In the latter case, the evasion of anti-angiogenic therapy is mediated by the development of alternative mechanisms to sustain tumor growth.

In part, the following adaptive can be involved: (i) activation and / or upregulation of alternative pro-angiogenic signaling pathways; (ii) activation of vasculogenesis; (iii) increased pericyte coverage of the tumor vessels, which confers resistance to therapy; (iv) increased invasion of cancer cells that allows them to access the blood supply of normal tissue without the necessity of neovascularization (Bergers and Hanahan, 2008).

Moreover, VEGF inhibition as a single therapy has been suggested to promote a switch of the cancer cells to a more invasive and more metastatic phenotype, possibly contributing to the limitations of patients' survival (Kerbel, 2008). Indeed, the results from pre-clinical studies on several tumor models confirmed that inhibition of angiogenesis as a monotherapy promotes tumor progression to malignancy, with heightened local invasion and increased metastatic capacity (Ebos et al., 2009; Paez-Ribes et al., 2009).

On the contrary to these 'vessel pruning' strategies, recent preclinical and initial clinical results revealed that 'normalization of the vascular abnormalities' in cancer is emerging as a complementary therapeutic approach to standardized cancer therapies (Carmeliet and Jain, 2011b; Jain, 2014).

3.1.2. VESSEL NORMALIZATION AS A NEW THERAPEUTHIC APPROACH TO BLOCK METASTASIS

In tumors, the production of angiogenic factors is excessive and leads to the development of functionally and structurally abnormal vessels. The strategy of tumor vessel normalization aims to restore the equilibrium of pro- and anti-angiogenic factors that are skewed in the tumor microenvironment. This would revert the utterly abnormal structure and function of the tumor vessels towards a more normal state (Goel et al., 2011). These changes would not only contribute to the development of less hypoxic tumors with lower invasive and metastatic

properties, but could also contribute to an improved chemoresponse by improving drug delivery.

The importance of vessel normalization has been recognized in 2001. The idea stemmed from the observation that monotherapy of bevacizumab had divergent outcomes compared to combined bevacizumab and chemotherapy on overall survival in patients (Jain, 2001). While monotherapy with an anti-VEGF monoclonal antibody failed to prolong the overall survival of patients, combined treatment with chemotherapy conferred a survival benefit (Jain, 2001; Jain, 2014). This beneficial effect was mediated by transient 'normalization' of the abnormal vasculature of tumors as a result of anti-angiogenic treatment that temporally improved tumor perfusion and reduced intratumoral hypoxia (known to promote resistance to chemotheraphy and radiotherapy). Thus, therapies that were administered during the window of time when tumor vessels were normalized might have achieved better efficacy (Jain, 2001; Jain, 2014).

Since 2001, several preclinical studies using direct and indirect anti-angiogenic agents supported the tumor vessel normalization hypothesis (Izumi et al., 2002; Tong et al., 2004; Winkler et al., 2004; Yuan et al., 1996). Moreover, a number of additional targets, present either in cancer cells or in stromal cells, have been implicated in facilitating or hindering vessel normalization (Jain, 2014). Among these, studies from our lab showed that genetic blockade of PHD2 in ECs promotes tumor vessel normalization (Mazzone et al., 2009). Moreover, we uncovered unanticipated activities of chloroquine (FDA-approved antimalarial drug) as a tumor vessel normalizing agent (Maes et al., 2014).

Altogether, these studies support the notion that tumor vessel 'normalization', rather than vessel 'pruning', presents a promising strategy to diminish cancel cell invasive and metastatic capacity, whilst improving drug-delivery and chemotherapy-response, thus promising a prolonged overall survival.

3.2. CANCER-ASSOCIATED FIBROBLASTS

CAFs are the most prominent cell type within the tumor stroma of many tumors, especially in breast, prostate and pancreatic carcinomas (Kalluri and Zeisberg, 2006; Pietras and Ostman, 2010). In fact, the fibroblast population in pancreatic cancers may comprise more than 90% of the overall tumor mass (Karagiannis et al., 2012).

The transformation of local fibroblasts is pathologically important in the progression of cancer. CAFs are a form of perpetually activated fibroblasts. They proliferate faster and deposit higher amounts of ECM components than resting fibroblasts in benign tissue (Kalluri and Zeisberg, 2006). While in the early phase of carcinogenesis fibroblasts can have tumor suppressing activities, the phenotype of activated fibroblasts (CAFs) switches to a tumor promoting state as the tumor progresses (Proia and Kuperwasser, 2005). CAFs have an important role in tumorigenesis and in malignant progression. They facilitate proliferation, invasion and motility of malignant cells, and eventually contribute to metastasis (Cirri and Chiarugi, 2011). Their pro-tumorigenic and pro-metastatic activities are related to several mechanisms (Figure 7).

First, CAFs facilitate tumor cell invasion through protease- and force-dependent matrix remodeling (Calvo et al., 2013; Gaggioli et al., 2007). They stimulate angiogenesis and provide building blocks (amino acids, nucleotides) and metabolites (glutamine, pyruvate, lactate) for cancer cell metabolism, promoting tumor growth, invasion and metastasis (Liu et al., 2011). CAFs and hypoxia are both crucial for tumor progression, however little is known about how hypoxia affects the recruitment and activation of CAFs. It has recently been indicated that the recruitment of fibrocytes (possible CAF precursors) / myofibroblasts to sites of pathological fibrosis may be driven by hypoxia (Giaccia and Schipani, 2010). Although it is unknown whether tumor hypoxia does indeed play a role in the recruitment of CAF precursors to the tumor, tumor hypoxia may

control the differentiation of CAFs from precursor cells through mechanisms involving TGF-β1 and endothelin-1 (ET-1) (Bellini and Mattoli, 2007). Overall, hypoxia might enhance most of the pro-tumorigenic activities of CAFs.

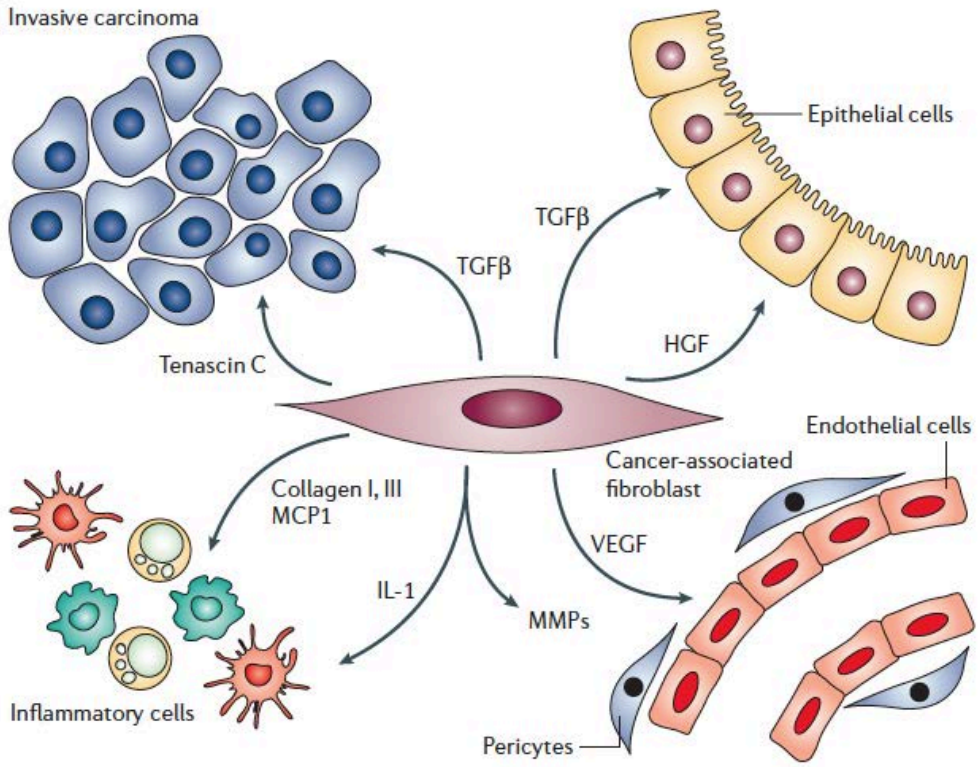

FIGURE 7: PLEIOTROPIC ACTIVITIES OF CAFS.
Within the tumor microenvironment CAFs communicate with several cell types: resident epithelial cells, cancer cells, ECs, pericytes, and inflammatory cells through either direct interaction or secretion of growth factors and chemokines. CAFs remodel the ECM of the tumor microenvironment by depositing collagen and expressing tenascin C, thus altering matrix structure. Moreover, CAFs are capable of proteolytically remodelling the ECM by secreting MMPs and contracting the matrix. These modifications eventually lead to the formation of tracks within the matrix that facilitate cancer cell migration and invasion. By secreting chemokines (MCP1, IL-1), CAFs mediate inflammatory responses and VEGF secreted by CAFs promotes angiogenesis. By releasing TGF-β and HGF they promote the transformation of normal epithelial cells and stimulate cancer cell invasion and proliferation. Adapted from (Kalluri and Zeisberg, 2006).

Secondly, CAFs produce ECM components that provide critical cues for growth, survival, motility of the cancer cells, and angiogenesis. It is generally believed that, in tumors, activated fibroblasts are the main cellular source of ECM. Recent studies show that matrix stiffness promotes BC progression via mechano-reciprocal induction of tumor cell contractility (Levental et al., 2009). The matrix

microenvironment is also important for tumor invasion and metastasis as tumor cells migrate along collagen fibers (Friedl and Gilmour, 2009). Reticular collagen surrounding mammary glands restrain invasion, while alignment of dense collagen fibers perpendicular to the tumor boundary promotes migration (Provenzano et al., 2008). Notably, increased mammographic density due to the stromal matrix is one of the greatest risk factors for developing BC (Boyd et al., 2002), and the presence of a tumor-associated collagen signature-3 (TACS-3) is an independent prognostic indicator regardless of tumor grade and size, estrogen or progesterone receptor status, node status or tumor subtype (Conklin et al., 2011). In fact, TACS-3 is characterized by bundles of straightly aligned collagen fibers that are oriented perpendicular to the tumor boundary, and regions containing TACS-3 correspond to sites of focal invasion into the stroma (Provenzano et al., 2006).

Hypoxia and HIFs have been linked to fibrosis in various tissues during pathological conditions and they act as strong stimuli for tumor matrix production and remodeling (Giaccia and Schipani, 2010). Hypoxia activates collagen synthesis in periarterial smooth muscle cells and in fibroblasts, stimulates the production of syndecan-4, galectin-1 and fibronectin. TGF-β1, the activity of which is increased in hypoxic areas (Higgins et al., 2008), promotes desmoplastic reactions in BC cells. Moreover, hypoxia modulates cell adhesion via integrin-dependent and -independent mechanisms (Jean et al., 2011), which are closely associated with ECM synthesis and remodeling (Geiger et al., 2001). It enhances integrin β1-expression in fibroblasts, leading to focal adhesion kinase (FAK) activation. Hypoxia also augments the expression of some selectin ligands, thereby facilitating endothelial cell adhesion to E-selectin on the surface of cancer cells (Jean et al., 2011). Lysyl oxidase (LOX), which enhances cell-to-matrix adhesion and the migration of tumor cells on modified collagen fibers, is increased in hypoxic human BC cells (Erler et al., 2006). However, hypoxia also influences ECM degradation through the production of matrix metalloproteinases

(MMPs) (Munoz-Najar et al., 2006). As a functional consequence, hypoxia mediated ECM synthesis and remodeling contributes to cancer invasion and metastasis.

Third, CAFs can foster metastasis in distant target organs. A particular challenge in the treatment of BC is early metastatic dissemination followed by long periods of cellular dormancy. The mechanisms responsible for maintaining survival and triggering outgrowth of dormant tumor cells remain largely unknown. One possible mechanism that may regulate tumor dormancy is the interaction of tumor cells with their microenvironment. It has been postulated more than a century ago by Paget that metastases will develop only when the tumor cell (the 'seed') and the microenvironment of a given tissue (the 'soil') are compatible (Goss and Chambers, 2010). Recent studies showed that adhesive interactions with ECM components, as well ECM remodeling (increased collagen I deposition) suffice to induce the switch from dormancy to proliferative tumor growth via integrin β1 signaling and cytoskeleton reorganization (Barkan et al., 2010). Moreover, metastatic cells can be accompanied by CAFs from the primary tumor (Duda et al., 2010) that create a nutritive microenvironment at the distant metastatic site, thereby increasing the number of metastases. Furthermore, CAFs and MSCs promote tumor growth, invasion, and metastasis via cytokine signaling (Karnoub et al., 2007; Orimo et al., 2005). Overall, CAFs are present in human BC and promote tumorigenesis, invasion, survival in the circulation, formation of the pre-metastatic niche and metastasis. Hypoxia signaling might also stimulate several of these processes, as indicated above.

Recent studies also demonstrated, however, tumor-inhibitory effects of CAFs in certain tumor types (pancreatic cancer) suggesting that CAFs exhibit phenotypic plasticity (Augsten, 2014; Ozdemir et al., 2014). CAFs are also being increasingly recognized as attractive therapeutic targets (Micke and Ostman,

2005; Takebe Naoko, 2013), and particulary in breast cancer, they also induce resistance to therapy (Mao et al., 2012; Ostman, 2012).

4. HYPOXIA SIGNALING

Hypoxia is a common feature of solid tumors, resulting from aberrant vessel function and rapid cancer cell proliferation. Cancer cells are able to survive under conditions of low oxygen by mounting adaptive responses to maintain metabolic, bio-energetic and redox demands (Majmundar et al., 2010). Several clinical and preclinical studies have demonstrated that intratumoral hypoxia is associated with poor prognosis, metastasis and resistance to cancer therapies (Fyles et al., 2002; Hockel et al., 1996a; Hockel et al., 1996b; Jubb et al., 2010). The ability of cells to adapt to hypoxia relies on the upregulation of hypoxia-inducible factors (HIFs) and nuclear factor-κB (NF-κB), among others (Cummins and Taylor, 2005; Taylor, 2008).

4.1. HYPOXIA INDUCIBLE FACTORS – FUNCTION, EXPRESSION AND REGULATION

HIFs play a central role in the cellular responses to hypoxia (Semenza, 2007). HIFs are transcription factors that induce the expression of hundreds of genes that regulate cell survival and apoptosis, erythropoiesis, angiogenesis, vascular tone, iron homeostasis, pH regulation, as well as adaptive changes in cellular metabolism (Semenza, 2007). HIFs are composed of an oxygen-regulated HIFα and a constitutive HIF-β subunit (also known as the aryl hydrocarbon nuclear translocator, ARNT). In normoxia, the HIFα subunit is continuously synthesized and degraded, whereas in hypoxia, its degradation is inhibited and it accumulates. Upon translocation to the nucleus, HIFα dimerizes with HIFβ through their helix-loop-helix (HLH) and PER-ARNT-SIM (PAS) domains (Figure

8). HIF heterodimers recognize and bind to hypoxia response elements (HREs; that have consensus sequence 5'-TACGTGCT-3') in target genes, and recruit co-activator proteins p300-CREBBP (CREB-binding protein), leading to increased transcription (Majmundar et al., 2010).

There are three isoforms of HIFα in mammals: HIF1α, HIF2α (also known as endothelial PAS domain-containing protein-1, EPAS-1), and HIF3α (or inhibitory PAS domain protein, IPAS), of which HIF1α and HIF2α are the best characterized (Kaelin and Ratcliffe, 2008). HIF3α lacks the C-terminal transactivation domain and is believed to be a negative regulator of hypoxia-regulated gene expression, most likely by binding competitively to HIFβ subunits, when they are limiting (Heikkila et al., 2011). HIF1α is expressed ubiquitously in all cells, while HIF2α and HIF3α are expressed only in certain tissues. HIF2α expression and transcriptional activity is restricted to vascular ECs, lung type II pneumocytes, kidney epithelial cells and the liver parenchyma. While HIF3α has been shown to be only expressed in cerebellar Purkinje cells, the corneal epithelium of the eye and in the thymus (Bertout et al., 2008).

While HIFs are the key regulator of cellular responses to hypoxia, there are other enzymes that are responsible for sensing the oxygen level and subsequently regulating HIFα activity, the oxygen sensors prolyl hydroxylase domain proteins (PHDs) (discussed in section 4.2). In normoxic conditions, HIFα subunits are hydroxylated by PHDs at the conserved proline residues Pro-402 and Pro-564 within the so-called oxygen-dependent degradation domains (ODDs). Hydroxylated HIFα subunits are recognized by the von Hippel-Lindau tumor suppressor (VHL), targeting it for polyubiquitination and degradation by the proteasome (Figure 8) (Ivan et al., 2001; Jaakkola et al., 2001; Mahon et al., 2001; Maxwell et al., 1999).

PHDs require oxygen and α-ketoglutarate (α-KG) as substrates, and ascorbic acid and ferrous iron (Fe^{2+}) as co-factors for hydroxylation (Bruick and

McKnight, 2001; Epstein et al., 2001; Wong et al., 2013). In addition to PHDs, the HIFα subunit is regulated by another oxygen-dependent hydroxylase, factor inhibiting HIF (FIH). FIH hydroxylates asparagine Asn-803 on the HIFα subunit and thereby reduces its affinity for p300/CREBBP co-factors, resulting in reduced transcriptional activity of HIF (Mahon et al., 2001; McNeill et al., 2002).

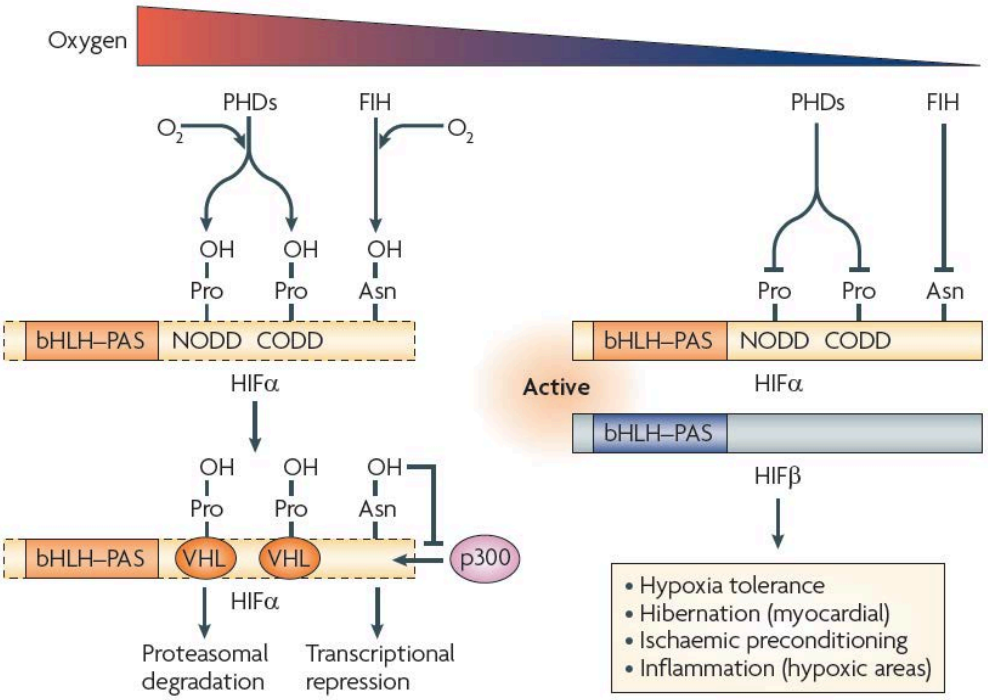

FIGURE 8: HIF ACTIVITY REGULATION IN NORMOXIA AND HYPOXIA.

In normoxic conditions, when the oxygen supply is abundant, prolyl hydroxylase domain-containing proteins (PHDs) and factor inhibiting HIF (FIH) hydroxylate proline or asparagine residues, respectively, on the HIFα subunit. The von Hippel-Lindau (VHL) protein complex recognizes hydroxylated proline residues, leading to proteosomal degradation of HIFα. Hydroxylation of asparagine residues represses transcriptional activity of HIF by blocking the interaction of HIFα and its co-activator p300. Insufficient oxygen supply leads to inactivation of PHDs and FIH. As a consequence, HIFα is stabilized and dimerizes with HIFβ to promote the transcription of a plethora of genes involved in adaptive responses to hypoxia. bHLH-PAS, basic heli-loop-helix-PAS protein domain; CODD, C-terminal oxygen degradation domain; FIH, factor inhibiting HIF; HIF, hypoxia-inducible factor; NODD, N-terminal oxygen degradation domain; PHDs, prolyl hydroxylase domain-containing proteins; VHL, von Hippel-Lindau protein; Adapted from (Fraisl et al., 2009).

4.2. OXYGEN SENSORS – PHDS AND FIH

To date, the family of oxygen sensors consists of: prolyl hydroxylase domain-containing protein 1 (PHD1), also known as HIF prolyl hydroxylase 3 (HPH-3) or egg-laying defective nine homologue 2 (EGLN2); prolyl hydroxylase domain-containing protein 2 (PHD2), also known as HPH-2 or EGLN1; prolyl hydroxylase domain-containing protein 3 (PHD3), also known as HPH-1 or EGLN3); and factor inhibiting HIF (FIH, also known as HIF1AN).

These oxygen sensing enzymes are α-KG–dependent dioxygenases that use oxygen as a substrate, and ferrous iron as a co-factor to catalyze hydroxylation. Interestingly, these enzymes have relatively low affinity for oxygen, with K_m values (the concentration of oxygen required for half-maximal catalytic rate) in the range 100-250 μM for PHDs (with the highest K_M reported for PHD2) (Ehrismann et al., 2007; Hirsila et al., 2003; Koivunen et al., 2006) and 90 μM for FIH (Koivunen et al., 2004). These oxygen levels required for half-maximal catalytic activities of PHDs and FIH are higher than the oxygen level in the tissue (Vaupel et al., 1991), and impaired diffusion in cancer likely creates even lower values. This discrepancy is the reason why these dioxygenases are highly sensitive to small changes in oxygen levels, thus acting as oxygen sensors.

The activity of PHD hydroxylases can also be regulated by metabolic intermediates. While α-KG is required for the enzymatic activity of PHDs, several tricarboxylic acid (TCA) cycle metabolites (fumarate, isocitrate and succinate) competitively inhibit PHDs (Hewitson et al., 2007; MacKenzie et al., 2007; Selak et al., 2005). Accumulation of these metabolites can result from genetic mutations in the metabolic enzymes succinate dehydrogenase and fumarate hydratase. In tumors, this leads to the inhibition of PHDs, HIF activation and promotion of tumorigenesis (Kaelin, 2011). Mutations in isocitrate dehydrogenase (IDH)-1 and IDH-2, common in human glioblastomas, gliomas and leukemias and other types of tumors, also reduce PHD activity by decreasing the cytosolic levels

of α-KG. Subsequent work provided a more in depth explanation suggesting that mutant IDH-1/IDH-2 decreases α-KG by preferentially producing the oncometabolite *(R)*-enantiomer of 2-hydroxyglutarate (*(R)*-2-HG). Structural similarity of *(R)*-2-HG to α-KG results in competitive inhibition of PHDs (Dang et al., 2009; Prensner and Chinnaiyan, 2011). On the contrary, a recent study reported that *(R)*-2-HG increases, not decreases, the activity of PHD1 and PHD2, lowered HIF signaling and surprisingly promoted cancer cell proliferation (Koivunen et al., 2012). These divergent, yet intriguing, results warrant further studies on the contextual molecular mechanism of *(R)*-2-HG activities.

Reactive oxygen species (ROS) have been shown to be a negative regulator of PHD activity by oxidizing ferrous iron to ferric iron, in a dose and time-dependent manner (Wong et al., 2013). Apart from ascorbic acid that reduces iron to its ferrous state (Schofield and Ratcliffe, 2004), other reducing agents, such as glutathione, could suffice to maintain a redox status of iron (Wong et al., 2013).

4.2.1. HIF-INDEPENDENT ACTIVITIES OF PHDS

In addition to their crucial role as regulators of HIF stability and activity, PHDs also regulate other downstream targets either by hydroxylation or by direct interaction.

One of the signalling pathways regulated by PHDs is the nuclear factor κ-light chain enhancer of activated B cells (NF-κB). The NF-κB pathway is involved in many cellular functions, including proliferation, cellular immune responses and cell survival (Perkins, 2007). It has been shown in several models that PHD1 and PHD3 inhibit IκB kinase (IKK), and consequently decrease NF-κB signalling (Cummins et al., 2006; Fu and Taubman, 2010; Fu and Taubman, 2013; Xue et al., 2010). PHD2 is also a negative regulator of the NF-κB pathway during arteriogenesis (Takeda et al., 2011) and vasculogenesis (Chan et al., 2009). A

recent study identified that PHD3, but not PHD1 or PHD2, interacts with and inhibits K63-linked ubiquitination of IKK subunit gamma (IKKγ). This interaction was independent of its hydroxylation activity (Fu and Taubman, 2013). However, it is not clear whether negative regulation of NF-κB signalling by other PHDs occurs via hydroxylation or in a hydroxylation-independent manner (Figure 9).

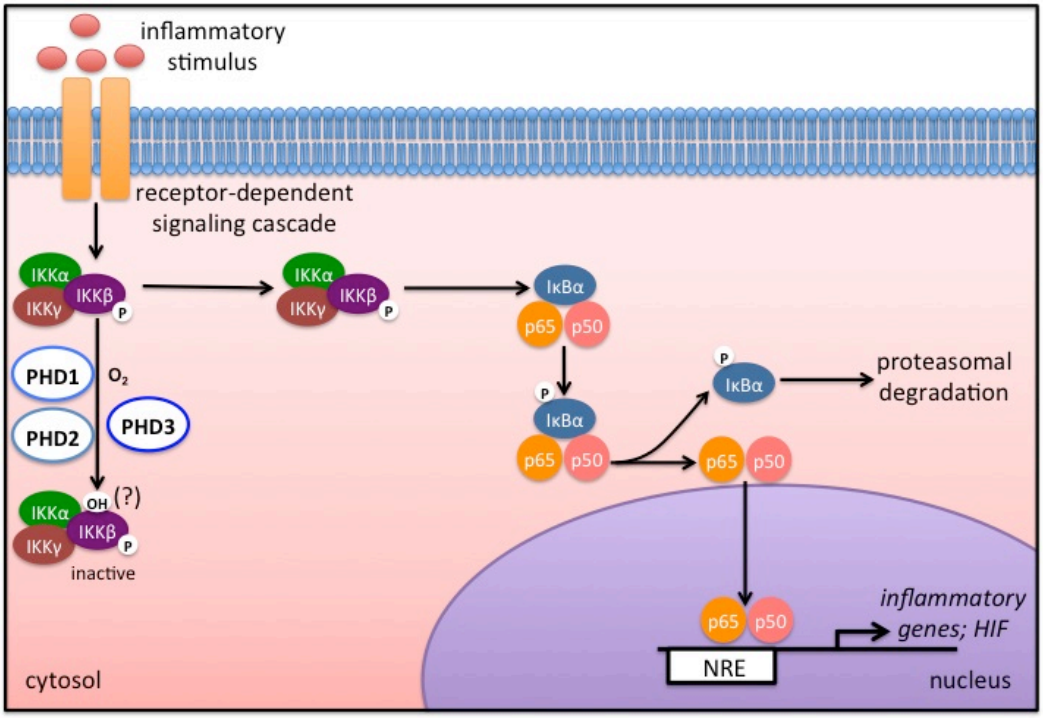

FIGURE 9: NF-κB activity is negatively regulated by PHDS.

Inflammatory stimuli and growth factor signaling cause phosphorylation of inhibitor of κB kinase (IKK)β, leading to complex formation with IKKα and IKKγ, resulting in the subsequent activation and phosphorylation of the inhibitor of transcription factor NF-κB (IκBα). Phosphorylated IκBα is then degraded by the proteasome, releasing the transcription factor NF-κB (consisting of p50 and p65 subunits), which translocates to the nucleus to activate proinflammatory genes via interaction with NF-κB-responsive elements (NRE). Prolyl hydroxylase domain enzymes PHD1, PHD2, and PHD3 were suggested to negatively regulate the IKK complex, possibly through hydroxylation, although the exact mechanism remains to be shown. PHD3 directly interacts with IKKβ in a hydroxylase-independent manner. This negative regulation of IKKβ by PHD3 may involve both steric hindrance and/or hydroxylation, whereas for PHD1 and PHD2, a hydroxylase-dependent negative regulatory mechanism cannot be excluded. Adapted from (Wong et al., 2013).

The regulation of cyclin D1 by PHD1 and PHD2 is also HIF-independent. In a cancer context, both PHD1 and PHD2 act as tumor promoters by upregulating

cyclin D1 in estrogen-dependent BC and pancreatic tumors, respectively (Su et al., 2012; Zhang et al., 2009).

Several independent studies also reported that PHD2 regulates TGF-β1 levels, though the regulation seems to be cell type-dependent. *Wottawa et al*. reported that silencing of PHD2 in the invasive MDA-MB-231 BC cell line resulted in decreased TGF-β1 processing by pro-protein convertase furin, impairing the secretion of the mature form of TGF-β1. TGF-β1 is an important regulator of tumor progression. By silencing PHD2, TGF-β1 secretion was decreased, impairing MDA-MB-231 BC progression *in vivo* (Wottawa et al., 2012). In line with these findings, TGF-β1 signalling was also decreased in PHD2-deficient keratinocytes resulting in increased keratinocyte proliferation and re-epithelialization, thereby promoting faster wound healing (Kalucka et al., 2013). On the contrary, PHD2 silencing in LM8 osteosarcoma, 3L-D122 Lewis lung carcinoma and B16BL6 melanoma increases TGF-β signalling. This is regulated on the transcriptional level as also transcript levels of TGF-β isoforms and their receptors were increased in PHD2-silenced cancer cells (Klotzsche-von Ameln et al., 2011). TGF-β signalling can also be regulated by PHD2 indirectly by other proteins. Indeed, PHD2 has been shown to regulate phosphodiesterase 4D, a key enzyme controlling the cytosolic cAMP levels. cAMP is an important second messenger, regulating many biological processes. Increased cAMP levels prevent TGF-β-induced Smad-specific gene transactivation, and antagonize the inductive effects of TGF-β on the expression of collagen, connective tissue growth factor, tissue inhibitor of matrix metalloproteinase-1, and plasminogen activator inhibitor type I, four prototypical TGF-β-responsive genes (Schiller et al., 2010). PHD2 has been found to upregulate cAMP levels in cardiomyocytes (Huo et al., 2012).

Moreover, PHD3 is also an important regulator of the DNA damage repair pathway during hypoxia (Xie et al., 2012). PHD3 associates with and

hydroxylates HCLK2, a component of the ATR/CHK1 pathway that mediates DNA damage repair and also induces apoptosis. Hydroxylation of HCLK2 is necessary for its binding to ATR, and activation of the ATR/CHK1 pathway. Inhibition of PHD3 or loss of its hydroxylase activity during hypoxia reduces DNA damage-induced apoptosis in cancer. In line with this, PHD3-deficiency *in vivo* desensitizes the mice to ionizing radiation and decreases thymic apoptosis (Xie et al., 2012). These results may provide underpinnings of the genetic instability of tumors, as PHD3 is downregulated by hypermethylation in various tumors (Place et al., 2011). On the contrary, another study reported that PHD2 and PHD3 induction during hypoxia by HIF protects glioblastoma cells from HIF-mediated cell death (Henze et al., 2010). In hypoxic conditions PHD3 is most robustly upregulated as compared to other PHDs (Henze et al., 2010). It is also induced through growth factor deprivation in neuronal cells (Henze et al., 2014). In glioblastoma, hypoxia co-operates with other growth-inhibiting factors to robustly increase PHD3 expression. In this context, PHD3 acts as a tumor suppressor; it regulates EGFR internalization to suppress tumor growth. PHD3 controls EGFR activity independent of its hydroxylase activity by acting as a scaffold protein that interacts with the endocytic adaptor and facilitates the internalization of EGFR. Loss of PHD3 in cancer cells results in impaired endocytosis of EGFR and hyperphosphorylation, leading to increased EGFR signaling and enhanced cell proliferation and survival (Garvalov et al., 2014; Henze et al., 2014).

Another study added another level of complexity to how PHD3 can indirectly regulate HIF activity. Cancer cells are usually highly glycolytic and they express high levels of pyruvate kinase muscle isoform 2 (PK-M2). Pyruvate kinase is a glycolytic enzyme that regulates the final step of glycolysis by converting phosphoenolpyruvate to pyruvate. Besides its glycolytic activity, PK-M2 can also increase the transcriptional activity of HIF1α. Binding of PK-M2 to HIF1α is facilitated by PHD3 through hydroxylation and direct binding to PK-M2 (Luo et al., 2011). Thus, depending on the oxygen level PHD3 can function as a

direct negative (in normoxia) or an indirect positive regulator of HIF1α (in hypoxia ~ 1% O_2), by hydroxylating HIF1α or PK-M2, respectively. The interaction between PHD3 and PK-M2 also inhibits its enzymatic activity in glycolysis (Chen et al., 2011). Additionally, PHD2 can also inhibit HIF1α transcriptional activity in hypoxic conditions, independent of HIFα hydroxylation, by forming a complex with inhibitor of growth protein-4 (ING-4). ING-4 is a tumor suppressor that mediates the ability of HIF to induce adaptive transcriptional responses (Ozer and Bruick, 2005). Binding of PHD2 to ING-4 inhibits it from activating HIF (Ozer et al., 2005). Overall, these and several other studies show a broad range of functions of PHDs, underlining their important biological functions.

4.2.2. Biological roles of PHDs: HIF-dependent and HIF-independent

PHDs have near-ubiquitous tissue expression, with PHD2 being the most abundant isoform in all cells of the body, except for the testis where PHD1 has the highest expression, and heart, where PHD3 is most highly expressed (Wong et al., 2013). Also FIH is expressed in a broad range of tissues (Zhang et al., 2010). Given its cellular abundance and lowest relative affinity to oxygen (see above), PHD2 has been considered to have a dominant role in oxygen sensing. Indeed, despite the presence of all PHDs, HIF1α activity is almost exclusively regulated by PHD2 at normoxia (Berra et al., 2003).

The crucial role of PHD2 is underlined by genetic studies, where systemic PHD2, but not PHD1 or PHD3, homozygous knockout mice die during embryonic development (E12.5 – E14.5) due to placental and cardiac defects (Takeda et al., 2006). PHD1 and PHD3 knockout mice develop normally and develop organ specific phenotypes, while the FIH knockout mice are viable, but have lower body mass due to enhanced metabolism, outlined in table 1.

Table 1. Summary of phenotypes in PHDs and FIH knockout mice.

Gene	*Genotype*	*Phenotype*	*Reference*
PHD1	-/-	Hypoxia tolerance of skeletal muscle and liver due to reprogramming to anaerobic metabolism	(Aragones et al., 2008; Schneider et al., 2010)
		Decreased Cyclin D1 level resulting in hypoproliferation of lactating mammary glands and inhibition of estrogen-dependent BC tumorigenesis	(Zhang et al., 2009)
PHD2*	-/- (prenatal)	Embryonic lethality (E12.5-E14.5) due to cardiac and placental defects	(Takeda et al., 2006)
	-/- (postnatal)	Increased angiogenesis	(Takeda et al., 2007)
		Polycythemia and congestive heart failure	(Minamishima et al., 2008)
	-/- (in cardiomyocytes)	No phenotype in cardiac filament structure and function, but increased cardiac capillary area and smaller myocardial infract area and necrosis after ligation (dependent on HIF1α - mediated switch to glycolytic metabolism)	(Holscher et al., 2011)
	Hypomorph Hif-p4h-2$^{gt/gt}$ mouse	These mice express decreased amounts of Hif-p4h-2 mRNA: 8% in the heart, 15% in skeletal muscle, 34-47% in the kidney, spleen, lung, and bladder, 60% in the brain and 85% in the liver No effect on: polycthemia, dilated cardiomyopathy, and angiogenesis but reduced myocardial infarct size by HIF1α and HIF2α - mediated cardioprotection resulting from the induction of many genes involved in glucose metabolim, cardiac function and blood pressure.	(Hyvarinen et al., 2010)
	-/- (in HSCs)	Hematopoietic progenitors are outcompeted under severe stress condtions.	(Singh et al., 2013)
	+/- (systmeic and myeloid-spcific)	Improved arteriogenesis, expansion of tissue-resident M2-like macrophages (NF-κB-dependent), improved limb perfusion and decreased necrosis in ischemia	(Takeda et al., 2011)
PHD3	-/-	Hypofunctional sympathoadrenal system and reduced blood pressure	(Bishop et al., 2008)
PHD1 PHD3	-/- -/-	Viable and fertile with smaller litters and modest erythrocytosis	(Takeda et al., 2008)
PHD2 PHD3	-/-;-/- (postnatal)	Premature lethality caused by hepatic steatosis and dilated cardiomyopathy	(Minamishima et al., 2009)
FIH	-/-	Viable, but lower body mass, enhanced metabolism, and increased insulin sensitiivity	(Zhang et al., 2010)

BC, breast cancer; FIH, factor inhibiting HIF; HIF, hypoxia indicible factor; HSC, hematopoietic stem cells; PHD, prolyl hydroxylase domain-containing proteins. * Cell type-dependent phenotypes of PHD2 in tumor are listed in Table 2.

Moreover, conditional PHD2 knockout mice revealed additional functions of PHD2 in adult organisms both in physiological and pathological conditions (also summarized in table 1).

4.2.3. CELL TYPE-DEPENDENT ROLES OF PHD2 IN TUMORS

Mounting evidence from recent studies support the notion that PHD2 has cell type-dependent activities in tumors. Not only the histotype of the tumor determines the effect of PHD2 on tumorigenesis and metastasis, the stromal cell compartment also contributes to these responses. In the following sections I will outline the cell type-dependent roles of PHD2 in tumorigenesis and metastasis, also summarized in table 2.

4.2.4. THE ROLE OF PHD2 IN CANCER CELLS

Several previous studies have investigated the role of PHD2 in cancer cells. It is becoming evident that PHD2 in cancer cells can display both an anti- and pro-tumorigenic effect depending on the cellular context (Bordoli et al., 2010; Chan et al., 2009; Couvelard et al., 2008; Klotzsche-von Ameln et al., 2011; Wottawa et al., 2012).

In a few studies, loss of PHD2 tumor-suppressing function was associated with increased levels of pro-angiogenic factors; VEGF and IL-8 in MCF-7 breast carcinoma xenografts (Bordoli et al., 2010) or angiogenin and IL-8 in HCT116 colorectal cancer xenografts (Chan et al., 2009). Upregulation of pro-angiogenic factors increased tumor angiogenesis or vasculogenesis, respectively, and fostered tumor growth in PHD-silenced cancer cells (Bordoli et al., 2010). In the context of PHD2 as a tumor suppressor, overexpression of PHD2 in several

pancreatic cancer lines reduced tumor growth through cyclin D1, angiogenesis and invasion (Su et al., 2012).

On the other hand, PHD2 can also display tumor-promoting activities. Silencing of PHD2 in LM8 osteosarcoma, Lewis lung carcinoma, and B16BL6 melanoma reduced tumor growth in a TGF-β- dependent manner (Klotzsche-von Ameln et al., 2011). Similarly, decreased TGF-β- secretion in MDA-MB-231 breast carcinoma reduced tumor xenograft growth upon PHD2 silencing (Wottawa et al., 2012).

Given that metastasis is the primary cause of death of most breast cancer patients, it is surprising that the role of PHD2 in regulating this process has been only minimally studied, and not at all in a clinically more relevant spontaneously arising tumor model. Only when using a transplantable xenograft model, a single recent study identified EGLN1 (PHD2) as one of the proteins that are upregulated in metastatic breast cancer cells (Naba et al., 2014). Silencing of PHD2 in the highly metastatic human mammary carcinoma xenograft, MDA-MB-231-LM2, implanted in the mammary fat pad of severely immunocompromised NOD/SCID/IL2Rγ-null mice, did not affect cancer cell invasion, but inhibited the spontaneous and experimental formation of pulmonary metastases (Naba et al., 2014). This suggests that PHD2 did not regulate the early (intravasation), but rather the late (extravasation, lodging, metastatic outgrowth) steps of metastasis in this experimental model (Naba et al., 2014). However, the underlying cellular mechanism and any possible involvement of stromal cells were not elucidated in this study.

Despite clear evidence from xenograft models, listed above, there are more human tumor types that overexpress PHD2 compared to their normal histological counterpart than tumor types that decreases the expression of this gene, suggesting that PHD2 rather acts as an oncogene than a tumor-suppressor (Klotzsche-von Ameln et al., 2011).

Table 2. Cell type-dependent functions of PHD2 in tumors.

PHD2-inhibited cell type	*Tumor growth*	*Meta stasis*	*Mechanism*	*Reference*
tumor cells				
human MCF-7 breast cancer cells	↑	?	- increased secretion of amphiregulin (HIF2-dependent), VEGF and IL-8 - increased angiogenesis	(Bordoli et al., 2010)
human AsPC-1, HPAF-II, MIA PaCa-2 and PANC-1 pancreatic cancer cells	↑	?	- downregulation of cyclin D1 - HIF-independent	(Su et al., 2012)
human HCT116 colon cancer cells	↑	?	- increased secretion of angiogenin and IL-8 - NF-κB-dependent but HIF-independent - increased tumor vascularization	(Chan et al., 2009)
murine LM8 osteosarcoma, B16 melanoma and LLC lung cancer cells	↓	?	- upregulation of MT1-MMP1 and MMP-2 - increased TGF-β activity - cytostatic effect of TGFβ - HIF1-independent	(Klotzsche-von Ameln et al., 2011)
human MDA-MB-231 breast cancer	↓	?	- impaired processing of TGF-β1 by furin - impaired secretion of TGF-β1	(Wottawa et al., 2012)
Human MDA-MB-231-LM2 (metastatic line)	=	↓	- decreased metastasis is likely due to impaired extravasation, seeding, survival, and grow in the target organ	(Naba et al., 2014)
stromal cells				
ECs (murine)	=	↓	- vessel normalization - reduced metastasis and intravasation - improved response to chemotherapy - protection from chemotherapy-induced side effects - HIF2-dependent	(Leite de Oliveira et al., 2012; Mazzone et al., 2009)
myeloid and T-cells (murine)	↓	?	- increased cell death (necrosis) - reduced cytokine secretion - partially HIF1-dependent	(Mamlouk et al., 2014)

LLC, Lewis lung carcinoma; ECs, endothelial cells; MMP, matrix metalloproteinase; MT1-MMP1, membrane type 1 matrix metalloproteinase 1.

4.2.5. THE ROLE OF PHD2 IN STROMAL CELLS

PHD2 is expressed in all cells in the body. Thus it is not surprising that it also exerts effects on tumor progression and metastasis when targeted in specific cell populations. Up to now, only a few studies reported the effect of PHD2 blockade

in the tumor stroma. *Mazzone et al.* revealed that PHD2 haplodeficiency in ECs does not affect primary tumor growth in several transplantable tumor models but reduces intravasation and pulmonary metastasis. They discovered that reduction in metastasis was due to normalization of abnormal tumor vessels in a HIF2α dependent manner. PHD2 haplodeficiency in ECs does not affect tumor vessel density or architecture, but improved endothelial cell lining and pericyte-coverage, leading to improved vessel function and decreased intratumoral hypoxia. Reduced hypoxia diminished the invasive phenotype of cancer cells, improved vessel structure and restrained cancer cell intravasation (Mazzone et al., 2009). To follow up on the clinical implication of these findings, they further investigated whether PHD2 haplodeficiency in ECs combined with standard chemotherapy would be beneficial. Indeed, PHD2 haplodeficiency in ECs not only improved the delivery of chemotherapeutics and the chemoresponse, it protected the mice from side effects of these chemotherapeutics by counteracting oxidative damage in the heart and kidney (Leite de Oliveira et al., 2012).

In another study, analysis of PHD2 deficiency in both myeloid cells and T-lymphocytes reduced primary tumor growth (LLC xenografts), but the effect on metastasis has not been investigated (Mamlouk et al., 2014). The reduced tumor volume was a result of a decreased secretion of pro-tumoral and anti-tumoral cytokines that caused an imbalance between enhanced cell death and improved cancer cell proliferation (Mamlouk et al., 2014).

Taken together, these results highlight that the treatment of cancer patients with a PHD2 pharmacological blocker might result in complex and divergent responses. Therefore, it is important to investigate the consequences of PHD2 blockade in both tumor and stromal cells to provide a unifying view on its effect on primary tumor growth and metastasis.

CHAPTER II

RATIONALE AND AIMS

Prolyl-hydroxylase 2 (PHD2) is an oxygen-sensing enzyme that regulates HIFα levels in normoxia by targeting HIFα via hydroxylation for proteasomal degradation. We focused on PHD2 because this oxygen sensor has a critical role in health and disease, and because hypoxia signaling influences metastasis. Even though the role of PHD2 in tumor progression has been previously studied by silencing PHD2 in cancer cells in transplantable tumor models, the following three medically important questions have not been addressed in these studies.

First, although metastasis kills >90% of cancer patients, the consequences of blocking PHD2, selectively in cancer or stromal cells, on metastasis have not been dissected in a spontaneously arising tumor model, which more closely mimics human cancer.

Second, it is unknown whether PHD2 regulates the behavior of CAFs, even though emerging evidence indicates that these stromal cells have important effects on tumor progression and metastasis.

Third, given that certain studies reported that PHD2 silencing in cancer cells stimulated tumor progression in transplanted tumor models (Bordoli et al., 2010; Chan et al., 2009), it is unknown if concomitant PHD2 inhibition in both malignant and stromal cells (mimicking treatment with a pharmacological blocker) *promotes* or *impairs* metastasis, when initiated before but certainly also after onset of tumor growth in a spontaneous tumor model.

In this study, we utilized the spontaneously arising Polyoma virus middle T antigen (PyMT)-oncogene driven breast cancer model to address these outstanding questions.

CHAPTER III

METHODOLOGY AND MATERIALS

1. MICE

Animal procedures were approved by the Institutional Animal Care and Research Advisory Committee (K.U. Leuven) and were performed in accordance with the institutional and national guidelines and regulations.

MMTV-PyMT SPONTANEOUS BC MODEL: MMTV-PyMT mice were obtained from The Jackson Laboratory (Guy et al., 1992). Mammary tumors in PyMT mice arise spontaneously in virgin animals due to mammary epithelium directed expression of the PyMT antigen by the mouse mammary tumor virus (MMTV)-long terminal repeat (LTR) promoter (Lin et al., 2003). PyMT exerts its tumorigenic effects by changes in signalling of the Src, Ras, and PI3K pathways (Dankort and Muller, 2000). Importantly, these signalling pathways are also activated by ErbB-2/Neu, a receptor tyrosine kinase that is commonly overexpressed in human breast cancers (Reese and Slamon, 1997). Extensive histological characterization of tumor progression in the PyMT model has also demonstrated reliable recapitulation of the morphological changes that occur during human breast cancer progression (Lin et al., 2003). Additionally, changes in gene expression concurrent with tumor progression in the PyMT model correlates with changes in gene expression observed in human breast cancer disease (Qiu et al., 2004). The PyMT model also provides an added advantage in the high rate of pulmonary metastasis that allows for the investigation of metastatic disease.

PHD2 GLOBAL AND CONDITIONAL KNOCKOUT MICE: The generation of $PHD2^{+/-}$ and $PHD2^{lox/lox}$ mice was described previously (Mazzone et al., 2009). Tie2-Cre mice (Kisanuki et al., 2001), or *VE-cadherin (PAC)-Cre^{ERT2}* mice (Benedito et al., 2012) were intercrossed with $PHD2^{lox/lox}$ mice and with MMTV-PyMT mice to obtain mice spontaneously developing metastatic mammary gland tumors with wild type PHD2 expression in endothelial cells ($PyMT^{Tie2\text{-}WT}$ or $PyMT^{VE\text{-}cadh\text{-}WT}$ mice, respectively) or with haplodeficiency of the PHD2 gene specifically in endothelial cells ($PyMT^{Tie2\text{-}HE}$ or $PyMT^{VE\text{-}cadh\text{-}HE}$ mice, respectively). PDGFRα:Cre^{ERT2} mice (Rivers et al., 2008) were intercrossed with $PHD2^{lox/lox}$ mice and with the MMTV-PyMT mice to obtain mice spontaneously developing metastatic mammary gland tumors with either wild type PHD2 expression in fibroblasts ($PyMT^{CAF\text{-}WT}$ mice) or with haplodeficiency of the PHD2 gene specifically in fibroblasts ($PyMT^{CAF\text{-}HE}$ mice). MMTV-Cre mice were from The Jackson Laboratory (Wagner et al., 1997) and were intercrossed with $PHD2^{lox/lox}$ mice and with the MMTV-PyMT mice to obtain mice spontaneously developing metastatic mammary gland tumors with wild type PHD2 expression in the tumor cells ($PyMT^{TC\text{-}WT}$ mice) or with haplodeficiency of the PHD2 gene specifically in tumor cells ($PyMT^{TC\text{-}HE}$ mice), respectively. Cell specific deletion of PHD2 was validated by qRT-PCR and immunoblotting. mT/mG reporter mice were from The Jackson Laboratory (Muzumdar et al., 2007) and were intercrossed with MMTV-PyMT mice to obtain mice harboring $mTomato^{+}$ tumor cells ($PyMT^{mT/mG}$). All the transgenic mice used in this study were backcrossed to FVB genetic background and their brief characterization is listed in table 1. Wild type FVB mice were obtained from the KU Leuven animal facility.

Table 1. List of the mouse lines and their characterization

Mouse line	Abbreviation	Specification	Background	Reference
PHD2ko:MMTV-PyMT	$PHD2^{+/+}$:MMTV-PyMT($PyMT^{+/+}$); $PHD2^{+/-}$:MMTV-PyMT ($PyMT^{+/-}$)	Global PHD2 haplodeficiency in all cell of tumor, cancer cells and stromal cells	FVB	(Lin et al., 2003; Mazzone et al., 2009)
Tie2-Cre:PHD2cko: MMTV-PyMT	$PHD2^{+/+}$:Tie2-Cre: MMTV-PyMT ($PyMT^{Tie2\text{-}WT}$); $PHD2^{+/lox}$:Tie2-Cre: MMTV-PyMT ($PyMT^{Tie2\text{-}HE}$)	PHD2 haplodeficiency in ECs and Tie2-expressing bone marrow derived cells, while the rest of the tumor stroma and cancer cells are wild type.	FVB	(Lin et al., 2003; Mazzone et al., 2009)
VE-cadherin (PAC)-Cre^{ERT2}:PHD2cko: MMTV-PyMT	$PHD2^{+/+}$:*VE-cadherin (PAC)-Cre^{ERT2}*: MMTV-PyMT ($PyMT^{Cdh5\text{-}WT}$); $PHD2^{+/lox}$:*VE-cadherin (PAC)-Cre^{ERT2}*: MMTV-PyMT ($PyMT^{Cdh5\text{-}HE}$)	PHD2 haplodeficiency in ECs, the rest of tumor stroma and cancer cells are wild type.	FVB	(Benedito et al., 2012; Lin et al., 2003; Mazzone et al., 2009)
PDGFRα-Cre^{ERT2}:PHD2cko: MMTV-PyMT	$PHD2^{+/+}$:PDGFRα-Cre^{ERT2}:MMTV-PyMT ($PyMT^{CAF\text{-}WT}$); $PHD2^{+/lox}$:PDGFRα-Cre^{ERT2}:MMTV-PyMT ($PyMT^{CAF\text{-}HE}$)	PHD2 haplodeficiency in PDGFRα-expressing cells, among which are CAFs, the rest of tumor stroma and cancer cells are wild type.	FVB	(Leite de Oliveira et al., 2012; Lin et al., 2003; Mazzone et al., 2009)
MMTV-Cre:PHD2cko: MMTV-PyMT	$PHD2^{+/+}$:MMTV-Cre:MMTV-PyMT ($PyMT^{TC\text{-}WT}$); $PHD2^{+/lox}$:MMTV-Cre:MMTV-PyMT ($PyMT^{TC\text{-}HE}$)	PHD2 haplodeficiency in cancer cells, CAFs are wild type.	FVB	(Lin et al., 2003; Mazzone et al., 2009; Wagner et al., 1997)
R26-Cre^{ERT2}:PHD2cko: MMTV-PyMT	$PHD2^{+/+}$:R26-Cre^{ERT2}: MMTV-PyMT ($PyMT^{R26\text{-}WT}$); $PHD2^{+/lox}$:R26-Cre^{ERT2}:MMTV-PyMT ($PyMT^{R26\text{-}HE}$) ; $PHD2^{lox/lox}$:R26-Cre^{ERT2}:MMTV-PyMT ($PyMT^{R26\text{-}HO}$)	Inducible global PHD2 haplodeficiency in all cell of tumor, cancer cells and stromal cells. In this study deletion of PHD2 was indeuced at 7 weeks of tumor progression.	FVB	(Leite de Oliveira et al., 2012; Lin et al., 2003; Mazzone et al., 2009)
MMTV-PyMT:mT/mG	MMTV-PyMT:mT/mG ($PyMT^{mT/mG}$)	The mT/mG line is a double-fluorescent Cre reporter mouse that expresses membrane-targeted tandem dimer Tomato (mT) prior to Cre-mediated excision and membrane-targeted green	FVB	(Muzumdar et al., 2007).

		fluorescent protein GFP (mG) after excision. For our experiments, PyMT$^{mT/mG}$ mice were not intercrossed with Cre-expressing mice and thus did not switch on the expression of GFP, but expressed Tomato reporter.		

GENOTYPING: Mice were genotyped by PCR. A tail biopsy (0.5-1cm) was digested overnight in 700µl lysis buffer (0,1M Tris-HCl (pH 8.5), 5 mM EDTA, 0.02% SDS, 0.2 M NaCl in distilled water) containing 7µl proteinase K (10 mg/ml proteinase K, dissolved in 47% glycerol in MQ-water). After centrifugation (10 min, 15,000 revolutions per minute (rpm)), the supernatant was mixed with isopropyl alcohol (600 µl) to precipitate the genomic DNA. The precipitated DNA was dissolved in 400 µl Tris-EDTA (10 mM Tris, pH7.5: 1 mM EDTA) by incubating for 1 hour at 55°C. 1 µl of DNA solution was pipetted into a PCR tube containing 12.5 µl GoTaq Green Master Mix (Promega), 1 µl each of the primers (10 µM), and adjusted to a total volume of 25 µl with RNase free water. The primers used are listed in table 2. PCR was performed using a PTC-200 Peltier thermal cycler with the following cycling program: one cycle of 30'' at 98°C, then 30 cycles of 5'' at 98°C, 5'' at 60°C, and 10'' at 72°C. Samples were separated on a 2% agarose (UltraPure Agarose, Invitrogen) gel, using a gel electrophorysis system (VWR, 700-0056).

Table 2. List of primers used for PCR to genotype the mice

Gene of interest	Primer name	Primer sequence	Pairs with	Allele	Band size (bp)
PHD2	WT MA 1	5' ACC-TAT-GAT-CTC-AGC-ATT-TGG-GAG 3'	ME 1	WT	340
	GETYPMA 1	5' TCA-GGA-CAG-TGA-AGC-CTA-GAA-ACT-CT 3'	ME 1	KO	380
	ME 1	5' AAA-TTC-TAA-TCG-TAG-CTG-ATG-TGA-GC 3'			
PHD2(cKO)	PHD2CKO C	5' CCT-TCC-ATG-TTG-GCT-CAT-TCC-ATT 3'			
	PHD2CKO D	5' TGC-TGA-ATT-GAG-TTG-CAT-			

		ACC-TTG 3'			
Tie2-Cre	Cre 850	5’ CGC-CGT-AAA-TCA-ATC-GAT-GAG-TTG-CTT-C 3’			
	Cre 403	5' GAT-GCC-GGT-GAA-CGT-GCA-AAA-CAG-GCT-C 3'			
	HIF 700	5' CAA-GCA-TTC-AAT-GTG-GAG-CTA-TCT 3'			
	HIF 960	5' TTG-TGT-TGG-GGC-AGT-ACT-GGA-AAG-ZTG 3'			
VE-cadherin (PAC)-Cre^{ERT2}	sCre1	5’ GCC-TGC-ATT-ACC-GGT-CGA-TGC-GA 3’			
	asCre2	5' GTG-GCA-GAT-GGC-GCG-GCA-ACA-CCA-TT 3'			
PDGFRα-Cre^{ERT2}	ATG Cre up	5’ CAG-GTC-TCA-GGA-GCT-ATG-TCC-AAT-TTA-CTG-ACC-GTA 3’			
	ATG Cre low	5' GGT-GTT-ATA-ACG-AAT-CCC-CAG-AA 3'			
MMTV-Cre	Cre 850	5’ CGC-CGT-AAA-TCA-ATC-GAT-GAG-TTG-CTT-C 3’			
	Cre 403	5' GAT-GCC-GGT-GAA-CGT-GCA-AAA-CAG-GCT-C 3'			
	Endo 1	5' CAA-ACC-TGC-TAC-CCG-AAG-GT 3'			
	Endo 2	5' CAG-TAT-GCG-GAA-GTT-CTA-GG 3'			
R26i-Cre	Cre 850	5’ CGC-CGT-AAA-TCA-ATC-GAT-GAG-TTG-CTT-C 3’			
	Cre 403	5' GAT-GCC-GGT-GAA-CGT-GCA-AAA-CAG-GCT-C 3'			
	HIF 700	5' CAA-GCA-TTC-AAT-GTG-GAG-CTA-TCT 3'			
	HIF 960	5' TTG-TGT-TGG-GGC-AGT-ACT-GGA-AAG-ZTG 3'			
MMTV-PyMT	IMR 15	5' CAA-ATG-TTG-CTT-GTC-TGG-TG 3'			
	IMR 16	5' GTC-AGT-CGA-GTG-CAC-AGT-TT 3'			
	IMR 384	5' GGA-AGC-AAG-TAC-TTC-ACA-AGG-G 3'			
	IMR 385	5' GGA-AAG-TCA-CTA-GGA-GCA-GGG 3'			
mT/mG	IMR 7318	5' CTC-TGC-TGC-CTC-CTG-GCT-TCT 3'			

	IMR 7319	5' CGA-GGC-GGA-TCA-CAA-GCA-ATA 3'			
	IMR 7320	5' TCA-ATG-GGC-GGG-GGT-CGT-T 3'			
MMTV-Cre	Cre 850	5' CGC-CGT-AAA-TCA-ATC-GAT-GAG-TTG-CTT-C 3'			
	Cre 403	5' GAT-GCC-GGT-GAA-CGT-GCA-AAA-CAG-GCT-C 3'			
	Endo 1	5' CAA-ACC-TGC-TAC-CCG-AAG-GT 3'			
	Endo 2	5' CAG-TAT-GCG-GAA-GTT-CTA-GG 3'			

2. TUMOR MODELS

PRIMARY TUMOR GROWTH: Progression from hyperplasia to adenoma and ultimately carcinoma was evaluated on H&E stained tumor sections as described before (Lin et al., 2003). Tumor growth was monitored by measuring the volume of each of the ten individual mammary tumors per MMTV-PyMT mouse once a week up to 16 weeks with a caliper using the formula: $V = \pi \times [d^2 \times D] / 6$, where D is the major tumor axis and d is the minor tumor axis. Per mouse the mean of the individual tumor volumes was calculated and used to determine the genotypic difference. To analyse the tumor weight and pulmonary metastasis, mice were euthanized by cervical dislocation at the end point and the tumors and lungs were dissected and analyzed as described below.

TUMOR CELL PROLIFERATION was detected by immunostaining of MMTV-PyMT tumor sections for PHH3. Mosaic pictures were taken, and $PHH3^+$ area was quantified and expressed as a % of total tumor area.

TUMOR CELL INITIATION: Analysis of MMTV-PyMT tumor initiation was done on whole mount carmine stained mammary glands. Inguinal and thoracic mammary

glands were dissected from 4 week old PyMT$^{TC\text{-}WT}$ and PyMT$^{TC\text{-}HE}$ mice. Mammary glands were stretched out on a glass slide and fixed with Carnoy's fixative for 2 hours at room temperature. The mammary glands were washed in 70% ethanol for 15 minutes and then hydrated by gradually changing to distilled water. Next they were stained in carmine alum overnight (2% carmine (Sigma-Aldrich, Bornem, Belgium), 5% potassium aluminum sulfate in distilled water). After staining, the mammary glands were gradually dehydrated (15 minutes each for 50%, 70%, 90%, 95%, and 100% ethanol), cleared in xylene, and mounted with DPX (Prosan). Imaging was performed using a stereomicroscope (Carl Zeiss, Munich, Germany). Intraepithelial neoplasias were delineated using ImageJ software and the area was determined across both inguinal and thoracic mammary glands.

ANALYSIS OF PULMONARY METASTASIS: Dissected lungs were perfused with 1 ml ink solution (15 volume% black ink in sterile water, 2-3 drops of 25% NH_3 per 50ml), washed with PBS and incubated in destaining solution (34% ethanol, 18% formaldehyde, 2.4% acetic acid) to visualize the metastatic nodules. Macroscopic metastatic lesions were counted under a dissecting microscope. The metastatic index was calculated as the number of metastases divided by total tumor weight.

DETECTION OF CIRCULATING TUMOR CELLS (CTCS): 100 µl blood samples were collected from tumor bearing mice at the end stage of the experiment. Blood samples were collected in RNA protect Animal Blood Tubes (Qiagen) and RNA was extracted with RNeasy Protect Animal Blood Kit (Qiagen), according to the manufacturer's instructions. The level of CTCs was analyzed by assessing *PyMT* and *Cytokeratin 8* transcript levels normalized to *Hprt* transcript levels.

ANALYSIS OF EXTRAVASATION AND COLONIZATION: 2,000,000 MMTV-PyMT tumor cells ($PyMT^{TC\text{-}WT}$ or $PyMT^{TC\text{-}HE}$) were injected in the tail vein of FVB mice. After 15 minutes, one, three or 24 hours, the mice were sacrificed and lungs were collected to assess tumor cell extravasation and colonization by assessing *PyMT* transcript levels normalized to *Hprt* transcript levels.

3. CELL ISOLATION AND CULTURE

CANCER CELLS AND CAFS FROM PYMT TUMORS: PyMT tumor cells and CAFs were isolated from MMTV-PyMT mice of different genotypes according to modified protocols of (Schwab et al., 2012) and (Calvo et al., 2013), respectively, cultured and used between passages 1 and 5. Briefly, dissected tumors were chopped and digested with 2 mg/ml collagenase (Sigma blend L, Sigma-Aldrich, Bornem, Belgium) in RPMI medium containing 5% fetal bovine serum (FBS) (5 ml/g tissue) for 1 hour at 37°C. Organoids were pelleted at 1,100 rpm, washed four times with digestion buffer and then plated into standard tissue culture flasks in plating medium (Ham F-12 medium supplemented with 10% FBS, 100:100 penicillin/streptomycin (Gibco, Invitrogen), 1.2% glutamine (Gibco, Invitrogen), 1 µg/ml hydrocortisone (Sigma-Aldrich, Bornem, Belgium), 50 µg/ml gentamicin (Gibco, Invitrogen), 5 µg/ml bovine insulin (Sigma-Aldrich, Bornem, Belgium), 10 ng/ml EGF (Gibco, Invitrogen), and 5 ng/ml cholera toxin (Gibco, Invitrogen)). The tumor suspension was plated for 30 minutes; adherent cells were enriched in CAFs. The non-adherent cell suspension was transferred to another flask to culture cancer cells. After plating for fibroblasts, the CAF enriched culture usually still contains some tumor cells. In order to obtain pure populations of CAFs, the cells were differentially trypsinized with dispase (Roche, Vilvoorde, Belgium) and 0.25% trypsin (Gibco, Invitrogen). CAFs were cultured in CAF medium (DMEM F-12, 10% FBS, 100:100 penicillin/streptomycin, 1.2% glutamine), and cancer cells in plating medium.

NORMAL LUNG FIBROBLASTS: fibroblasts were freshly isolated from lungs of FVB mice, cultured and used between passages 1 and 5. Briefly, dissected lungs were chopped and digested in a solution of 2 mg/ml collagenase (Sigma blend L, Sigma-Aldrich) in RPMI medium containing 5% fetal bovine serum (FBS) (5 ml/ lungs) for 1 hour at 37°C. Organoids were pelleted at 1,100 rpm, washed four times with digestion solution and then plated into standard tissue culture flasks in CAF medium. The day after isolation, the medium was refreshed. Cells were then routinely maintained in 5% CO_2 and 95% air (normoxia) at 37°C and the medium was replaced every second day.

TREATMENTS: Mitotic inactivation was achieved by culturing the cells for 24 hours in the presence of 2 µg/ml mitomycin C, and was confirmed using a [^{3}H]-Thymidine proliferation assay (see below). Culture under hypoxia was done in 5% CO_2 and 0.5% O_2. Tumor cell conditioned medium was obtained from tumor cell cultures seeded at a density of 20 million cells per 10 cm dish in plating medium. After one day, confluent cells were washed with DPBS (Gibco, Invitrogen) and the medium was changed to 5 ml of full plating medium without FBS. Conditioned medium was collected from these dishes 24 hours later.

4. LENTIVIRAL TRANSDUCTIONS

Lentiviral transductions were performed as described (De Bock et al., 2013). Briefly, a lentiviral vector (pLVx-shRNA2; Clontech) encoding a green fluorescent reporter (ZsGreen, for convenience abbreviated as GFP in the text and figures) and into which a nonsense scrambled shRNA was cloned (De Bock et al., 2013), was used at a multiplicity of infection (MOI) of 10. Cells were transduced overnight in the presence of 0.5 µg/ml polybrene (Sigma-Aldrich, Bornem, Belgium), and refreshed with regular medium the next day. Transduced cells were used in functional assays at least 3 to 4 days post-transduction.

5. IN VITRO ASSAYS

CELLULAR PROLIFERATION was quantified by incubating the cells for 2 hours with 1 µCi/ml [^{3}H]-thymidine. Thereafter, cells were fixed with 100% ethanol for 15 minutes at 4°C, precipitated with 10% TCA and lysed with 0.1N NaOH. The amount of [^{3}H]-thymidine incorporated into DNA was measured by scintillation counting.

SCRATCH WOUND MIGRATION ASSAY: was performed with MMTV-PyMT cancer cells on 24-well plates 18 hours after seeding. A scratch wound was applied on the confluent MMTV-PyMT cancer cell monolayer using a 200 µl tip. After applying the wound and photography (T_0), the cultures were further incubated for 18 hours, and photographed again (T_{18hr}). Endpoint pictures (T_{18hr}) were taken after several wash steps with DPBS (Gibco, Invitrogen) to clear the cellular debris. Mean migration distance (gap area at T_0 minus gap area at T_{18hr}, normalized by the width of the migration front (measured as a straight line, parallel to the migration front)) was measured with NIH ImageJ software and is expressed in arbitrary units.

SPHEROID TUMOR CELL INVASION ASSAY: MMTV-PyMT cancer cells (50,000 cells) were incubated for 3 days in hanging drops in plating medium (see above) containing 20% methylcellulose (Sigma-Aldrich, Bornem, Belgium), to form spheroids. Spheroids were then embedded in collagen gel as described (Korff et al., 2004) and cultured for 72 hours to induce invasion. Cultures were fixed and images were captured with an inverted microscope (Zeiss Axiovert 40CFL). Analysis of the entire cancer cell spheroid (as a measure of the collective cancer cell invasion) was done using the NIH ImageJ software.

SPHEROID CAF INVASION ASSAY: CAFs (1,000 cells) were incubated overnight in hanging drops in CAF medium (see above) containing 20% methylcellulose

(Sigma-Aldrich, Bornem, Belgium), to form spheroids. Spheroids were then embedded in collagen gel as described (Korff et al., 2004) and cultured for 18 hours to induce invasion. Cultures were fixed and images were captured with an inverted microscope (Zeiss Axiovert 40CFL). Analysis of the number of sprouts and the total sprout length (cumulative length of primary sprouts and branches per spheroid) was performed using NIH ImageJ.

CHIMERIC TC-CAF SPHEROID INVASION ASSAY: Tomato^{+} PyMT$^{mT/mG}$ tumor cells (TCs) (1,000 cells) and GFP^{+} CAFs (1,000 cells) were co-incubated overnight in hanging drops in plating medium (see above) containing 20% methylcellulose (Sigma-Aldrich, Bornem, Belgium), to form spheroids. Spheroids were then embedded in collagen gel as described (Korff et al., 2004) and cultured for 48 hours to induce invasion. Cultures were fixed and images were captured with Zeiss LSM 780 confocal microscope (Carl Zeiss, Munich, Germany). The number of the individual TCs invading into the collagen gel was analyzed.

CO-CULTURE ASSAYS: A CAF organotypic culture system was set up to analyse the effect of CAF-mediated ECM remodelling on TC invasion into a collagen gel. Briefly, 250,000 CAFs/ml were embedded in a collagen matrix. After the base layer of collagen gel with non-transduced or GFP^{+} CAFs was solidified at 37°C, Tomato^{+} PyMT$^{mT/mG}$ cancer cell spheroids (50,000 cancer cells/spheroid), aggregated 72 hours in advance, were pipetted on top of the base layer, and overlayed by a top layer of collagen with non-transduced or GFP^{+} CAFs. Spheroids were cultured for 48 hours to induce invasion. Cultures were fixed and images were captured with Zeiss LSM 780 confocal microscope (Carl Zeiss, Munich, Germany). Analysis of the invasive tumor area was done using the NIH ImageJ software.

CLONOGENIC GROWTH ASSAY: A base layer of agar was prepared in 12-well plates. Agar (high-gel strength, Serva) was dissolved at 0.5% in sterile distilled water

(Gibco, Invitrogen) in a microwave oven and was mixed with pre-warmed (56°C) Ham's F12 medium (Gibco, Invitrogen) at a 1:1 ratio. The base layer of agar mixture was pipetted into a 12-well plate at 1.5 ml per well, and was left to solidify at room temperature. Cancer cells were suspended as a single-cell suspension (5,000 cancer cells per 1.5 ml, 1.5 ml per well) and plated on top of the base agar. Cancer cell colonies were counted visually under an inverted microscope (Motic AE31) after 10 days of incubation at 37°C in normoxia.

ECM-REMODELLING ASSAY: to assess force-mediated matrix remodelling, CAFs were uniformly dispersed in 300 µl of collagen I lattices (in volume%: 38% rat tail tendon collagen I (1.25 mg/ml, Biomatrix), 14% $NaHCO_3$ (15,6 mg/ml, Sigma-Aldrich, Bornem, Belgium), 1% NaOH (1M) and 47% DMEM/F12 (Gibco, Invitrogen) containing 250,000 cells/ml CAFs) and seeded in a 24-well plate (300 µl/well, Corning). Once the gel was solidified, the cells were maintained in CAF medium. Gel contraction was monitored daily for 4 days, by taking photographs of the gels. To obtain the gel contraction value, the relative diameters of the well and the gel were measured using NIH ImageJ software, and the percentage of contraction was calculated using the formula (100% - gel area/well area%) (Calvo et al., 2013; Tomasek et al., 1992).

EXTRACELLULLAR MATRIX SYNTHESIS: 350,000 MMTV-PyMT cancer cells or CAFs were seeded in 6-well plates in plating or CAF medium, respectively, supplemented with 5 mCi/ml [^{3}H]-L-proline (PerkinElmer) and 50 µg/ml ascorbic acid which was refreshed every second day. At day 8, cancer cells or CAFs were denudated with pre-warmed extraction buffer (20 mM NH_4OH, 0.5% Triton X-100 in PBS). The remaining residues of cells were digested with 10 µg/ml DNase I (Roche, Vilvoorde, Belgium) in PBS^+ (containing calcium and magnesium). Thereafter, the remaining matrix was collected in lysis buffer (4% SDS, 0.1 M Tris-HCl, 0.1 M DTT), and equal volumes were counted in liquid scintillation

buffer. For imaging purposes, the matrices, after denudation of the cells, were washed twice with PBS^+ and were stored at 4°C in PBS^+ or used immediately for immunostaining of collagen I.

CAF ACTIVATION ASSAY: Lung fibroblasts were seeded into a 6-well culture plate at a density of 200,000 cells per well. 24 hours after seeding, the culture medium was aspirated and the cells were washed with PBS. Serum-free control or MMTV-PyMT cancer cell conditioned medium (see above) supplemented with or without 5 µg/ml polyclonal TGF-β-neutralizing antibody (R&D Systems) was added to the experimental wells and the cells were further cultured for 8 days. The medium was refreshed every third day. On day 8, the cultures were lysed for RNA preparation for expression analysis of activation markers, or the cells were reseeded for proliferation assessment.

6. RNA ANALYSIS

RNA EXTRACTION AND cDNA SYNTHESIS: RNA was extracted from cells or tissue using a premade kit (PureLink RNA Mini Kit, Invitrogen), according to the manufacturer's instructions. One microgram of total RNA was used for reverse transcription with the QuantiTect Reverse Transcription Kit (Qiagen).

EC ISOLATION FOR VALIDATION OF KNOCKDOWN EFFICIENCY: EC were isolated from the lungs of $PyMT^{Tie2\text{-}WT}$, $PyMT^{Tie2\text{-}HE}$, and tamoxifen treated $PyMT^{Cdh5\text{-}WT}$ and $PyMT^{Cdh5\text{-}HE}$ mice as described before (Mazzone et al., 2009). Briefly, mice were sacrificed by cervical dislocation and lungs were harvested. After a wash in PBS, lungs were minced in RPMI medium containing 0.1% collagenase type I and incubated for 1 h at 37°C with gentle agitation. The digested tissue was centrifuged for 5 min at 1200 rpm, resuspended in RPMI medium containing 5% FBS and filtered by a 40 µm-pore size mesh. Filtered cells were incubated with magnetic beads previously coated with rat anti-CD31 (BD,Pharmingen), negative selection for $CD45^+$ cells was performed using magnetic beads previously

coated with rat anti-CD45 (BD,Pharmingen). $CD31^+$ ECs were selected under magnetic filed. Cell purity was assessed by qRT-PCR for *Cdh5*, *Cd31*, *VegfR2*, *Cd105*, *Pdgfrβ*, *Cd45*, *Vim*, *Sm22a*. $CD31^+$ ECs were used for assessment of *Egln1* knockdown efficiency by qRT-PCR in $PyMT^{Tie2\text{-}WT}$, $PyMT^{Tie2\text{-}HE}$, $PyMT^{Cdh5\text{-}WT}$ and $PyMT^{Cdh5\text{-}HE}$ mice.

QUANTITATIVE REVERSE TRANSCRIPTION PCR: RNA Quantitative reverse transcription (qRT)-PCR was performed using TaqMan Fast Universal PCR Master Mix (Applied Biosystems) and in-house-designed primers and probes or premade primer sets (Applied Biosystems and Integrated DNA Technologies). Primer sequences or premade primer set ID numbers are listed in tables 3 and 4. Analyses were performed using ABI7500 Fast Real-Time PCR System (Applied Biosystems). Gene transcription was calculated as the number of mRNA copies relative to the number of mRNA copies of the housekeeping gene hypoxanthine guanine phosphoribosyl transferase (*Hprt*).

Table 3. List of primers, used for qRT-PCR

Gene	Probe	Forward	Reverse
Egln1	ACG-AAA-GCC-ATG-GTT-GCT-TGT-TAC-CCA	GCT-GGG-CAA-CTA-CAG-GAT-AAA-C	CAT-AGC-CTG-TTC-GTT-GCC-T
Pymt	/56-FAM/AGAATCAGA/ZEN/CCC TCCCATGGACTCA/3IABkFQ/	GAA-CAA-GTA-CCC-CAG-CTC-ATC	CAT-TCT-CTG-ACT-CGC-ATC-TAG-G

Table 4. List of commercially available primers, used for qRT-PCR

Gene	Manufacturer	Sequence ID
Hprt	Integrated DNA Technologies	Mm.PT.42.12662529
E-Cadherin	Applied Biosystems	Mm00486906_m1
N-Cadherin	Applied Biosystems	Mm00483213_m1
Egln1	Integrated DNA Technologies	Mm.PT.51.8105240

Twist1	Applied Biosystems	Mm00442036_m1
Vimentin	Applied Biosystems	Mm00449201_m1
Occludin	Applied Biosystems	Mm00500907_m1
Zonula Occludens Protein-1	Applied Biosystems	Mm00493699_m1
Cytokeratin 8	Applied Biosystems	Mm00835759_m1
PDGFRα	Applied Biosystems	Mm01205760_m1
Fsp-1	Applied Biosystems	Mm00803371_m1
Lox	Applied Biosystems	Mm00495386_m1
Mmp2	Applied Biosystems	Mm00439506_m1
Mmp9	Applied Biosystems	Mm00442991_m1
Vegf-A	Applied Biosystems	Mm00437306_m1
Vegf-B	Applied Biosystems	Mm00442102_m1
Sele	Applied Biosystems	Mm00441278_m1
Vcam	Applied Biosystems	Mm01320970_m1
Plgf	Applied Biosystems	Mm00435613_m1
Ang2	Applied Biosystems	Mm00545822-m1

7. PROTEIN ANALYSIS

IMMUNOBLOT ANALYSIS: Protein extraction and immunoblot analysis were performed using a modified Laemmli sample buffer (125 mM Tris-HCl, pH 6.8 buffer containing 2% SDS and 20% glycerol) (Carmeliet et al., 2001) or using RIPA buffer in the presence of protease and phosphatase inhibitors (Roche, Vilvoorde, Belgium). Lysates were separated by SDS-PAGE under reducing conditions, the protein was transferred to a nitrocellulose or PVDF membrane,

and analyzed by immunoblotting. Primary antibodies used were E-cadherin (Novus Biologicals), N-cadherin (BD Pharmingen, Erembodegem, Belgium), fibronectin (Sigma-Aldrich Bornem, Belgium), α-actin (Cell Signaling Technology, Bioké, Leiden, the Netherlands), fibronectin (Sigma-Aldrich Bornem, Belgium), lamin A/C (Cell Signaling Technology, Bioké, Leiden, the Netherlands), and β-actin (Cell Signaling Technology, Bioké, Leiden, the Netherlands). Appropriate secondary antibodies were from Dako (Enschede, the Netherlands). Signal was detected using the ECL system (Amersham Biosciences, GE Healthcare, Diegem, Belgium) according to the manufacturer's instructions. Quantifications were done by densitometry of the bands using the NIH ImageJ software.

ELISA: Tumor cell conditioned medium was prepared as described above. The conditioned medium (5 ml) was concentrated using Centricon tubes (Vivaspin 20, Sartorius) and 100 µl was used to quantify TGF-β1 levels. The TGF-β1 level in tumor extracts (prepared as described above) or in the concentrated conditioned medium was determined using a sandwich ELISA kit (Quantikine ELISA, R&D Systems), according to the manufacturers' instructions.

8. HISTOLOGY, IMMUNOSTAININGS AND MORPHOMETRIC ANALYSES

All methods for histology and immunostaining have been performed as described by *Fischer et al.* (Fischer et al., 2007).

CELLS AND TISSUE PREPARATION: Cell cultures were fixed in 4% paraformaldehyde (PFA) for 10 min at 37°C. Mouse tissue samples were immediately frozen in OCT compound (for 7 µm and 40 µm serial sections) or fixed in 4% PFA overnight at 4°C, dehydrated and embedded in paraffin (for 7 µm serial sections).

STAININGS: Immunostainings were performed using the following primary antibodies: anti-CD105 and anti-PDGFRα (R&D systems, Minneapolis, MN,

USA), anti-α-smooth muscle actin-Cy3 (Sigma-Aldrich Bornem, Belgium), anti-PHH3 (from Cell Signaling Technology, Bioké, Leiden, the Netherlands), anti-S100a4 (Dako, Heverlee, Belgium), and anti-collagen I (Abcam, Cambridge, United Kingdom). Sections were then incubated with the appropriate fluorescently conjugated secondary antibodies (Alexa 488 or 546, Molecular Probes®, Invitrogen, Life Technologies, Ghent, Belgium) or with peroxidase-labeled IgGs (Dako, Heverlee, Belgium), followed by amplification with the proper tyramide signal amplification systems when needed (Perkin Elmer, Life Sciences, Zaventem, Belgium). Nuclei were counterstained with DAPI (Molecular Probes®, Invitrogen, Life Technologies, Ghent, Belgium). H&E or Harris Haematoxylin (HH) staining and Picro Sirius Red staining of paraffin sections was done using standard protocols. Whole mount carmine alum staining of mammary glands was done as detailed above.

MORPHOMETRIC ANALYSES: For morphometric analyses, mosaic pictures of the whole tumor or 15-20 random optical fields (20x or 40x magnification) per tumor section were taken by a Zeiss Axioplan upright microscope or Leica DMI 6000 B inverted microscope (Leica Microsystems, Mannheim, Germany), respectively and analyzed using the NIH ImageJ or Leica MM AF powered by MetaMorph ® analysis software. Confocal imaging was performed using a Zeiss LSM 510 Meta NLO or Zeiss LSM 780 confocal microscope (Carl Zeiss, Munich, Germany). Polarized light microscopy (Leica DMRB microscope) was used to visualize the birefringence of Picro Sirius Red stained collagen to distinguish between thin and cross-linked thick collagen fibres.

SCANNING ELECTRON MICROSCOPY: Small tumor pieces were fixed overnight in 2.5% glutaraldehyde in 0.1 M Na-cacodylate buffer, pH 7.2-7.4 at 4 °C. Three rinses of 30 min with 0.1 M Na-cacodylate buffer were followed by vibratome sectioning (HM 650V, Thermo Scientific Microm, Loughborough, UK) of the

tissues (400 µm) embedded in 5% low melting temperature SeaPlaque ® agarose (Lonza, Rockland, ME, USA). Sections were postfixed with 2% osmiumtetroxide in 0.1 M Na-cacodylate buffer for 2 hrs at room temperature. Following dehydration in a graded ethanol series (30-50-70-100%) the organs were critical-point dried (BAL-TEC CPD 030, Balzers, Germany). Critical-point dried tissues were mounted on stubs with double-sided adhesive carbon tape. The stubs were coated with gold (SPI-MODULE^{TM} Sputter Coater, SPI Supplies, West Chester, PA, USA). Images were obtained with a scanning electron microscope (JEOL JSM-6360, Tokyo, Japan) at 10 kV (KU Leuven, Molecular Physiology of Plants and Micro-organisms Section). I am thankful to Stefan Vinckier from the VIB Vesalius Research Center for assistance in SEM analysis.

9. STATISTICS

Data represent mean ± SEM of representative experiments unless otherwise stated. Each experiment was performed at least 3 times, each showing statistical significance using the appropriate statistical test. Unless otherwise indicated, statistical significance was calculated by standard two-sided t-test with F-testing to confirm equality of variance (Prism v6.0b). When the two populations have different variance two-sided t-test with Welch's correction was used (Prism v6.0b). When inter-experimental variability was large in *in vitro* experiments performed with isolated cells, mixed model statistics (SAS statistical software version 9.3) was used with experiment (i.e. donor mouse) as random factor to correct for variation between individual mice. $p < 0.05$ was considered significant.

CHAPTER IV

RESULTS

PHD2 HAPLODEFICIENCY DOES NOT AFFECT BREAST CANCER PROGRESSION

To explore the consequences of PHD2 haplodeficiency in tumor and stromal cells on breast cancer, PHD2 haplodeficient ($PHD2^{+/-}$) mice were intercrossed with mice expressing the PyMT oncoprotein under control of the MMTV-long terminal repeat (LTR) promoter (MMTV-PyMT), a model that spontaneously develops metastatic mammary gland tumors and recapitulates many features of human ductal breast cancer (Lin et al., 2003). In all experiments, $PHD2^{+/+}$:MMTV-PyMT mice (referred to as $PyMT^{+/+}$) were compared with $PHD2^{+/-}$:MMTV-PyMT (referred to as $PyMT^{+/-}$) littermates.

Tumor onset at 4 weeks of age was comparable in $PyMT^{+/+}$ and $PyMT^{+/-}$ mice. In both genotypes, the primary tumors enlarged from 4 to 16 weeks, however without differences in growth rate, as analyzed by measuring tumor size and end-stage weight (Figure 1A,B). Breast cancers developed at comparable (full) penetrance in both genotypes. Morphometric analysis showed no differences in the number of tumor nodules and the area of intraepithelial neoplastic foci at early stages of tumor progression (4 weeks) (Figure 1C-E). Analysis of proliferation, by immunostaining for PHH3, revealed no differences in tumor cell proliferation in tumors at different stages of progression and age (Figure 1F). Also, [^{3}H]-thymidine incorporation assays showed no difference in the proliferation rates of tumor cells isolated from $PyMT^{+/+}$ and $PyMT^{+/-}$ mice at end stage (16 weeks) (Figure 1G).

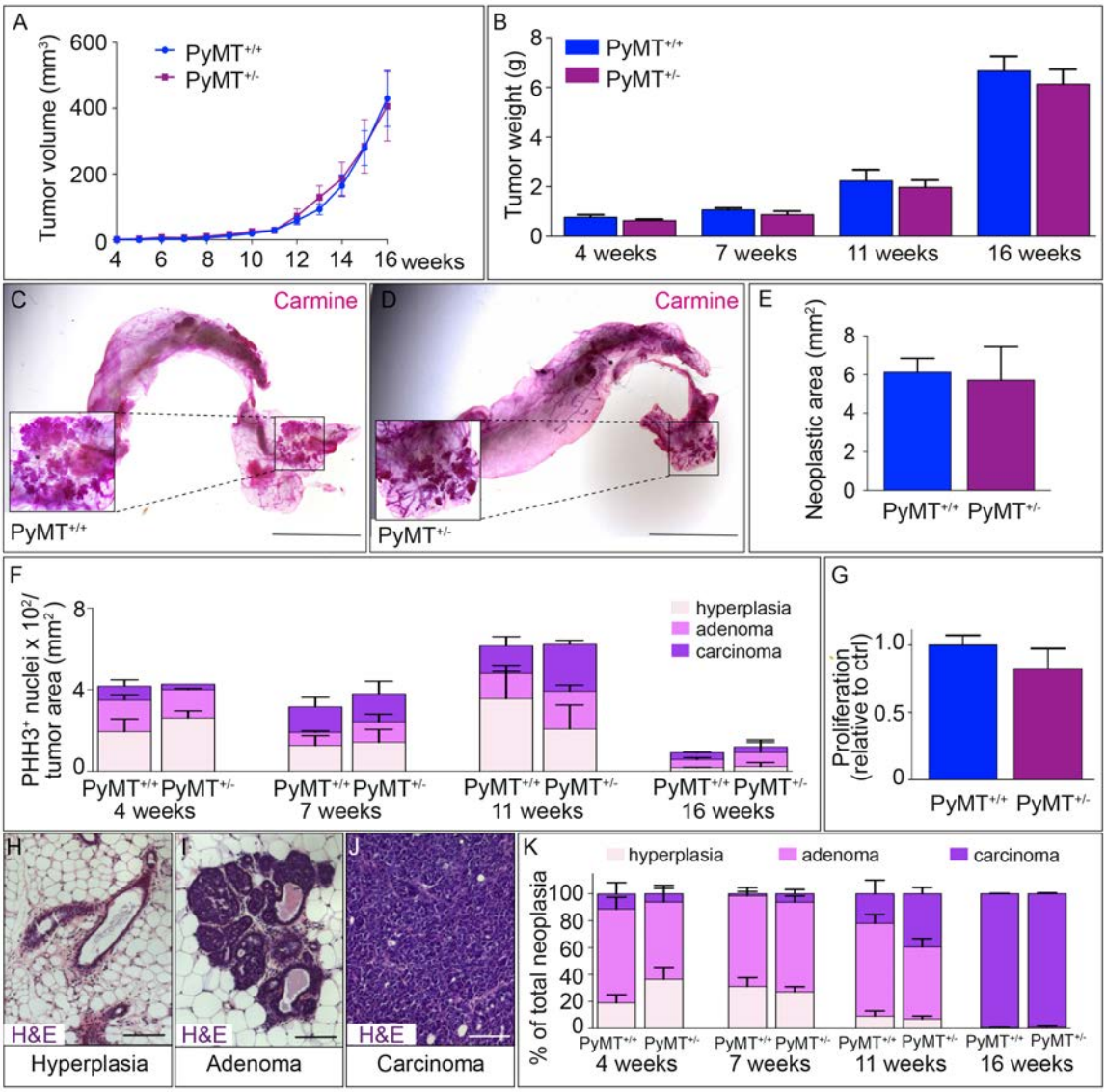

FIGURE 1: EFFECT OF GLOBAL PHD2 HAPLODEFICIENCY ON TUMOR GROWTH AND PROGRESSION
A, Growth curve of individual tumors in PyMT$^{+/+}$ and PyMT$^{+/-}$ mice (n = 23-28 ; p = ns). **B**, Tumor weight of tumors in PyMT$^{+/+}$ and PyMT$^{+/-}$ mice at 4, 7, 11 and 16 weeks of age (n > 6; p = ns). **C-E,** Carmine-stained inguinal mammary glands from 4 week old PyMT$^{+/+}$ (C) and PyMT$^{+/-}$ (D) mice. Panel E: quantification of neoplastic area (n = 3-4; p = ns). **F,** Quantification of the PHH3^{+} area on tumors from 4, 7, 11 and 16 week old PyMT$^{+/+}$ and PyMT$^{+/-}$ mice (n = 3-4; p = ns). **G**, Proliferation ([^{3}H]-thymidine incorporation assay) of cancer cells isolated from 16 week old PyMT$^{+/+}$ and PyMT$^{+/-}$ mice, expressed as relative values to control (n = 6; p = ns). **H-J**, H&E staining of tumors in PyMT mice representing hyperplasia (H), adenoma (I) and carcinoma (J). **K,** Quantification of hyperplastic, adenoma or carcinoma lesion area on tumors from 4, 7, 11 and 16 week old PyMT$^{+/+}$ and PyMT$^{+/-}$ mice (n = 3-7; p = ns). Bar: 5 mm (C,D), 100 µm (H-J). All quantitative data are mean ± SEM.

Three distinct stages of tumor progression can be identified in PyMT-induced mammary gland tumors: hyperplasia, adenoma, and carcinoma (Figure 1H-J).

Consistent with previous reports (Lin et al., 2003), PyMT tumors did not develop as homogeneous populations of cancer cells within a single stage, but rather consisted of a heterogeneous mix of cancer cells at various stages (Figure 1K). Thus, tumors at 4 weeks contained not only hyperplastic lesions, but also cancer cells at adenoma and carcinoma stages were already present. Tumor progression to adenoma, and then carcinoma was also not affected by PHD2 haplodeficiency as largely similar fractions of hyperplastic, adenoma and carcinoma lesions were found in $PyMT^{+/+}$ and $PyMT^{+/-}$ mice at 4, 7, 11 and 16 weeks (Figure 1K). At end stage (16 weeks), carcinoma cells prevailed in tumors of either genotype (Figure 1K).

Thus, PHD2 haplodeficiency did not alter PyMT tumor progression and did not change the tumor phenotype.

PHD2 HAPLODEFICIENCY REDUCES METASTASIS

The PyMT transgenic mice exhibit a high frequency of pulmonary metastasis. Already at 11 weeks, ~43% of mice (8 of 15 $PyMT^{+/+}$ mice *versus* 5 of 15 $PyMT^{+/-}$ mice; p = ns; Fischer's exact test) developed macroscopically visible metastatic pulmonary nodules, but on average, only one nodule was detected per mouse. However, by 16 weeks, all (22 of 22) $PyMT^{+/+}$ mice developed numerous large pulmonary metastases, while only 74% (17 of 23; * p = 0.0216; Fischer's exact test) of $PyMT^{+/-}$ mice formed pulmonary metastases which were also fewer in number (Figure 2A-C). Also the metastatic index, *i.e.* the number of metastases normalized to tumor weight, was reduced in $PyMT^{+/-}$ mice (Figure 2D). We also analyzed the extent of micro- and macro-metastasis by measuring the area of metastasis (expressed as % of total lung area) on cross sections of lungs from $PyMT^{+/+}$ and $PyMT^{+/-}$ mice at 11 and 16 weeks. This analysis revealed that already at 11 weeks $PyMT^{+/-}$ mice showed a trend to reduced metastatic area as

compared to PyMT$^{+/+}$ mice, and that this difference became even more pronounced at 16 weeks (Figure 2E).

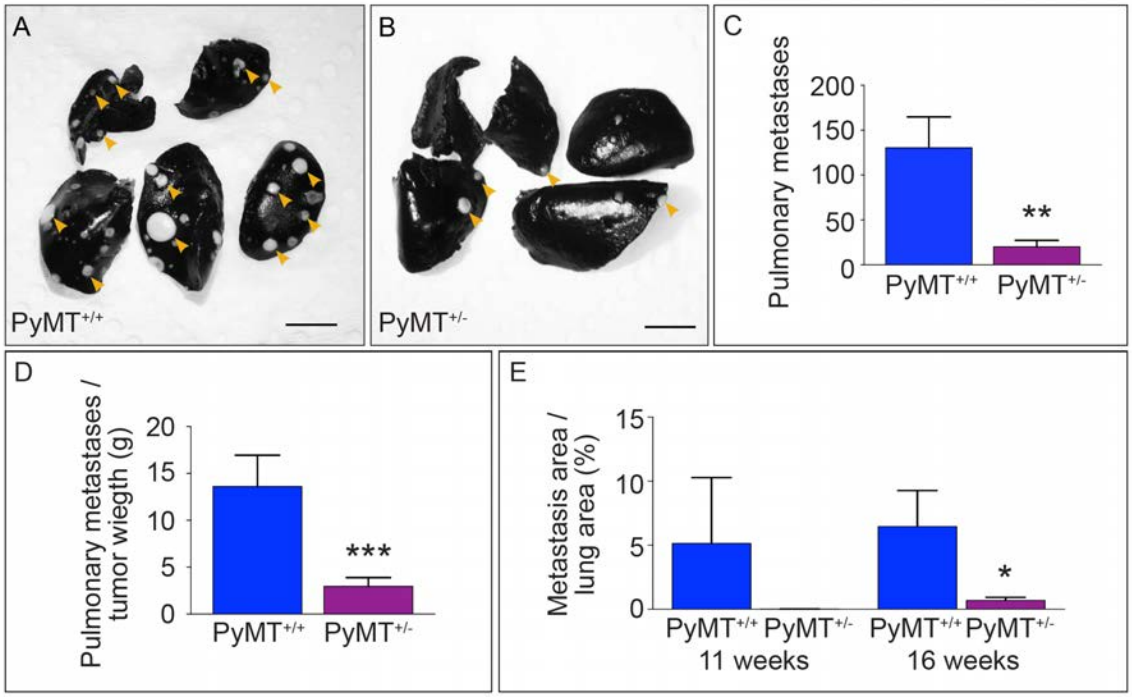

FIGURE 2: EFFECT OF GLOBAL PHD2 HAPLODEFICIENCY ON METASTASIS.
A,B, Pulmonary metastatic nodules (arrowheads) in 16 week old PyMT$^{+/+}$ and PyMT$^{+/-}$ mice, visualized by Indian ink perfusion. **C,** Pulmonary metastases number in PyMT$^{+/+}$ and PyMT$^{+/-}$ tumor bearing 16 week old mice (n = 22-23; t-test with Welch's correction). **D,** Metastatic index (number of metastases corrected for tumor weigth) (n = 22-23; t-test with Welch's correction). **E,** Morphometric quantification of metastatic area on hemotoxylin and eosin (H&E)-stained lungs sections from PyMT$^{+/+}$ and PyMT$^{+/-}$ tumor bearing 11 and 16 week old mice (n = 4 for 11 week old mice; n = 28-33 for 16 week old mice; t-test with Welch's correction). Bar: 5 mm (A,B). All quantitative data are mean ± SEM. * $p < 0.05$, ** $p < 0.01$, *** $p < 0.001$.

PHD2 HAPLODEFICIENCY DOES NOT AFFECT LYMPHATIC DISSEMINATION

As cancer cells can enter the blood directly by intravasating into venous capillaries or indirectly via lymphatic vessels, it is important to first evaluate which pathway is impaired by PHD2 haplodeficiency as a route to egress from the primary site. In breast cancer, lymph nodes are often the first site to harbor metastases (Stacker et al., 2002). To assess whether PHD2 haplodeficiency affects cancer cell dissemination to lymph nodes, we evaluated the expression of cytokeratin 8 as a marker of cancer cells, in axillary and popliteal lymph nodes

(Figure 3A) from PyMT$^{+/+}$ and PyMT$^{+/-}$ mice at end stage. Inguinal lymph nodes were not analyzed considering that they are localized in the middle of mammary gland tissue. This analysis revealed no differences in metastatic dissemination to lymph nodes (Figure 3B-F). Lymphatic vessel development was minimal in PyMT tumors, and was also not different in the primary tumors of PyMT$^{+/+}$ and PyMT$^{+/-}$ mice at end stage, as assessed by LYVE-1 immunostaining (Figure 3G-I). We then explored whether PHD2 haplodeficiency impairs metastatic dissemination through hematogenous routes.

PHD2 HAPLODEFICIENCY REDUCES INTRAVASATION

Hematogenous metastasis is a complex process consisting of several steps. Therefore, we investigated which step of this metastatic process was impaired in PyMT$^{+/-}$ mice. As previous reports from the host lab showed that selective EC haplodeficiency of PHD2 impaired cancer cell intravasation, we first focused on this step. Determination of circulating tumor cells (CTCs) by RT-PCR analysis of the mRNA levels of cancer cell-specific markers (PyMT; cytokeratin 8 (*Krt8*), marker of luminal epithelial cells) in the peripheral blood revealed that fewer CTCs were present in PyMT$^{+/-}$ mice (Figure 3J,K). Since the number of CTCs is not only dependent on cancer cell intravasation, but is also determined by their survival in the blood, we analyzed cancer cell viability in non-adherent conditions (as is the case in the circulation). However, an *in vitro* clonogenic assay revealed a comparable viability of PyMT$^{+/+}$ and PyMT$^{+/-}$ cancer cells in these conditions (Figure 3L), implying that the reduction in CTCs could be explained by reduced intravasation.

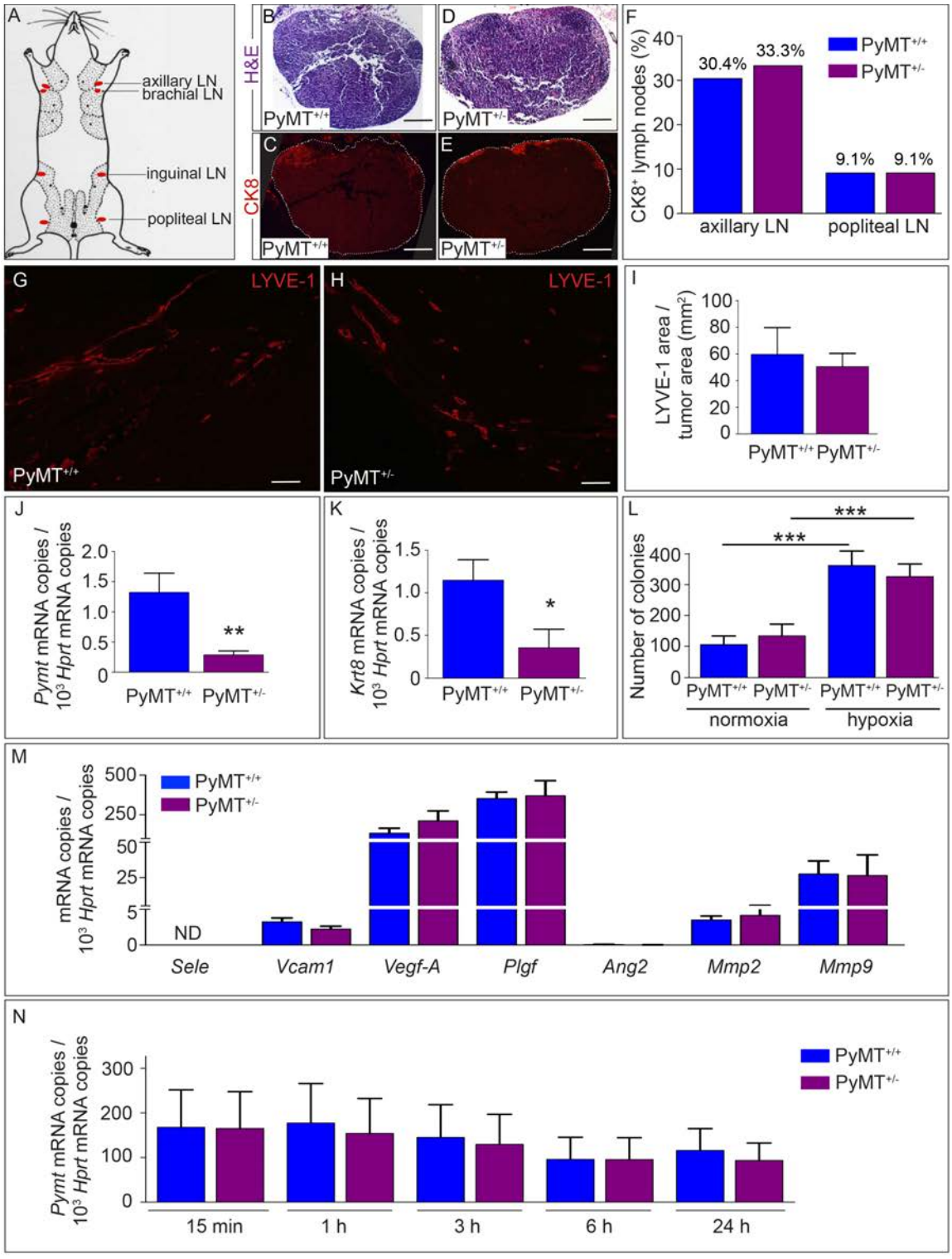

FIGURE 3: PHD2 HAPLODEFICIENCY EFFECT ON LYMPHATIC AND HEMATOGENOUS CANCER CELL DISSEMINATION

A, Schematic representation of the lymph nodes (LN), in red, in mouse. Mammary gland localization is annotated as dotted area. **B-F,** Representative images of axillary lymph nodes from 16 week old $PyMT^{+/+}$ (B,C) and $PyMT^{+/-}$ (D,E) mice stained with H&E or cytokeratin 8 (CK8; a marker of cancer cells). Panel F: Histogram showing LN metastasis frequencies in 16 week old $PyMT^{+/+}$ and $PyMT^{+/-}$ mice (n = 12-23 for axillary LN; n = 11-22 for popliteal LN; p = ns; Fisher's

exact test). **G-I,** Representative images of LYVE-1 staining on tumors from 16 week old PyMT$^{+/+}$ (G) and PyMT$^{+/-}$ (H) mice. Panel I: quantification of the LYVE-1^{+} area (n = 5; p = ns). **J,** RT-PCR analysis for *Pymt* in blood samples as a measure of the number of CTCs in PyMT$^{+/+}$ and PyMT$^{+/-}$ mice (n = 15-17; t-test with Welch's correction). **K**, RT-PCR analysis of *Krt8* mRNA levels in blood samples as a measure of circulating tumor cells in PyMT$^{+/+}$ and PyMT$^{+/-}$ tumor bearing mice (n = 10). **L,** Quantification of the number of colonies of PyMT$^{+/+}$ and PyMT$^{+/-}$ cancer cells grown in non-adherent conditions in normoxia or hypoxia (n = 4-5; p = ns). **M**, RT-PCR analysis of the mRNA levels of genes, involved in the various steps of cancer cell extravasation, including adhesion to the endothelium (*Sele*, *Vcam1*), permeabilization of the endothelial cell barrier (*Vegf-A*, *Plgf*, *Ang2*) and proteolytic matrix degradation (*Mmp2*, *Mmp9*), in PyMT$^{+/+}$ and PyMT$^{+/-}$ cancer cells (n = 5-6). ND, not detectable. *Sele*: E-selectin; *Vcam1*: Vascular adhesion molecule 1; *Ang2*: angiopoietin-2; *Mmp*: matrix metalloproteinase. **N**, RT-PCR analysis of *Pymt* mRNA levels in the lungs at the indicated times after intravenous injection of PyMT$^{+/+}$ and PyMT$^{+/-}$ cancer cells in recipient wild type mice, as a measure of cancer cell colonization (n = 10-12). Bar: 200 µm (B-E), 50 µm (G,H). All quantitative data are mean ± SEM. * $p < 0.05$, ** $p < 0.01$, *** $p < 0.001$.

We next examined whether the reduced metastasis of PyMT$^{+/-}$ tumors could also be partly attributable to a difference in cancer cell trapping in pulmonary vessels, extravasation or lodging. First, RT-PCR analysis of genes, involved in cancer cell extravasation, did not show changes in mRNA levels in PyMT$^{+/-}$ cancer cells that could explain the reduced metastasis of PyMT$^{+/-}$ mice (Figure 3M). Second, analysis of PyMT transcript levels in the lungs at 15 minutes, and at 1, 3, 6 and 24 hours after intravenous injection of PyMT$^{+/-}$ or PyMT$^{+/+}$ cancer cells in wild type (WT) recipient mice did not reveal significant differences (Figure 3N). Hence, PHD2 haplodeficiency did not affect cancer cell extravasation and colonization, but reduced their intravasation.

PHD2 HAPLODEFICIENCY DOES NOT AFFECT CANCER CELL-INTRINSIC INVASION

We then sought to explore the mechanism underlying the decrease in intravasation and metastasis of PyMT$^{+/-}$ tumors. For cancer cells to be able to intravasate, they must travel through the tumor matrix and breach the endothelial barrier, which requires an invasive behavior (van Zijl et al., 2011). We therefore analyzed whether PHD2 haplodeficiency impaired the invasive properties of cancer cells. These analyses were performed in both normoxic and hypoxic

conditions (48h at 0.5% O_2), given the occurrence of hypoxia in the tumor milieu. To invade the surrounding stroma, certain cancer cell types can undergo epithelial-to-mesenchymal transition (EMT), whereby they lose cell polarity and cell-cell adhesion, but acquire more invasive mesenchymal cell characteristics (Waldmeier et al., 2012). Hypoxia is one of the main regulators of EMT (Foubert et al., 2010; Gort et al., 2008; Yang et al., 2008) and thus a driver of invasive phenotype of cancer cells. Since PHD2 is a key regulator of HIF1α and HIF2α, we first analyzed HIF1α and HIF2α levels in nuclear and cytoplasmic fractions of isolated cancer cells from $PyMT^{+/+}$ and $PyMT^{+/-}$ mice. Consistent with the literature, PHD2 haplodeficiency (Figure 4A) increased HIF1α and HIF2α protein levels in both fractions of cancer cell lysates (Figure 4B-G). Similarly, hypoxia increased HIF1α and HIF2α protein levels, but PHD2 haplodeficiency did not further augment their levels under hypoxic conditions (Figure 4B-G).

Although PHD2 haplodeficiency increased pro-invasive HIF1α levels in the cancer cells (Figure 4B-D), isolated cancer cells from $PyMT^{+/+}$ and $PyMT^{+/-}$ mice had a typical epithelial cobblestone-like morphology, and did not show clear signs of EMT when cultured as a monolayer (Figure 5A,B).

Also, analysis of isolated tumor cells did not show any genotypic differences in immunoreactive levels of E-cadherin, N-cadherin and fibronectin or in the mRNA transcript levels of the junctional molecules N-cadherin (*Cdh2*), Vimentin (*Vim*) and zonula occludens (ZO-1, *Tjp1*), Occludin (*Ocln*), of the pro-EMT transcription factor *Twist1* and of the known pro-invasive factors *Mmp2* and *Mmp9* (Figure 3M; Figure 5C-E). Additionally, cancer cell migration or invasion, as analysed by scratch wound assay or 3D spheroids invasion embedded into a collagen I matrix, respectively, did not show genotypic differences neither in normoxia, nor in hypoxia (Figure 5F-K).

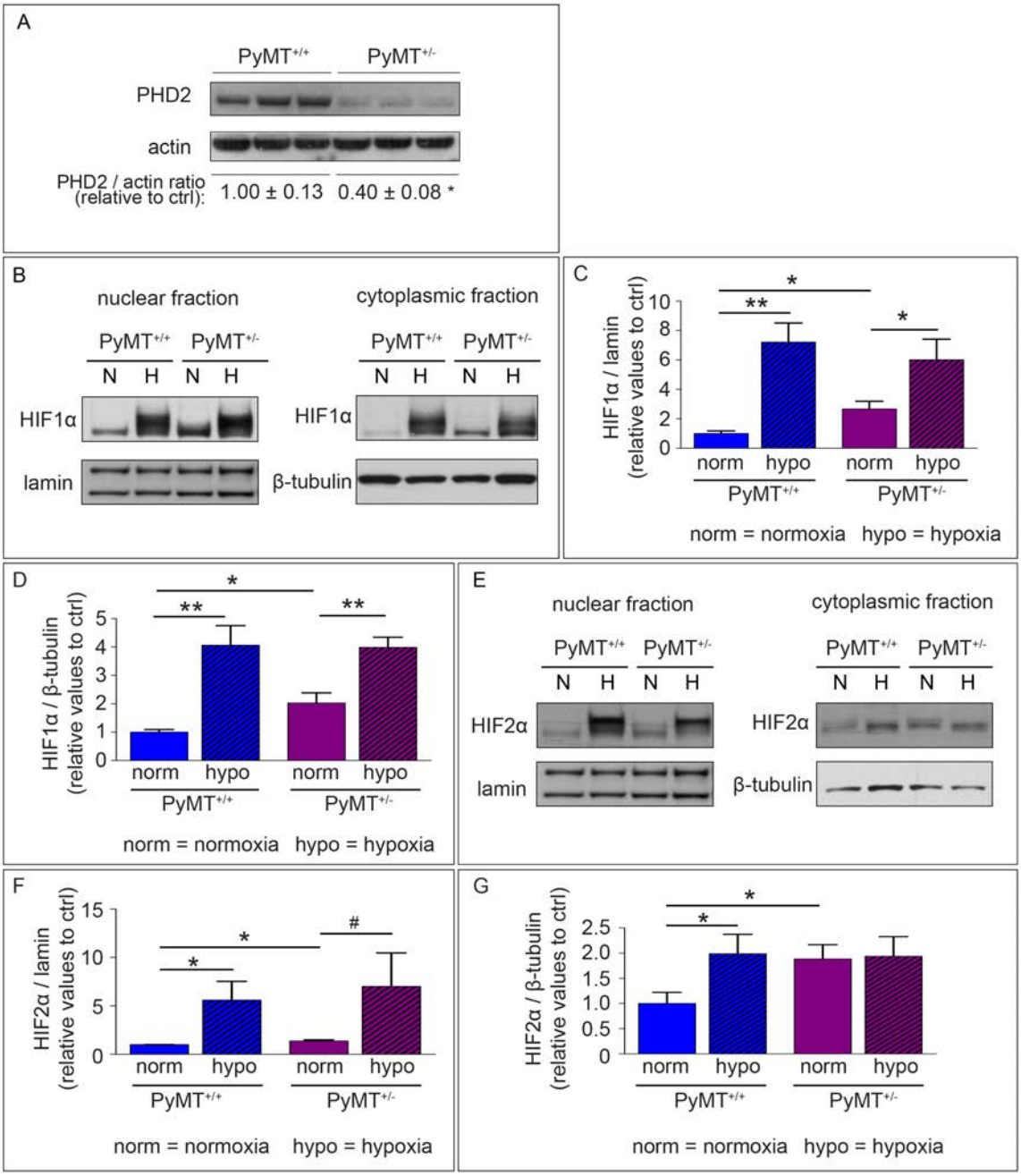

FIGURE 4: PHD2 HAPLODEFICIENCY INCREASES HIF1α AND HIF2α LEVELS IN CANCER CELLS.
A, Immunoblotting for PHD2 of total PyMT$^{+/+}$ and PyMT$^{+/-}$ cancer cell lysates. β-actin was used as loading control. Densitometric quantification is indicated (n = 4-6 independent experiments). **B-D,** Immunoblotting for HIF1α of nuclear and cytoplasmic lysates of PyMT$^{+/+}$ and PyMT$^{+/-}$ cancer cells cultured in normoxia (N) or hypoxia (H). β-tubulin or lamin was used as loading control. Panels C,D: Densitometric quantification relative to control (PyMT$^{+/+}$ normoxia) in nuclear (C; n = 5-6; t-test with Welch's correction) or cytoplasmic (D; n = 5-6; t-test with Welch's correction) fractions. **E-G,** Immunoblotting for HIF2α of nuclear and cytoplasmic PyMT$^{+/+}$ and PyMT$^{+/-}$ cancer cell lysates cultured in normoxia (N) or hypoxia (H). β-tubulin or lamin was used as loading control. Panels F,G: Densitometric quantification relative to control (PyMT$^{+/+}$ normoxia) in nuclear (F; n = 5-6; t-test with Welch's correction) or cytoplasmic (G; n = 5-6; t-test with Welch's correction) fractions. All quantitative data are mean ± SEM. * $p < 0.05$, ** $p < 0.01$, $^{\#}$ $p = 0.07$.

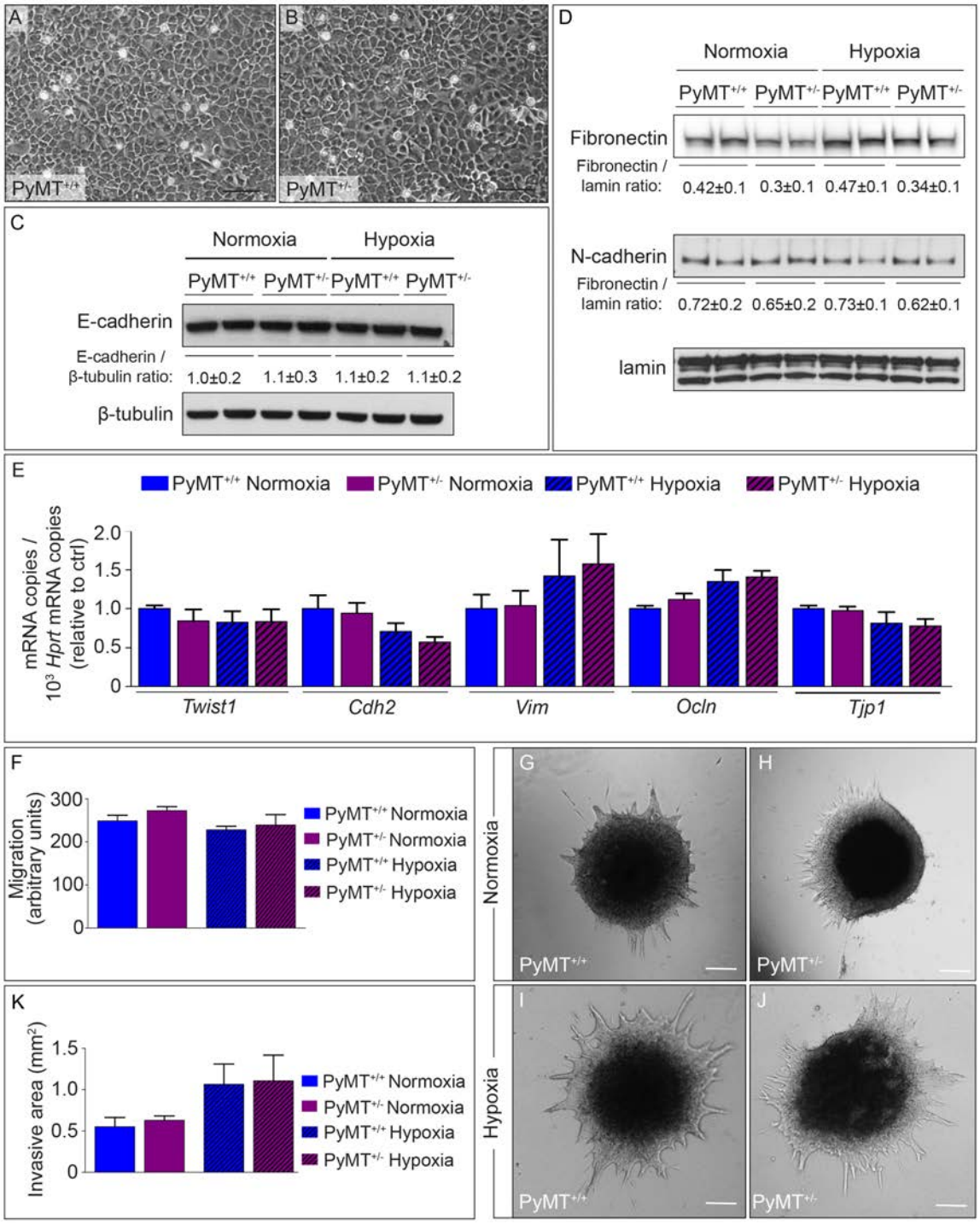

FIGURE 5: PHD2 HAPLODEFICIENCY DOES NOT AFFECT CANCER CELL INVASION

A,B, Representative images of monolayer of cancer cells isolated from PyMT$^{+/+}$ and PyMT$^{+/-}$ tumors at the end stage. **C,D,** Immunoblotting of EMT protein levels (E-cadherin (C), N-cadherin, fibronectin (D)) in PyMT$^{+/+}$ and PyMT$^{+/-}$ cancer cell lysates. β-tubulin or lamin was used as loading control. Densitometric quantification is indicated (n = 4-6 independent experiments; p = ns). **E,** RT-PCR analysis of EMT genes in PyMT$^{+/+}$ and PyMT$^{+/-}$ cancer cells (n = 3 independent experiments; p = ns). **F,** Scratch wound assay: analysis of PyMT$^{+/+}$ and PyMT$^{+/-}$ cancer cell migration in normoxia or hypoxia (n = 3; p = ns). **G-J,** Cancer cell spheroid invasion assay: analysis of collective invasion of PyMT$^{+/+}$ (G,I) and PyMT$^{+/-}$ (H,J) cancer cells into a collagen I

matrix in normoxia (G,H) or hypoxia (I,J). Note that cancer cells invade collectively as sheets with emerging sprouts. Panel K shows the morphometric quantification of the area of the entire invasive spheroid (see methods) (n = 3-5 independent experiments; p = ns). Bar: 75 μm (A,B), 200 μm (G-J). All quantitative data are mean ± SEM.

Despite there being no changes in cancer cell-intrinsic invasive behavior, and previous studies that documented only minimal EMT in malignant epithelial cells from the MMTV-PyMT tumor model, these cancer cells are still capable of disseminating (Trimboli et al., 2008; Waldmeier et al., 2012). We therefore investigated additional mechanisms by which PHD2 haplodeficiency might reduce intravasation and dissemination.

PHD2 HAPLODEFICIENCY DECREASES INTRATUMORAL HYPOXIA

Since hypoxia promotes tumor cell invasion and metastasis (De Bock et al., 2011), we assessed the level of intratumoral hypoxia by staining sections of tumors at various stages for the hypoxia marker pimonizadole. At early stages (up to 11 weeks), only a minimal level of hypoxia was present in $PyMT^{+/+}$ tumors (Figure 6A). In agreement with reports that breast cancer cells progressively outgrow their vascular supply, hypoxia levels substantially increased during the last weeks of $PyMT^{+/+}$ tumor progression, when tumors enlarged exponentially (Figure 6A). In $PyMT^{+/-}$ tumors, hypoxia levels tended to be lower at early stages, and were significantly reduced by 16 weeks (Figure 6A-C). However, immunoblotting revealed that HIF1α protein levels were similar in end-stage $PyMT^{+/-}$ and $PyMT^{+/+}$ tumors (Figure 6D). Likely, the environmental level of hypoxia-induced HIF1α protein was balanced by genetic programming in PHD2 haplodeficient tumor cells (Figure 4B-D). Thus, the reduction in environmental hypoxia coincided with the reduction in metastasis, suggesting a possible causal link.

PHD2 HAPLODEFICIENCY DOES NOT AFFECT VESSEL DENSITY

Given that endothelial cell haplodefiency of PHD2 improves tumor oxygenation by inducing normalization of tumor vessels in xenografts models (Leite de Oliveira et al., 2012; Mazzone et al., 2009), we explored whether reduced intratumoral hypoxia and impaired intravasation in MMTV-PyMT tumors also is related to tumor vessel normalization. We, thus, examined the vascular network at different stages to assess whether decreased intratumoral hypoxia in $PyMT^{+/-}$ mice is a result of increased vascularization and / or improved functionality.

In the MMTV-PyMT tumor model blood vessels co-evolve with tumor progression to meet the increasing demand for oxygen and nutrients, required for tumor growth. Initially, when the tumor is small, diffusion is the major way to support its metabolic needs. However, diffusion distance is restricted, e.g. for oxygen it is limited to the distance of 20-200 µm (Carmeliet and Jain, 2000; Pries and Secomb, 2014). Thus, when tumors have grown beyond the size of 1-2 mm in diameter the development of new tumor vasculature is required to support the increased metabolic demands (Bergers and Benjamin, 2003). The induction of this vasculature is termed the angiogenic switch and can occur at various stages of tumor progression, depending on the tumor type and the environment. By analyzing vessel number and perfusion at 4, 7, 11 and 16 weeks we were able to determine at which stage the onset of the angiogenic switch occurs. We also analyzed whether PHD2 haplodeficiency provided a functional advantage from the start of tumorigenesis or whether this only occured in the course of tumor progression.

Double immunostaining for CD105 and cytokeratin 8 of tumor sections from $PyMT^{+/-}$ and $PyMT^{+/+}$ mice at 4, 7, 11 and 16 weeks of age were used to analyze vessel area as a percent of tumor area (Figure 6E-M).

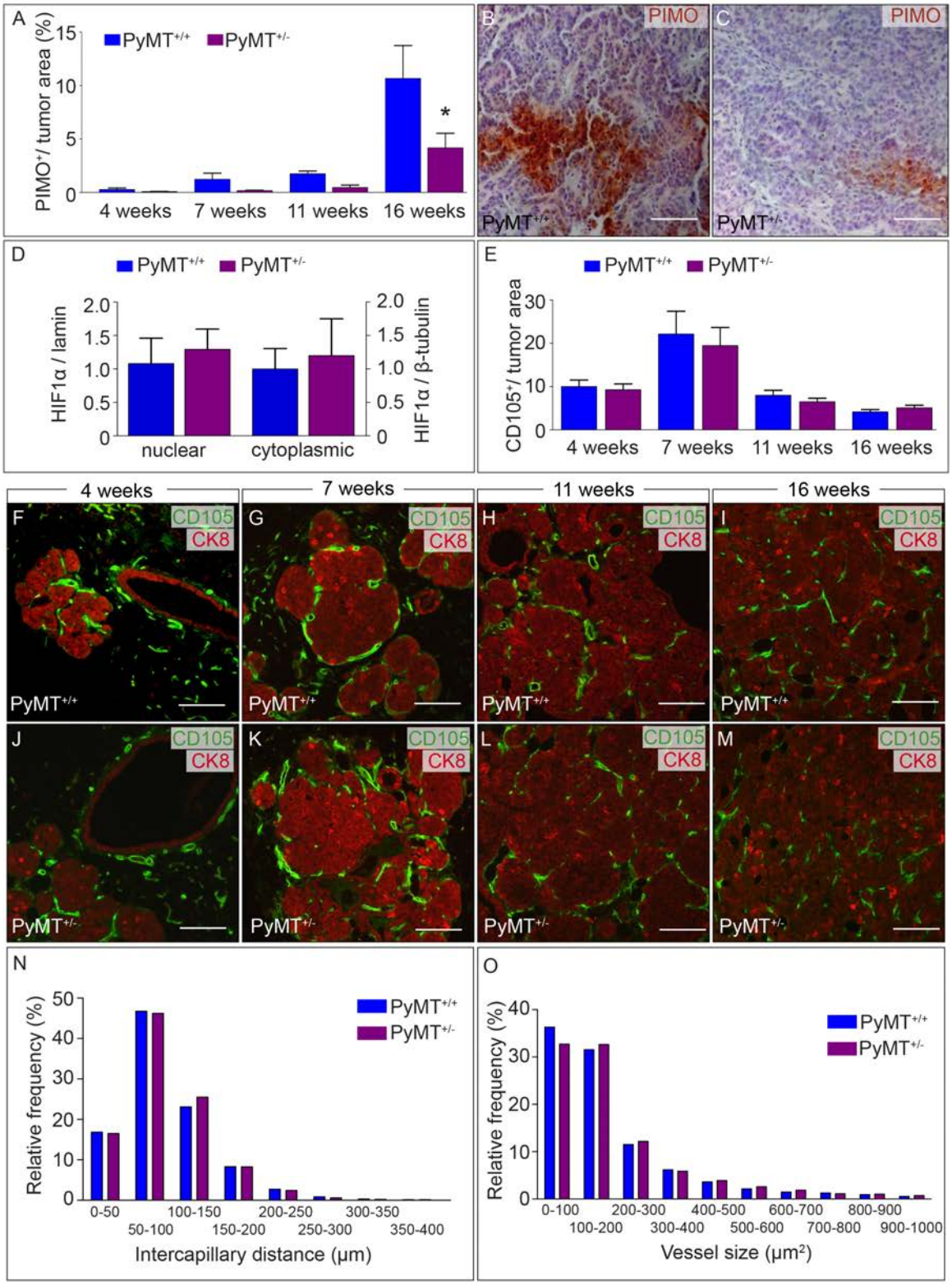

FIGURE 6: PHD2 HAPLODEFICIENCY DECREASES INTRATUMORAL HYPOXIA BUT DOES NOT AFFECT VESSEL DENSITY

A-C, Quantification of $PIMO^{+}$ hypoxic tumor area (% of total) in tumors from $PyMT^{+/+}$ and $PyMT^{+/-}$ mice at 4, 7, 11 and 16 weeks of age (n = 6-15). Representative micrographs of PIMO staining (brown) in end stage $PyMT^{+/+}$ (B) and $PyMT^{+/-}$ (C) tumors. **D,** Densitometric quantification of

HIF1α immunoblotting in nuclear or cytoplasmic fractions of $PyMT^{+/+}$ and $PyMT^{+/-}$ tumor lysates at 16 weeks of tumor progression (n = 4-6). Lamin (for nuclear fraction) or β-tubulin (for cytoplasmic fraction) was used as loading control. **E-M,** Tumors from $PyMT^{+/+}$ and $PyMT^{+/-}$ mice at 4, 7, 11 and 16 weeks of age were immunostained for CD105 and cytokeratin 8 (CK8) (F-M) and quantified for vessel area expressed as a percent of tumor area (E) (n = 8-11). **N,** Histogram of intercapillary distance, revealing a comparable distribution of vessel intercapillary distance in $PyMT^{+/+}$ and $PyMT^{+/-}$ tumors of 16 week old mice. **O**, Histogram of vessel size, revealing a comparable distribution of vessel size in $PyMT^{+/+}$ and $PyMT^{+/-}$ tumors of 16 week old mice. Bar: 50 µm (B,C), 100 µm (F-M). All quantitative data are mean ± SEM. * $p < 0.05$.

This analysis revealed that the increase in vessel number, relative to tumor area, was highest at 7 weeks (Figure 6E), suggesting that the 'angiogenic switch' preceded the progression to carcinoma stage. However, there were no genotypic differences in tumor vessel area and intercapillary distance (Figures 6E-N). Also, the distribution of tumor vessels in $PyMT^{+/-}$ and $PyMT^{+/+}$ tumors from 16 weeks old mice according to their size was overlapping in both genotypes, indicating that there was no shift from small to large vessels (or vice versa) (Figures 6O). As lack of the changes in vessel density could not explain reduced hypoxia, we then explored whether PHD2 haplodeficiency improved vessel function.

PHD2 HAPLODEFICIENCY IMPROVES VESSEL FUNCTION AND STRUCTURE

A hallmark of many cancers is a structurally and functionally abnormal vasculature, which reduces tumor perfusion and enhances hypoxia, stimulating cancer cell invasion and metastasis (De Bock et al., 2011). To analyze vessel functionality, we injected 4, 7, 11 and 16 week old $PyMT^{+/+}$ and $PyMT^{+/-}$ mice with lectin-FITC to label perfused vessels and co-stained the tumor sections for CD31 to identify all vessels (perfused and non-perfused) so that the percentage of perfused vessels could be determined. This analysis revealed that in the control tumors already at 4 weeks only 43.5% of the vessels were perfused and vessel perfusion gradually decreased with tumor progression to 14.6% at 16 weeks (Figure 7A-I). Compared to $PyMT^{+/+}$ tumors, PHD2 haplodeficiency increased the

fraction of perfused lectin-FITC$^+$ CD31$^+$ vessels already from 7 weeks onwards (Figure 7A-I). At the early stage (4 weeks), the fraction of perfused lectin-FITC$^+$ CD31$^+$ vessels was modestly, but not significantly increased in PyMT$^{+/-}$ tumors (Figure 7A,E,I, p = 0.147).

As perivascular stromal cells, pericytes and mural cells provide structural support to blood vessels and regulate their stability and function, we evaluated whether differences in vessel maturation underlined the improved function of tumor vessels in PyMT$^{+/-}$ mice. To this end we double-stained tumor sections from 16 week old PyMT$^{+/+}$ and PyMT$^{+/-}$ mice for the mural cell marker α-smooth muscle actin (αSMA) and the endothelial marker CD31. Analysis of vessel coverage with pericytes (expressed as a percent of total CD31) revealed more αSMA$^+$ cell - covered tumor vessels in PyMT$^{+/-}$ tumors (Figure 7J,K).

A major obstacle to blood-borne transport in tumors is their heterogeneous microvascular architecture. Tumors are known to contain many tortuous vessel, shunts, vascular loops and widely variable intervascular distance. Local heterogeneity in the blood flow and locally increased resistance to blood flow due to vessel tortuosity limits the blood-borne transport and thus reduces tumor perfusion (Baish et al., 1996; Stylianopoulos and Jain, 2013). Analysis of whole mount stainings of thick tumor sections for CD31 revealed that the three-dimensional architecture of the tumor vessels was comparable in PyMT$^{+/+}$ and PyMT$^{+/-}$ tumors isolated from 16 week old mice (Figure 7L,M). However, similar to what was already observed in xenograft tumor models (Mazzone et al., 2009), PHD2 haplodeficiency improved endothelial cell lining in 16 weeks PyMT$^{+/-}$ tumors as analysed by scanning electron microscopy analysis of the endothelial layer (Figure 7N,O). Altogether, PHD2 haplodeficiency in tumor and stromal cells promotes normalization of the tumor vasculature in the spontaneously developing MMTV-PyMT model.

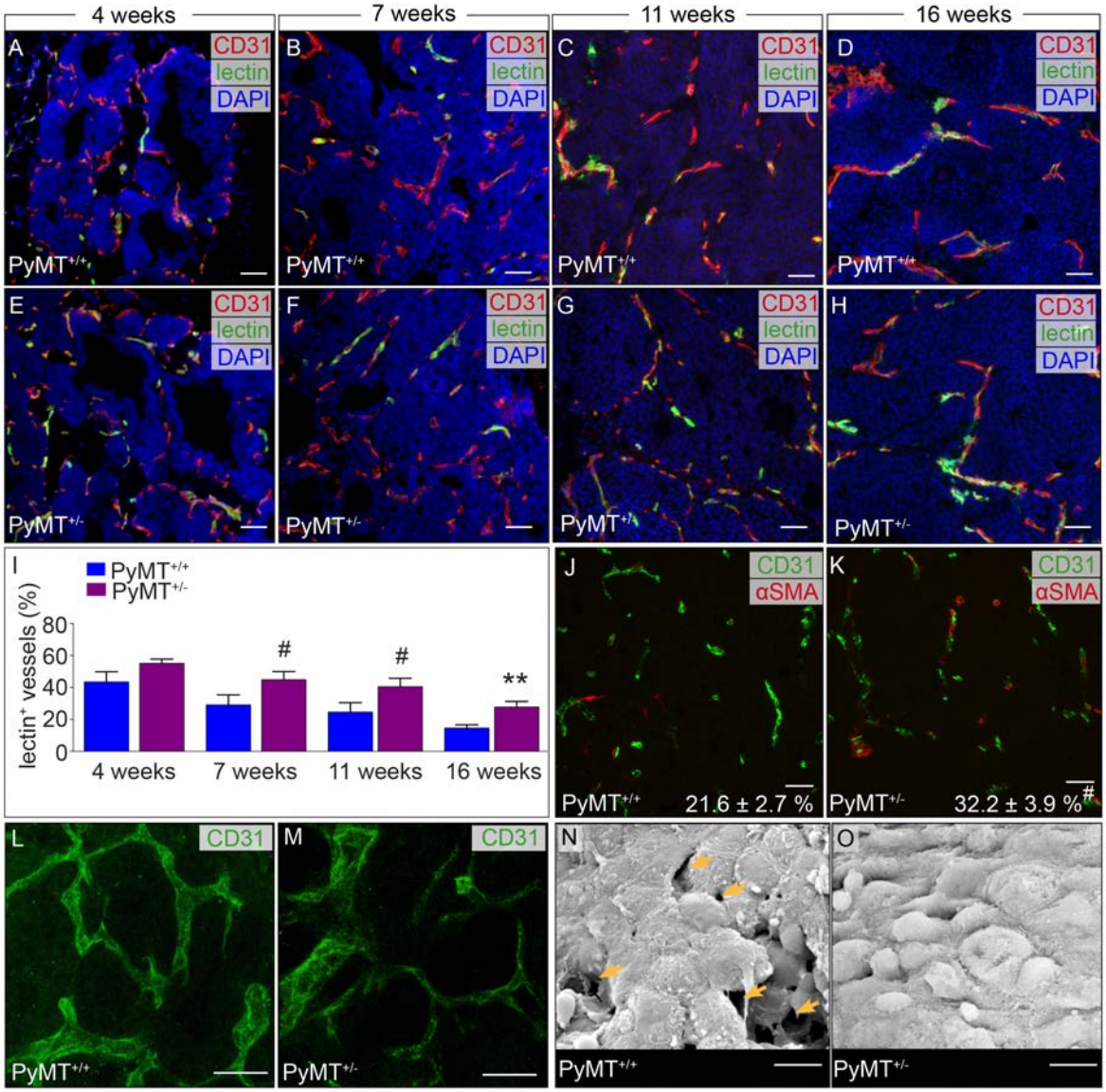

FIGURE 7: PHD2 HAPLODEFICIENCY IMPROVES VESSEL FUNCTION, BUT DOES NOT AFFECT THEIR ARCHITECTURE

A-I, Micrographs of lectin-FITC perfused and CD31-stained vessels in tumors from $PyMT^{+/+}$ and $PyMT^{+/-}$ mice at 4, 7, 11 and 16 weeks of age. Panel I: Quantification of perfusion is indicated ($CD31^{+}LECTIN^{+}$ area, % of total $CD31^{+}$ area) (n = 5-7; # p=0.07). **J,K,** Micrographs of αSMA and CD31-stained vessels in end stage $PyMT^{+/+}$ (J) and $PyMT^{+/-}$ (K) tumors. Quantification of vessel maturation is indicated (% of $αSMA^{+}$ covered vessels) (n = 5; # p=0.05). **L,M,** Confocal images of CD31 immunostaining of the vascular network of $PyMT^{+/+}$ (L) and $PyMT^{+/-}$ (M) tumors. **N,O,** Scanning electron microscopy of $PyMT^{+/+}$ (N) and $PyMT^{+/-}$ (O) tumors. Arrows indicates gaps in endothelial lining. Bar: 50 µm (A-H,J,K), 20 µm (L,M), 5 µm (N,O). All quantitative data are mean ± SEM. ** $p < 0.01$.

PHD2 HAPLODEFICIENCY IN ECS REDUCES METASTASIS AND INDUCES TUMOR VESSEL NORMALIZATION

Since haplodeficiency of PHD2 in ECs suffices to cause tumor vessel normalization (Leite de Oliveira et al., 2012; Mazzone et al., 2009), we also intercrossed $PHD2^{+/lox}$:Tie2-Cre mice with MMTV-PyMT mice ($PyMT^{Tie2\text{-}HE}$). RT-PCR analysis of ECs revealed that *Egln1* mRNA expression in $PyMT^{Tie2\text{-}HE}$ mice was reduced by 50% (Figure 8A). While tumor growth was not altered in $PyMT^{Tie2\text{-}HE}$ mice, metastasis and metastatic index were significantly reduced (Figure 8B-E). Indeed, EC-specific haplodeficiency of PHD2 phenocopied the vascular parameters of $PyMT^{+/-}$ tumors. While vessel number was not altered (Figure 8F), vessel maturation was improved (Figure 8G-I) and intratumoral hypoxia was reduced (Figure 8J-L).

Given the limitations of the Tie2-Cre line concerning EC specificity (the Tie2 promoter is also active in the hematopoietic lineage), we have also validated these results in another line. For this purpose *VE-cadherin(PAC)-Cre^{ERT2}* mice, an EC-specific inducible Cre-driver line (Benedito et al., 2012), was intercrossed with $PHD2^{+/lox}$ mice and further with MMTV-PyMT mice and was treated with tamoxifen for 7 days at the age of 3 weeks (before the onset of tumorigenesis in the MMTV-PYMT model). $PHD2^{+/lox}$:VE-cadherin(PAC)-Cre^{ERT2}:MMTV-PyMT mice are referred to as $PyMT^{Cdh5\text{-}HE}$ and their control littermates $PHD2^{+/+}$:VE-cadherin(PAC)-Cre^{ERT2}:MMTV-PyMT as $PyMT^{Cdh5\text{-}WT}$. RT-PCR revealed decreased *Egln1* levels in ECs isolated from $PyMT^{Cdh5\text{-}HE}$ mice (Figure 9A). The analyses indicate that also in this line PHD2 haplodeficiency in ECs reduced pulmonary metastasis and metastatic index (Figure 9B,C). Analysis of vascular parameters revealed that the vessel number was not altered in $PyMT^{Cdh5\text{-}HE}$ tumors, however, we observed an increase in vessel maturation (Figure 9D-G) and decreased intratumoral hypoxia (Figure 9H-J).

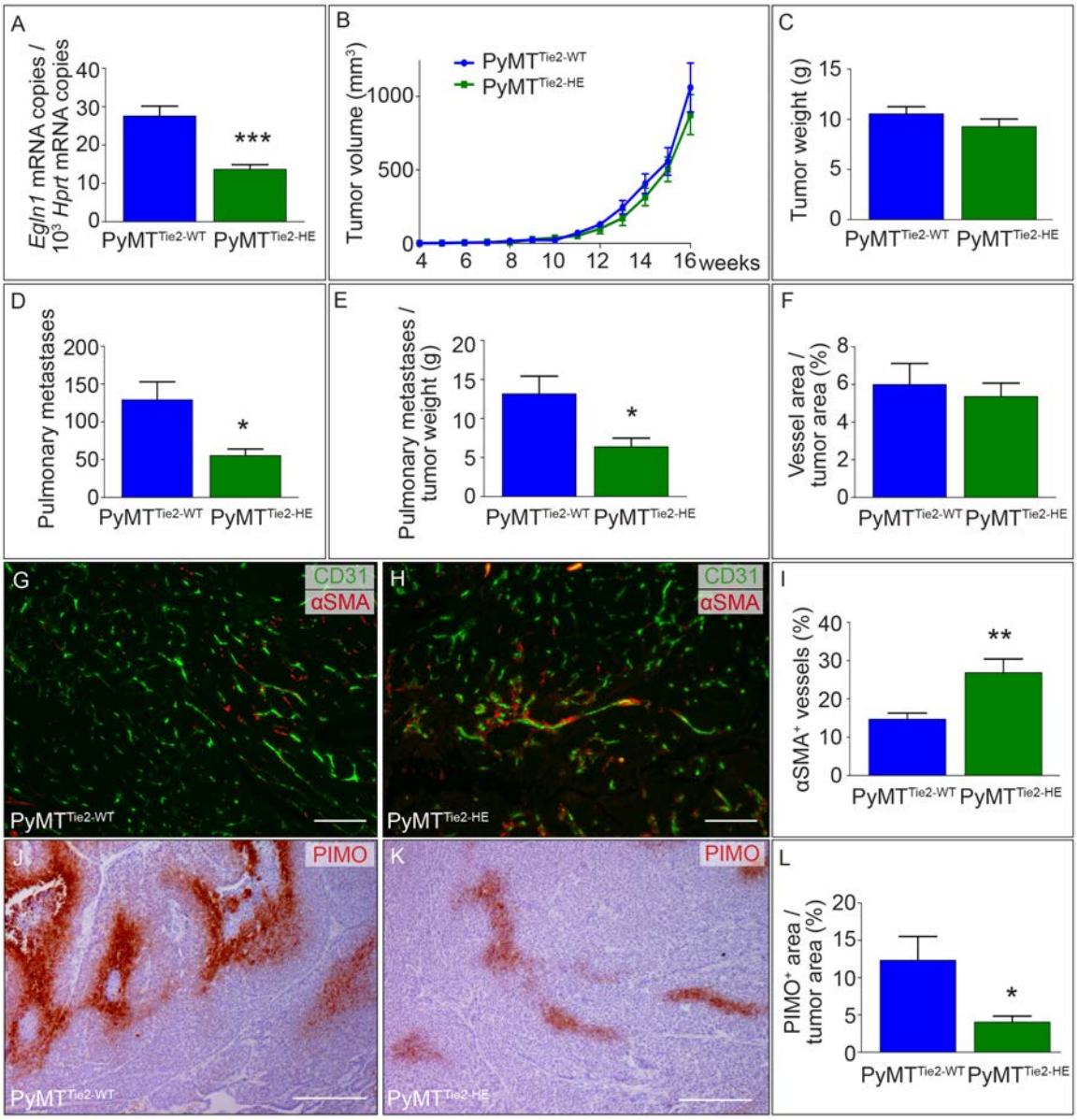

FIGURE 8: TIE2-CRE EC-PHD2 HAPLODEFICIENCY NORMALIZES TUMOR BLOOD VESSELS AND REDUCES METASTASIS

A, RT-PCR analysis of *Egln1* mRNA level in lung ECs isolated from PyMT$^{Tie2\text{-}WT}$ and PyMT$^{Tie2\text{-}HE}$ mice (n = 4-6). **B,** Growth curve of individual tumors in PyMT$^{Tie2\text{-}WT}$ and PyMT$^{Tie2\text{-}HE}$ mice (n = 11-20 ; p = ns). **C,** Tumor weight in PyMT$^{Tie2\text{-}WT}$ and PyMT$^{Tie2\text{-}HE}$ tumor bearing 16 week old mice (n = 29-46; p = ns). **D,** Number of pulmonary metastases in PyMT$^{Tie2\text{-}WT}$ and PyMT$^{Tie2\text{-}HE}$ tumor bearing 16 week old mice (n = 29-46; t-test with Welch's correction). **E,** Metastatic index (number of metastases corrected for tumor weight) in PyMT$^{Tie2\text{-}WT}$ and PyMT$^{Tie2\text{-}HE}$ mice (n = 29-46; t-test with Welch's correction). **F,** Quantification of vessel area expressed as a percent of tumor area (n = 4-5). **G-I** Micrographs of αSMA and CD31-stained vessels in end stage PyMT$^{Tie2\text{-}WT}$ (G) and PyMT$^{Tie2\text{-}HE}$ (H) tumors. Panel I: quantification of vessel maturation (% of αSMA^{+} covered vessels) (n = 10). **J-L,** Representative micrographs of PIMO staining (brown) in end stage PyMT$^{Tie2\text{-}WT}$ (J) and PyMT$^{Tie2\text{-}HE}$ (K) tumors. Quantification of PIMO^{+} hypoxic tumor area (% of total) in tumors from PyMT$^{Tie2\text{-}WT}$ and PyMT$^{Tie2\text{-}HE}$ mice at 16 weeks of age is indicated in panel L (n = 6-7). Bar: 100 µm (G,H), 200 µm (J,K). All quantitative data are mean ± SEM. * $p < 0.05$, ** $p < 0.01$, *** $p < 0.01$.

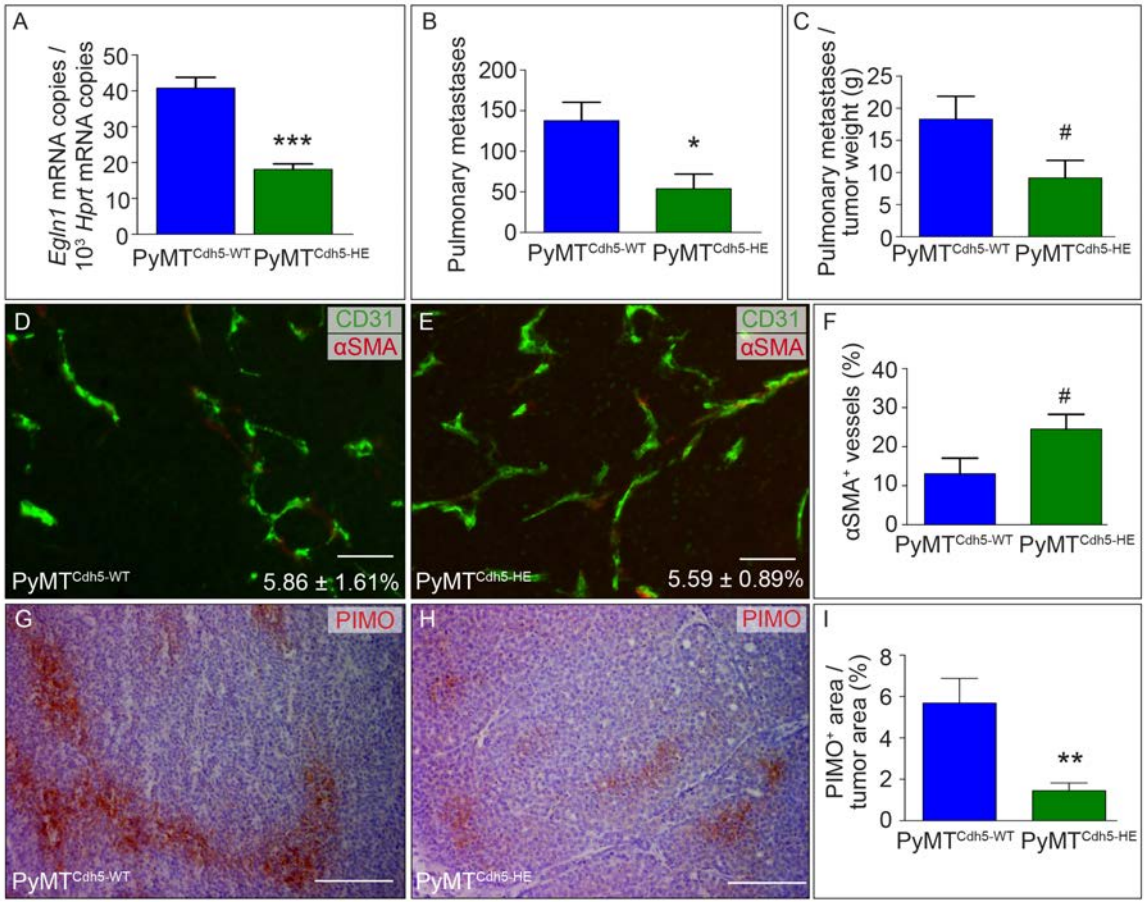

FIGURE 9: VE-CADHERIN-CRE-DRIVEN EC-PHD2 HAPLODEFICIENCY NORMALIZES TUMOR BLOOD VESSELS AND REDUCES METASTASIS

A, RT-PCR analysis of *Egln1* mRNA level in lung ECs isolated from $PyMT^{Cdh5\text{-}WT}$ and $PyMT^{Cdh5\text{-}HE}$ mice (n = 5-6). **B,** Number of pulmonary metastases in $PyMT^{Cdh5\text{-}WT}$ and $PyMT^{Cdh5\text{-}HE}$ mice (n = 14-19). **C,** Metastatic index (number of metastases corrected for tumor weight) in $PyMT^{Cdh5\text{-}WT}$ and $PyMT^{Cdh5\text{-}HE}$ mice (n = 14-19). **D-F** Micrographs of αSMA and CD31-stained vessels in end stage $PyMT^{Cdh5\text{-}WT}$ (D) and $PyMT^{Cdh5\text{-}HE}$ (E) tumors. Quantification of vessel area expressed as a percent of tumor area is indicated in the insets (n = 6-8). Panel F: quantification of vessel maturation (% of αSMA^+ covered vessels) (n = 6-8). **G-I,** Representative micrographs of PIMO staining (brown) in end stage $PyMT^{Cdh5\text{-}WT}$ (G) and $PyMT^{Cdh5\text{-}HE}$ (H) tumors. Quantification of $PIMO^+$ hypoxic tumor area (% of total) in tumors from $PyMT^{Cdh5\text{-}WT}$ and $PyMT^{Cdh5\text{-}HE}$ mice at 16 weeks of age is indicated in panel I (n = 6-8). Bar: 50 µm (D,E), 200 µm (G,H). All quantitative data are mean ± SEM. * $p < 0.05$, ** $p < 0.01$, *** $p < 0.01$, # $p = 0.06$.

These results further support the finding that endothelial haplodeficiency of PHD2 induced tumor vessel normalization and suggest that reduced metastasis in full PHD2 haplodeficient mice ($PyMT^{+/-}$) is at least partly caused by functional and morphological changes of tumor vessels. However, when we compared the magnitude of reduction of pulmonary metastasis in endothelial PHD2

haplodeficient mice (Figure 8D,E; Figure 9B,C) to that in mice with global PHD2 haplodeficiency (Figure 2A-D), we observed that pulmonary metastasis in the latter was more severely diminished than in EC-specific PHD2 haplodeficient mice. This discrepancy in magnitude of metastasis reduction might be explained by the contribution of PHD2 haplodeficiency in another cell type to the reduction in metastasis in $PyMT^{+/-}$ tumors. We thus explored whether PHD2 haplodeficiency in additional cell types could influence the metastatic process.

PHD2 HAPLODEFICIENCY DOES NOT AFFECT TAMS

Tumor-associated macrophages (TAMs), recruited to the tumor, promote tumor invasion and metastasis (Goswami et al., 2005; Mantovani et al., 2008). As PHD2 haplodeficiency influences TAM infiltration and polarization in the limb ischemia model (Takeda et al., 2011), and as such a change in TAMs might contribute to the reduced intravasation and metastasis, we analyzed TAM infiltration and polarization in the MMTV-PyMT tumors. However, staining for F4/80 failed to reveal any genotypic differences in the accumulation of TAMs in $PyMT^{+/+}$ and $PyMT^{+/-}$ tumors (Figure 10A). Additionally, double immunostaining for F4/80 and mannose receptor-2 (MRC1) also did not show differences in the skewing of macrophages towards M2 polarization (Figure 10B).

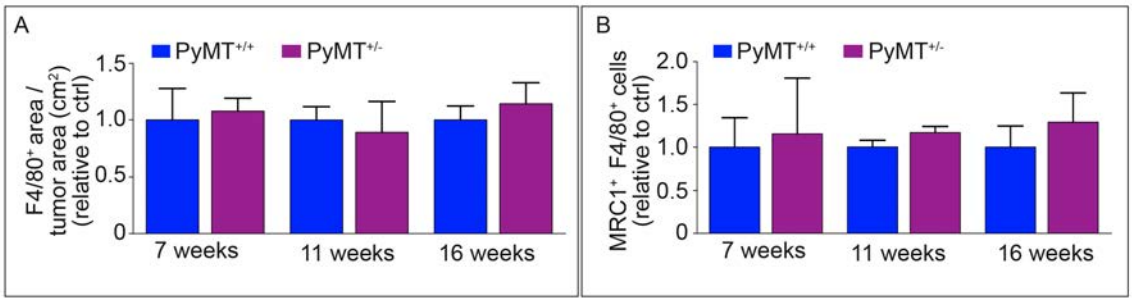

FIGURE 10: PHD2 HAPLODEFICIENCY DOES NOT AFFECT MACROPHAGE
A, Quantification of F4/80 macrophage infiltration into $PyMT^{+/+}$ and $PyMT^{+/-}$ tumors at 7, 11 and 16 week of age, expressed as relative values to control ($PyMT^{+/+}$ tumor) (n = 3-6; p = ns). **B**, Quantification of MRC1 colocalization with F4/80 to assess macrophage polarization in $PyMT^{+/+}$ and $PyMT^{+/-}$ tumors at 7, 11 and 16 week of age (n = 3-6; p = ns). All quantitative data are mean ± SEM.

REDUCED ACTIVATION OF CAFS IN PYMT$^{+/-}$ TUMORS

We then focused our attention on cancer-associated fibroblasts (CAFs), which promote tumorigenesis and metastasis (Kalluri and Zeisberg, 2006). Compared to PyMT$^{+/+}$ tumors, PyMT$^{+/-}$ tumors contained substantially fewer activated CAFs (Figure 11A-C). Notably, this genotypic difference in CAF activation became especially evident beyond 11 weeks, when the genotypic difference in metastasis was also evident. Previous studies already showed that CAFs became more abundant in PyMT tumors when progressing from adenoma to carcinoma (Calvo et al., 2013) (which occurs around 11 weeks of age; Figure 1K), precisely when pulmonary macro-metastases first became detectable in the PyMT model (Figure 2E). This temporal association between the genotypic difference in CAF activation and metastasis raised the question whether both processes were also functionally linked to each other.

To further investigate the properties of CAFs, we isolated stromal mesenchymal cells from PyMT$^{+/+}$ and PyMT$^{+/-}$ tumors. Previous studies documented that, once normal fibroblasts become activated to CAFs in tumors *in vivo*, they maintain their features *in vitro* even when cultured for several passages, in part because they sustain their activation status through continued autocrine production of TGF-β1, SDF-1α and other signals (Kojima et al., 2010). Indeed, gene expression profiling revealed that PyMT$^{+/+}$ CAFs expressed high transcript levels of *Tgf-β1* and *Sdf-1α* and their receptors *Tgf-βR2 and Cxcr4* in culture (Figure 11D).

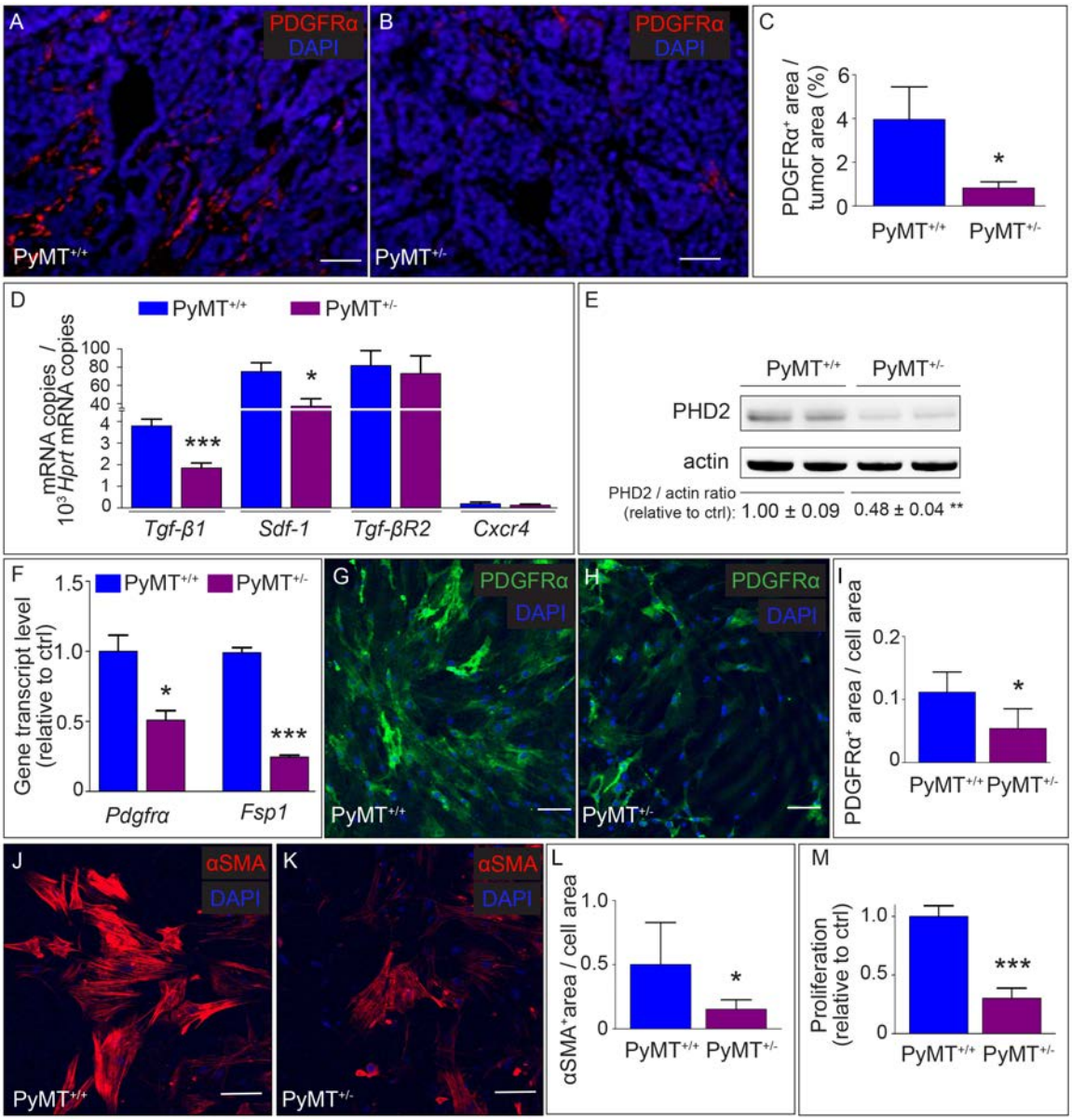

FIGURE 11: PHD2 HAPLODEFICIENCY REDUCES CAF ACTIVATION.

A-C, Staining of tumor sections from PyMT$^{+/+}$ (A) and PyMT$^{+/-}$ (B) 16 week old mice for the CAF-enriched activation marker PDGFRα, counterstained with DAPI. Panel C: quantification of the PDGFRα^{+} area (% of tumor area) in both genotypes (n = 5-6). **D,** RT-PCR analysis of *Sdf-1*, *Tgf-β1*, *Tgf-βR2* and *Cxcr4* mRNA levels in CAFs, isolated from PyMT$^{+/+}$ and PyMT$^{+/-}$ tumors (n = 6-8). **E,** Immunoblotting for PHD2 of PyMT$^{+/+}$ and PyMT$^{+/-}$ CAFs total lysates. Actin was used as loading control. Densitometric quantification is shown underneath the lanes (n = 3). **F,** RT-PCR analysis of genes associated with CAF activation (*Pdgfrα, Fsp1*) in CAFs isolated from end-stage PyMT$^{+/+}$ and PyMT$^{+/-}$ tumors (n = 3). **G-L,** Immunostaining of CAFs, isolated from PyMT$^{+/+}$ (G,J) or PyMT$^{-/-}$ (H,K) tumors, for the CAF activation markers PDGFRa (G,H), or αSMA (J,K). Quantification of the marker positive area per cell is shown in panels I,L (n = 3-6). **M,** Proliferation (thymidine incorporation) of CAFs isolated from PyMT$^{+/+}$ and PyMT$^{+/-}$ tumors (n = 3). Bar: 50 µm (A,B), 100 µm (G,H,J,K). All quantitative data are mean ± SEM. * p < 0.05, ** p < 0.01, ***p < 0.001.

We took advantage of this "phenotypic memory" to analyze distinct CAF behavioral phenotypes in culture. Analysis of PHD2 protein level revealed 50% decrease in $PyMT^{+/-}$ CAFs as compared to $PyMT^{+/+}$ CAFs (Figure 11E). First, gene expression profiling and immunostaining studies confirmed that stromal cells isolated from $PyMT^{+/-}$ tumors expressed lower levels of markers, enriched in activated CAFs, such as FSP1 (fibroblast-specific protein-1, also known as S100A4), PDGFRα and αSMA (Figure 11F-L). As the majority of the $PyMT^{+/+}$ stromal cell population expressed these markers (Figure 11G-L), we termed them $PyMT^{+/+}$ CAFs. Second, stromal cells isolated from $PyMT^{+/-}$ tumors ($PyMT^{+/-}$ CAFs) exhibited a lower proliferation rate, as measured by [^{3}H]-thymidine incorporation into DNA (Figure 11M). Overall, $PyMT^{+/-}$ CAFs were less activated, less proliferative, and expressed lower levels of the contractile protein αSMA.

IMPAIRED INVASION OF $PyMT^{+/-}$ CAFS

We then explored whether CAFs might regulate cancer cell invasion, and therefore we first examined their own invasive behavior. More in particular, since activated CAFs are highly invasive and assist cancer cell invasion (Calvo et al., 2013; Kalluri and Zeisberg, 2006), we examined whether PHD2 haplodeficiency impaired the invasive ability of CAFs. We embedded CAF spheroids in a collagen I gel and monitored their ability to form invasive sprouts (Kalluri and Zeisberg, 2006; Liu et al., 2011). Notably, compared to cancer cells, CAFs were capable of forming more and longer invasive sprouts (Figure 12A,B; compare to Figure 5G,H), indicating that they were more invasive. However, $PyMT^{+/-}$ CAFs formed fewer and shorter sprouts than $PyMT^{+/+}$ CAFs (Figure 12A-D). In agreement with these findings, the expression levels of various matrix metalloproteinases

(*Mmp2*, *Mmp9*), previously implicated in proteolytic ECM degradation during CAF invasion (Lu et al., 2012), were reduced in PyMT$^{+/-}$ CAFs (Figure 12E). Thus, PyMT$^{+/-}$ CAFs exhibited profound invasion defects.

INVASION OF WT PYMT TUMOR CELLS IS REDUCED BY PYMT$^{+/-}$ CAFS

Since CAFs can promote the invasion of tumor cells by direct remodelling of the extracellular matrix (ECM) (Duda et al., 2010; Gaggioli et al., 2007; Goetz et al., 2011), we assessed whether the reduced activation state of PyMT$^{+/-}$ CAFs influenced tumor cell invasion in collagen gels. We studied whether CAFs influenced the invasion of cancer cells by embedding spheroids consisting of a 1:1 mixture of cancer cells and CAFs. More in particular, given that PHD2 haplodeficiency impaired the invasion of CAFs, we assessed whether the reduced activation of PyMT$^{+/-}$ CAFs influenced the invasion of WT cancer cells. To distinguish cancer cells from CAFs, and to visualize their spatial position relative to each other, we stably transduced CAFs, isolated from PyMT$^{+/+}$ or PyMT$^{+/-}$ mice, with a lentiviral vector expressing GFP, and isolated Tomato (red) labelled cancer cells from wild type MMTV-PyMT mice that were intercrossed with mT/mG mice (abbreviated as PyMT$^{mT/mG}$). The mT/mG line is a double-fluorescent Cre reporter mouse that expresses membrane-targeted tandem dimer Tomato (mT) prior to Cre-mediated excision and membrane-targeted green fluorescent protein GFP (mG) after excision (Muzumdar et al., 2007). For our experiments, we did not intercross PyMT$^{mT/mG}$ mice with Cre-expressing mice (and thus did not switch on the expression of GFP), but took advantage of the constitutive expression of the Tomato reporter by the cancer cells.

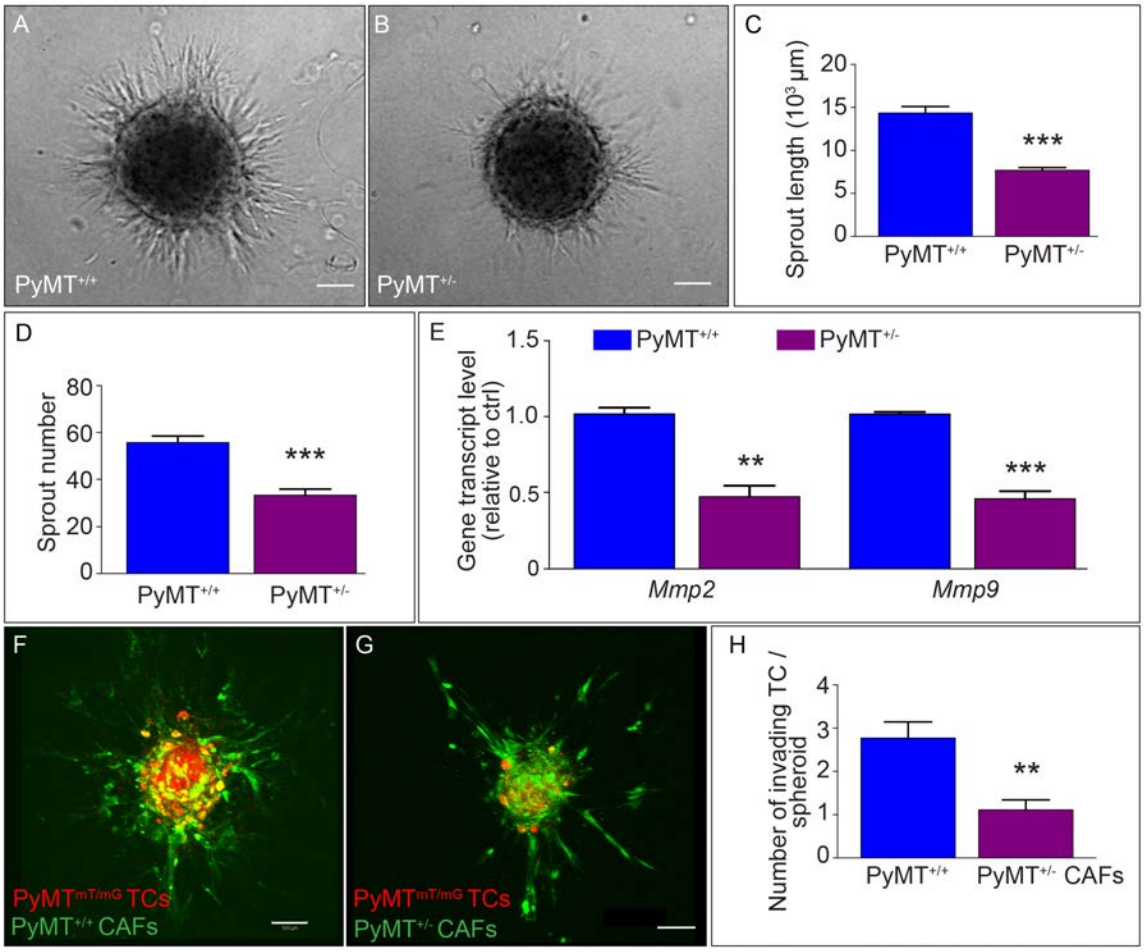

FIGURE 12: PHD2 HAPLODEFICIENCY REDUCES CAF INVASION.
A-D, CAF spheroid invasion assay using CAFs isolated from PyMT$^{+/-}$ (A) and PyMT$^{+/-}$ (B) tumors. Quantification of invasive sprout number and length is shown in panels C and D, respectively (n > 14 spheroids). **E,** RT-PCR analysis of *Mmp2* and *Mmp9* in CAFs isolated from PyMT$^{+/+}$ and PyMT$^{+/-}$ end stage tumors (n = 3). **F-H,** Invasion assay using spheroids consisting of a 1:1 mixture of Tomato^{+} PyMT$^{mT/mG}$ tumor cells (TCs, wild type for PHD2; red) and GFP^{+} CAFs (green), isolated either from PyMT$^{+/+}$ (F) or from PyMT$^{+/-}$ (G) tumors. Quantification of the number of individual invading tumor cells is shown in panel H (n > 45 spheroids). Since in this model, tumor cells co-invaded together with CAFs (often in the same sprout), we counted the number of individual tumor cells that migrated from the spheroid. Bar: 100 µm (A,B,F,G). All quantitative data are mean ± SEM. ** $p < 0.01$, *** $p < 0.001$.

Analysis of spheroids consisting of a 1:1 mixture of Tomato^{+} PyMT$^{mT/mG}$ cancer cells and GFP^{+} CAFs, isolated from PyMT$^{+/+}$ or PyMT$^{+/-}$ tumors, showed that fewer cancer cells invaded into the gel when they were co-cultured with PyMT$^{+/-}$ CAFs as compared to when they were co-cultured with PyMT$^{+/+}$ CAFs (Figure 12F-H). This genotypic difference in invasive behavior of cancer cells,

determined by CAFs, could contribute to the genotypic difference observed in intravasation and metastasis.

IMPAIRED MATRIX DEPOSITION AND CROSS-LINKING BY PyMT$^{+/-}$ CAFS

Previous studies documented that CAFs can facilitate cancer cell invasion through various effects on the ECM. For instance, CAFs can promote the invasion of cancer cells by depositing bundles of cross-linked collagen I, which cancer cells use as preferred migration tracks (Calvo et al., 2013; Lu et al., 2012; Maller et al., 2013). We first verified that CAFs represented a significant source of ECM production in PyMT tumors, to which end we compared the relative amount of matrix production by CAFs *versus* cancer cells. Analysis of [^{3}H]-L-proline incorporation into the deposited matrix indeed revealed that CAFs produced much larger amounts of matrix than PyMT cancer cells (Figure 13A).

Several lines of evidence indicated that PyMT$^{+/-}$ CAFs produced less extracellular matrix than PyMT$^{+/+}$ CAFs, both *in vivo* and *in vitro*. First, Picro Sirius Red staining showed that PyMT$^{+/-}$ tumors contained smaller amounts of fibrillar collagen (Figure 13B-D). Second, we took advantage of the birefringency of cross-linked collagen, which upon polarized light microscopy appears red, while non-cross-linked collagen appears green. This analysis showed that PyMT$^{+/-}$ tumors contained fewer thick bundles of cross-linked collagen compared to PyMT$^{+/+}$ tumors (Figure 13E-G). Third, analysis of [^{3}H]-L-proline incorporation into the matrix deposited by CAFs over a period of eight days showed that CAFs isolated from PyMT$^{+/-}$ tumors produced less matrix *in vitro* (Figure 13H). Fourth, the reduced matrix production in culture was not only a result of the decreased proliferation rate of PyMT$^{+/-}$ CAFs, since immunostaining of isolated CAFs also

showed lower immunoreactive levels of collagen I per cell in PyMT$^{+/-}$ than PyMT$^{+/+}$ CAFs (Figure 13I-K). Thus, CAFs from PyMT$^{+/-}$ tumors produced fewer cross-linked collagen fibers, thereby decreasing the amount of available migration tracks for cancer cells.

IMPAIRED REMODELING OF THE EXTRACELLULAR MATRIX BY PyMT$^{+/-}$ CAFS

CAFs can also facilitate cancer cell invasion via another mechanism, i.e. by remodelling the extracellular matrix through active contraction (Calvo et al., 2013), a process that results in matrix stiffening and is known to promote cancer cell invasion and metastasis (Calvo et al., 2013; Lu et al., 2012). Since CAFs require a contractile cytoskeleton for matrix contraction (Calvo et al., 2013), and PyMT$^{+/-}$ CAFs had decreased amounts of immunoreactive αSMA^{+} actin stress fibers (Figure 11J-L), we studied whether the ability of PyMT$^{+/-}$ CAFs to remodel the ECM via matrix contraction was impaired. We therefore used the "collagen contraction assay", in which CAFs are uniformly dispersed throughout a collagen I gel (Calvo et al., 2013). By contracting the gel, CAFs are able to reduce the size of the gel. Notably, this analysis revealed that, compared to PyMT$^{+/+}$ CAFs, PyMT$^{+/-}$ CAFs contracted the collagen gel less, as evidenced by the larger size of the gels after incubation (Figure 13L).

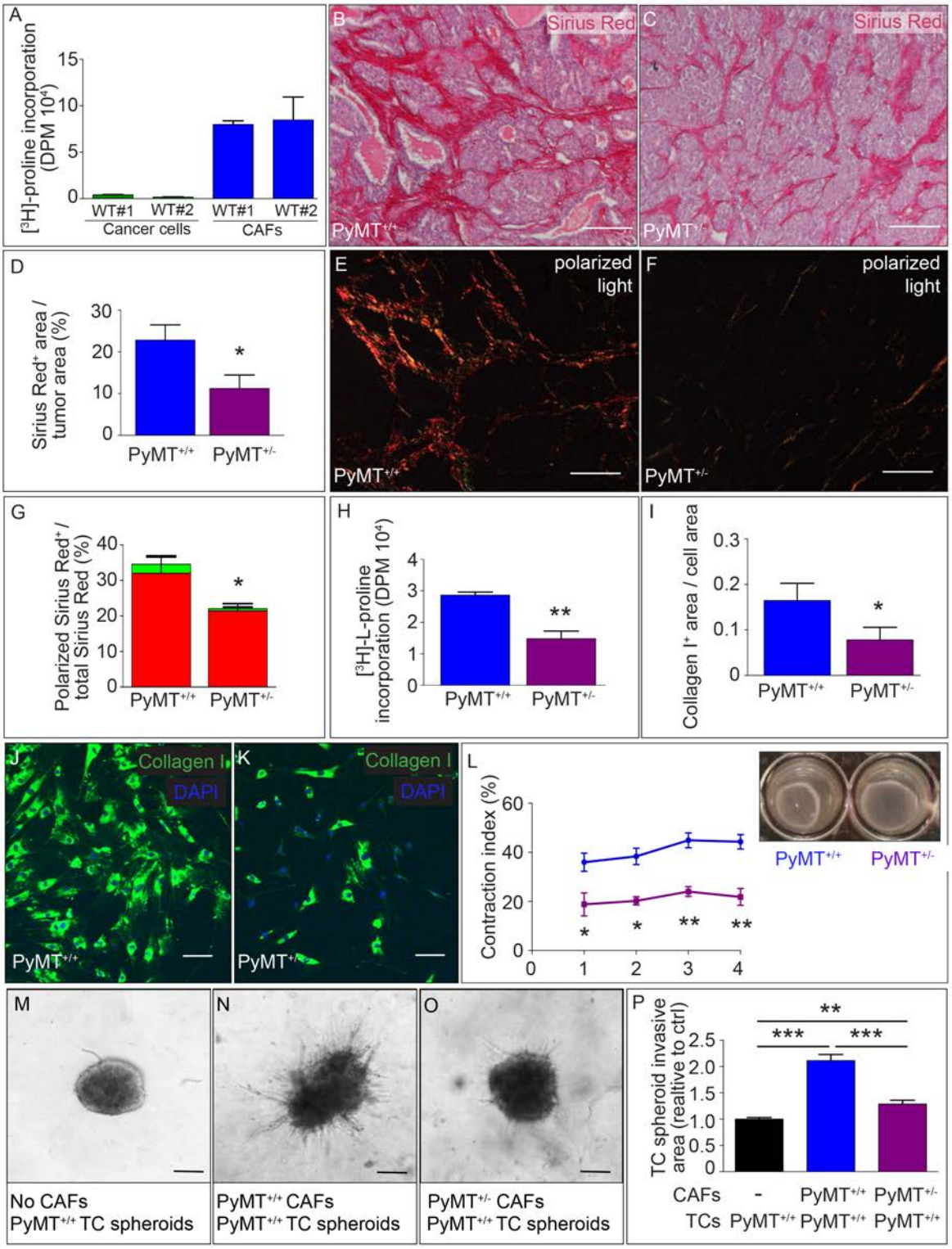

FIGURE 13: EFFECT OF PHD2 HAPLODEFICIENCY ON ECM PRODUCTION AND REMODELLING BY CAFS
A, Quantification of ECM deposition by cancer cells or CAFs isolated from $PyMT^{+/+}$ tumors, measured by the [^{3}H]-L-proline incorporation assay (see methods). Data are shown for 2 independent isolations from different $PyMT^{+/+}$ mice (n = 3). DPM, disintegrations per minute. **B-D,** Picro Sirius Red staining of $PyMT^{+/+}$ (B) and $PyMT^{+/-}$ (C) tumor sections. Panel D: quantification of Picro Sirius Red+ area (n = 5). **E-G**, Polarized light microscopy analysis of Picro

Sirius Red stained PyMT$^{+/+}$ (E) and PyMT$^{+/-}$ (F) tumors to visualize thick cross-linked (red) versus thin non-cross-linked (green) collagen fibers. Panel G: quantifications of cross-linked and thin fibers (n = 5; t-test with Welch's correction). **H**, Quantification of matrix synthesis by CAFs isolated from PyMT$^{+/+}$ or PyMT$^{+/-}$ tumors as measured by an in vitro [^{3}H]-L-proline incorporation assay (n = 3); DPM, disintegrations per minute. **I-K,** Immunostaining of CAFs, isolated from PyMT$^{+/+}$ (J) or PyMT$^{+/-}$ (K) tumors, for collagen I. The DAPI nuclear counterstain is shown in blue. Quantification of the collagen I-immunoreactive area per cell is shown in panel I (n = 3). **L,** Collagen gel contraction assay using CAFs isolated from PyMT$^{+/+}$ (blue) or PyMT$^{+/-}$ (purple) tumors (n = 4; t-test with Welch's correction). Inset: representative pictures of contracted gels. To determine the contraction index, the area of the gel at the indicated time was subtracted from the initial area of the gel at the beginning of the experiment, and this value was expressed as a percentage of the initial gel area. **M-P**, Invasion assay using spheroids of PyMT$^{+/+}$ tumor cells in collagen gels with no CAFs (M), or into which CAFs isolated from PyMT$^{+/+}$(N) or from PyMT$^{+/-}$ (O) tumors were homogeneously dispersed. Panel P: quantification of the area of the entire cancer cell spheroids (n > 18 spheroids). Bar: 50 µm (B,C,E,F,J,K), 200 µm (M-O). All quantitative data are mean ± SEM. * $p < 0.05$, ** $p < 0.01$, *** $p < 0.001$.

To assess whether remodelling of the collagen gel by the CAFs' contractile activity altered the invasion of wild type cancer cells, we embedded cancer cell spheroids into a collagen gel, in which CAFs had been uniformly dispersed throughout the gel, largely as previously described (Calvo et al., 2013). Compared to PyMT$^{+/+}$ cancer cell spheroids alone, co-embedding dispersed PyMT$^{+/+}$ CAFs in the gel accelerated collective cancer cell invasion by a day, indicating that CAFs promoted cancer cell invasion. Notably however, PyMT$^{+/+}$ cancer cells invaded the collagen gel less when they were co-embedded with PyMT$^{+/-}$ than PyMT$^{+/+}$ CAFs (Figure 13M-P). Hence, in conditions where CAFs were capable of remodelling the ECM, CAFs from PyMT$^{+/-}$ tumors did not stimulate the invasive behavior of the cancer cells to the same extent as PyMT$^{+/+}$ CAFs.

PyMT$^{+/-}$ CAFs HAVE REDUCED CAPACITY TO PROMOTE METASTASIS IN TUMOR GRAFTS AS COMPARED TO PyMT$^{+/+}$ CAFs

To assess whether PyMT$^{+/-}$ CAFs also impaired promoting cancer cell invasion activities *in vivo*, we orthotopically transplanted PyMT$^{+/+}$ tumor cells with or without PyMT$^{+/+}$ or PyMT$^{+/-}$ CAFs as a 1:2 mixture in WT mice. Analysis of primary tumor growth confirmed previous findings (Orimo et al., 2005) that co-transplantation of CAFs increased primary tumor growth, both upon co-transplantation of either PyMT$^{+/+}$ or PyMT$^{+/-}$ CAFs (Figure 14A). Also metastatic dissemination, at 6 weeks after transplantation, was increased upon co-transplantation of PyMT$^{+/+}$ tumor cells and PyMT$^{+/+}$ CAFs (Figure 14B,C). Interestingly, fewer pulmonary metastases could be detected in the group where PyMT$^{+/+}$ tumor cells were co-implanted with PyMT$^{+/-}$ CAFs (Figure 14B,C) than in the group where tumor cells were co-implanted with PyMT$^{+/+}$ CAFs. These results further confirm that PyMT$^{+/-}$ CAFs have impaired capacity to mediate tumor cell invasion and metastasis.

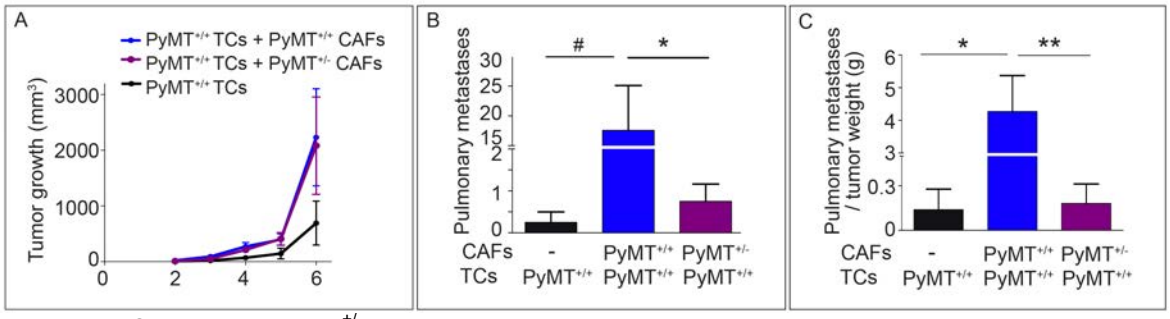

FIGURE 14: CAFs FROM PyMT$^{+/-}$ TUMORS HAVE IMPAIRED PRO-METASTATIC CAPACITY.
A, Growth curve of PyMT tumor xenografts upon PyMT$^{+/+}$ cancer cell transplantation (alone; black), or co-transplanted with PyMT$^{+/+}$ (blue) or PyMT$^{+/-}$ (purple) CAFs (n = 4-7). **B**, Number of pulmonary metastases evaluated 6 weeks after PyMT$^{+/+}$ cancer cell transplantation (alone; black), or co-transplanted with PyMT$^{+/+}$ (blue) or PyMT$^{+/-}$ (purple) CAFs (n = 4-7; t-test with Welch's correction). **C**, Metastatic index (number of metastases corrected for tumor weight) in mice injected with PyMT$^{+/+}$ cancer cells alone (black), or co-transplanted with PyMT$^{+/+}$ (blue) or PyMT$^{+/-}$ (purple) CAFs (n = 4-7; t-test with Welch's correction). All quantitative data are mean ± SEM. * $p < 0.05$, ** $p < 0.01$, $^{\#}$ $p = 0.06$.

HAPLODEFICIENCY OF PHD2 IN CAFS DOES NOT AFFECT CAF ACTIVATION AND PYMT TUMOR METASTASIS

In order to explore whether PHD2 in CAFs orchestrated metastasis *in vivo*, we intercrossed MMTV-PyMT x $PHD2^{+/lox}$ mice with PDGFRα:Cre^{ERT2} mice (Leite de Oliveira et al., 2012; Rivers et al., 2008) and treated them at the age of 3 weeks with tamoxifen for 7 days to obtain mice with PHD2 haplodeficiency in the fibroblasts *in vivo* (abbreviated as $PyMT^{CAF\text{-}HE}$ mice). Analysis of PHD2 protein level in CAFs, isolated from these mice, showed that PHD2 levels were reduced by 43.1 ± 3.8% ($n = 3$; $p < 0.05$). Surprisingly, analysis of $PyMT^{CAF\text{-}HE}$ mice revealed that neither tumor growth nor pulmonary metastasis were altered when compared to $PyMT^{CAF\text{-}WT}$ mice (Figure 15A-C).

Furthermore, analysis of CAF accumulation as determined by immunostaining for PDGFRα and analysis of their capacity to deposit an ECM (by Picro Sirius red staining) in tumors from $PyMT^{CAF\text{-}WT}$ and $PyMT^{CAF\text{-}HE}$ mice revealed no differences (Figure 15D-I). To further validate these findings we have assessed *in vitro* characteristics of CAFs isolated from $PyMT^{CAF\text{-}WT}$ and $PyMT^{CAF\text{-}HE}$ mice. PHD2 haplodeficiency in fibroblasts did not change their capacity to proliferate or to remodel collagen gel by contraction (Figure 15J,K). Altogether these results showed that selective PHD2 haplodeficiency in fibroblasts did not affect the activation of CAFs and tumor cell metastasis. We therefore explored other possible mechanisms that could explain the reduced activation of CAFs in mice with global PHD2 haplodeficiency ($PyMT^{+/-}$).

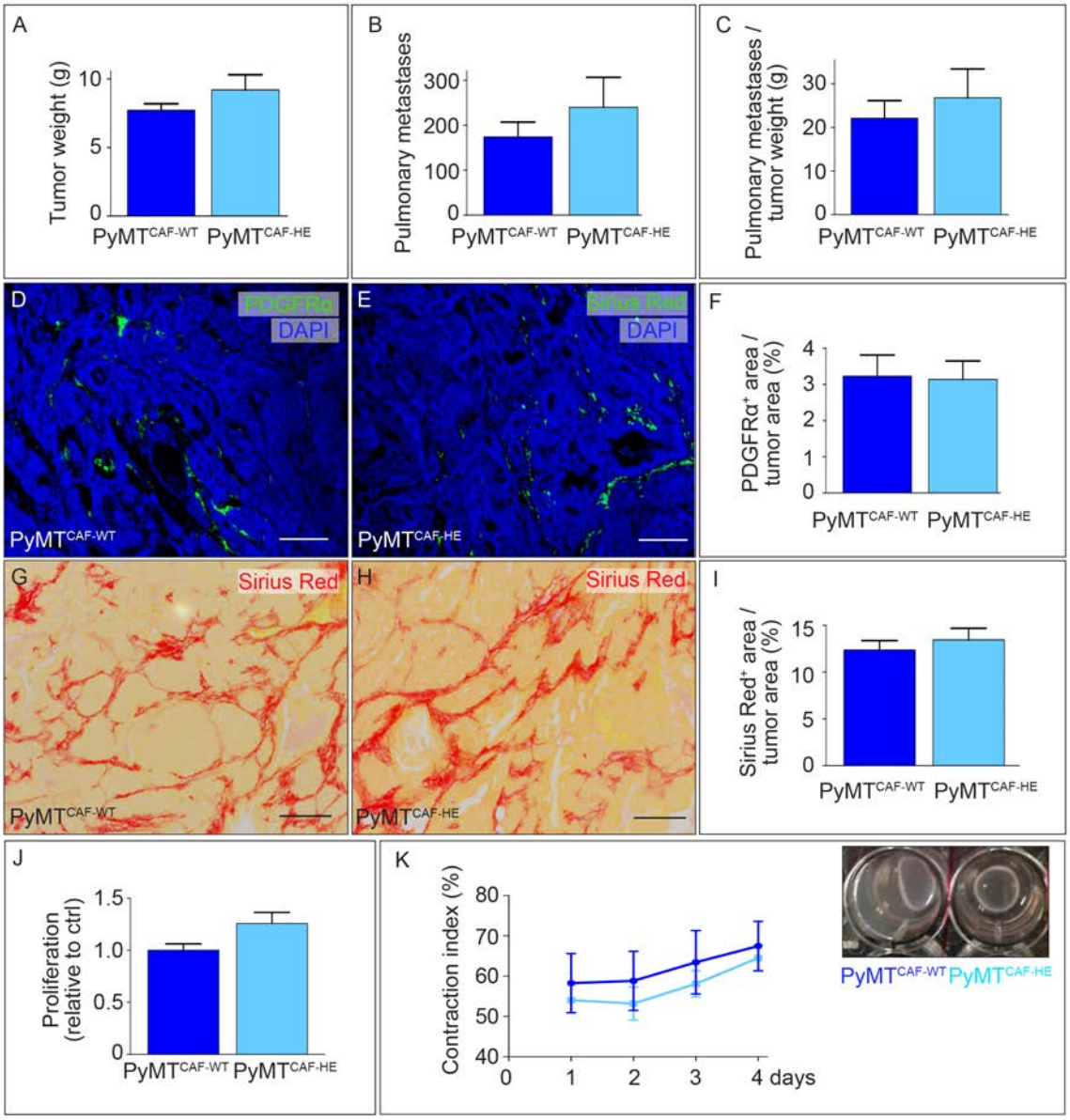

FIGURE 15: CAFS FROM PyMT$^{CAF\text{-}HE}$ TUMORS HAVE NORMAL PRO-METASTATIC CAPACITY AND ACTIVATION CHARACTERISTICS.

A, Weight of PyMT$^{CAF\text{-}WT}$ and PyMT$^{CAF\text{-}HE}$ tumors collected at the end-stage (16 week of age) (n = 16-22; p = ns). **B**, Number of pulmonary metastases in PyMT$^{CAF\text{-}WT}$ and PyMT$^{CAF\text{-}HE}$ tumor bearing 16 week old mice (n = 16-22; p = ns; t-test with Welch's correction). **C,** Metastatic index (number of metastases corrected for tumor weight) in PyMT$^{CAF\text{-}WT}$ and PyMT$^{CAF\text{-}HE}$ tumor bearing 16 week old mice (n = 16-22; p = ns; t-test with Welch's correction). **D-F,** Staining of tumor sections from PyMT$^{CAF\text{-}WT}$ (D) and PyMT$^{CAF\text{-}HE}$ (E) mice for the CAF-enriched activation marker PDGFRα, counterstained with DAPI. Panel F: quantification of the PDGFRα^{+} area (% of tumor area) in both genotypes (n = 9-10; p = ns). **G-I,** Picro Sirius Red staining of PyMT$^{CAF\text{-}WT}$ (G) and PyMT$^{CAF\text{-}HE}$ (H) tumor sections. Panel I: quantification of Picro Sirius Red^{+} area (n = 8-9; p = ns). **J,** Proliferation ([3H]-thymidine incorporation) of CAFs isolated from PyMT$^{CAF\text{-}WT}$ and PyMT$^{CAF\text{-}HE}$ tumors (n = 4). **K,** Collagen gel contraction assay using CAFs isolated from PyMT$^{CAF\text{-}WT}$ or PyMT$^{CAF\text{-}HE}$ tumors (n = 4). Scale bar: 100 μm (D,E,G,H). All quantitative data are mean ± SEM.

DECREASED TGF-ß1 SECRETION IN PHD2 HAPLODEFICIENT CANCER CELLS

The origin of CAFs has not been fully elucidated yet, but the most commonly accepted hypothesis is that the majority of CAFs trans-differentiate from resident fibroblasts upon stimulation by a plethora of cytokines and growth factors secreted by cancer cells, such as TGF-β1, PDGF, FGF2 and SDF1 (Quail and Joyce, 2013). Previous studies reported that silencing of PHD2 in a breast cancer cell line or epithelial cells reduced the secretion of TGF-β1 (Kalucka et al., 2013; Wottawa et al., 2012). We therefore investigated whether reduced activation of CAFs is related to a reduction in TGF-β1 secretion by $PyMT^{+/-}$ cancer cells. ELISA measurements indeed showed that TGF-β1 levels were reduced in the supernatant of cultured $PyMT^{+/-}$ tumor cells (TCs) (Figure 16A). Interestingly, analysis of 40 other secreted chemokines and cytokines revealed no differences in the supernatants of $PyMT^{+/+}$ and $PyMT^{+/-}$ cancer cells (Figure 16B-D). We therefore focused on TGF-β1 signalling pathway in our subsequent analyses.

To explore whether decreased secretion of TGF-β1 by PHD2 haplodeficient TCs would be sufficient to reduce CAF activation and thus impair metastasis *in vivo*, we intercrossed $PHD2^{+/lox}$ mice with MMTV-Cre and MMTV-PyMT mice, yielding mice with PHD2 haplodeficiency selectively in the TCs (abbreviated as $PyMT^{TC-HE}$). These $PyMT^{TC-HE}$ mice were compared to their wild type littermates (abbreviated as $PyMT^{TC-WT}$). RT-PCR and protein analysis of tumor cells, freshly isolated from these tumors, revealed that PHD2 protein level and *Egln1* mRNA in $PyMT^{TC-HE}$ cancer cells was reduced (Figure 16E,F). This effect was selective to cancer cells as *Egln1* mRNA levels were the same in $PyMT^{TC-WT}$ and $PyMT^{TC-HE}$ CAFs (Figure 16G).

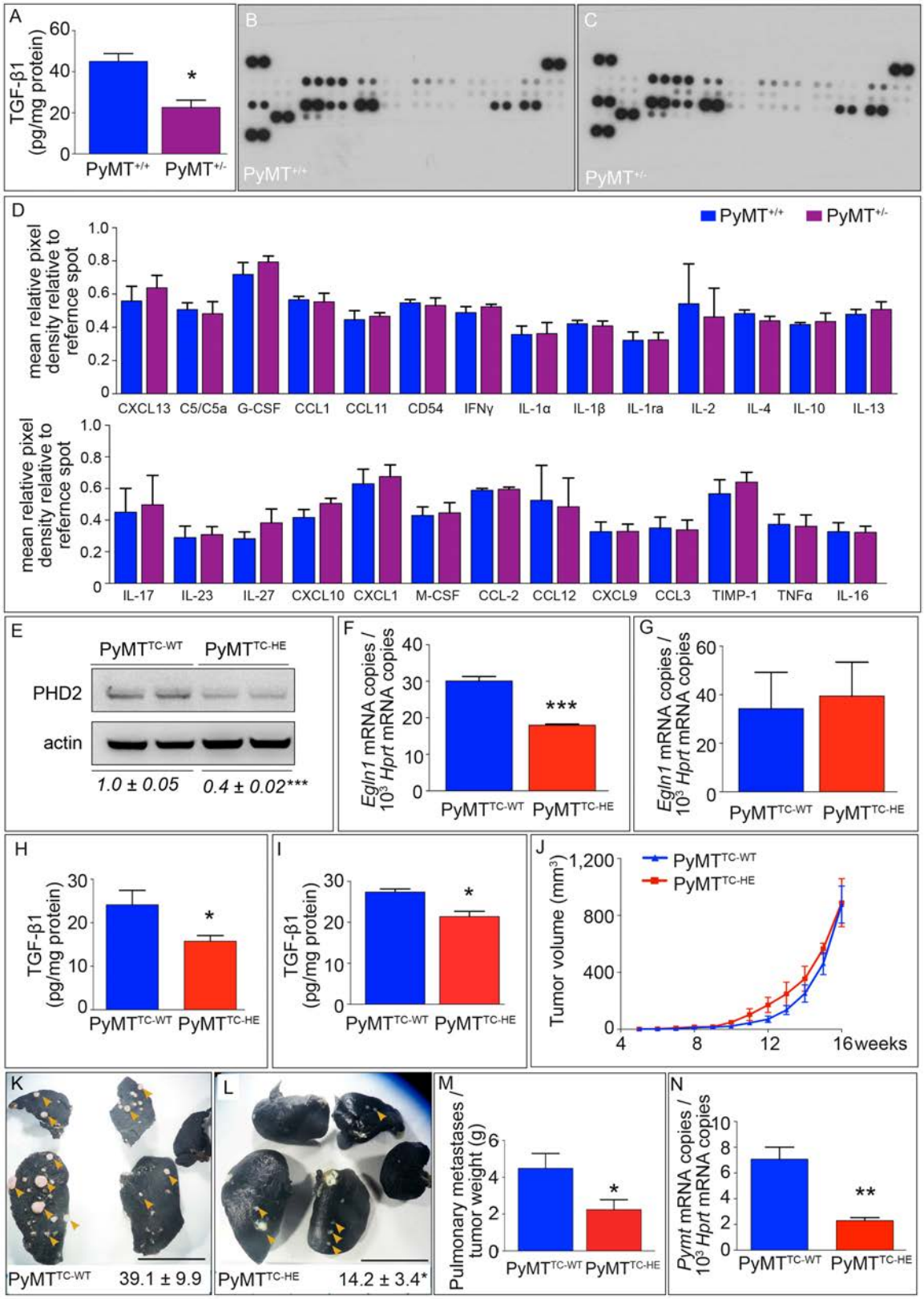

FIGURE 16: PHD2 HAPLODEFICIENCY IN CANCER CELLS DECREASES TGF-β1 SECRETION AND DECREASED THE NUMBER OF CTCS AND METASTASIS

A, ELISA analysis of TGF-β1 levels in culture medium conditioned by $PyMT^{+/+}$ or $PyMT^{+/-}$ cancer

cell cultures (n = 3). **B-D,** Profiling of proteins in supernatant from $PyMT^{+/+}$ (A) and $PyMT^{+/-}$ (B) cancer cells. Quantification of detected proteins is indicated in panel D (n = 3; p = ns; only proteins detected in 3 independent experiments have been included in the quantification). **E,** Immunoblotting for PHD2 of $PyMT^{TC\text{-}WT}$ and $PyMT^{TC\text{-}HE}$ cancer cell total lysates. Actin was used as loading control. Densitometric quantification is shown underneath the lanes (n = 3). **F,G**, RT-PCR analysis of *Egln1* mRNA levels in cancer cells (F) and CAFs (G), isolated from $PyMT^{TC\text{-}WT}$ and $PyMT^{TC\text{-}HE}$ tumors (n > 3). **H,I**, ELISA analysis of TGF-β1 levels in extracts of $PyMT^{TC\text{-}WT}$ or $PyMT^{TC\text{-}HE}$ tumors (H; n = 5) or in culture medium conditioned by $PyMT^{TC\text{-}WT}$ or $PyMT^{TC\text{-}HE}$ cancer cell cultures (I; n = 3). **J,** Growth curve of individual tumors in $PyMT^{TC\text{-}WT}$ and $PyMT^{TC\text{-}HE}$ mice (n = 5-10; p = ns). **K,L,** Pulmonary metastatic nodules (arrowheads) in 16 week old $PyMT^{TC\text{-}WT}$ (K) and $PyMT^{TC\text{-}HE}$ (L) mice, visualized by Indian ink perfusion. The number of pulmonary metastases is indicated (n = 18-28; t-test with Welch's correction). **M,** Metastatic index in $PyMT^{TC\text{-}WT}$ and $PyMT^{TC\text{-}HE}$ tumor bearing mice (n = 18-28; t-test with Welch's correction. **N,** RT-PCR analysis for *Pymt* in blood samples as a measure of the number of CTCs in $PyMT^{TC\text{-}WT}$ and $PyMT^{TC\text{-}HE}$ mice (n = 6-8; t-test with Welch's correction). Bar: 750 μm (K,L). All quantitative data are mean ± SEM. * p < 0.05, ** p < 0.01, *** p < 0.001.

Analysis TGF-β1 in tumor cell supernatans as well as in $PyMT^{TC\text{-}HE}$ tumor extracts confirmed the reduced levels of secreted TGF-β1 (Figure 16H,I). Similar to $PyMT^{+/-}$ mice, tumor growth was not affected (Figure 16J), while metastasis and circulating tumor cells (CTCs) were decreased in $PyMT^{TC\text{-}HE}$ mice (Figure 16K-N). These results suggest that PHD2 haplodeficiency in TCs could explain the reduced activation of CAFs and metastasis in globally haplodeficient $PyMT^{+/-}$ mice.

PHD2 HAPLODEFICIENCY SELECTIVELY IN CANCER CELLS DOES NOT AFFECT CANCER CELL INTRINSIC PROPERTIES

To exclude that this reduction in metastasis was dependent on PHD2-mediated tumor cell-intrinsic changes, we analysed the invasive behaviour and EMT-phenotype of $PyMT^{TC\text{-}WT}$ and $PyMT^{TC\text{-}HE}$ cancer cells. These tests confirmed that no changes in cancer cell migration, tumor spheroids invasion and minimal changes in EMT are caused by PHD2 haplodeficiency in tumor cells (Figure 17A-I), in line with previous findings which documented that in the MMTV-PyMT tumor model malignant epithelial cells undergo only minimal EMT, yet are capable of disseminating (Trimboli et al., 2008; Waldmeier et al., 2012).

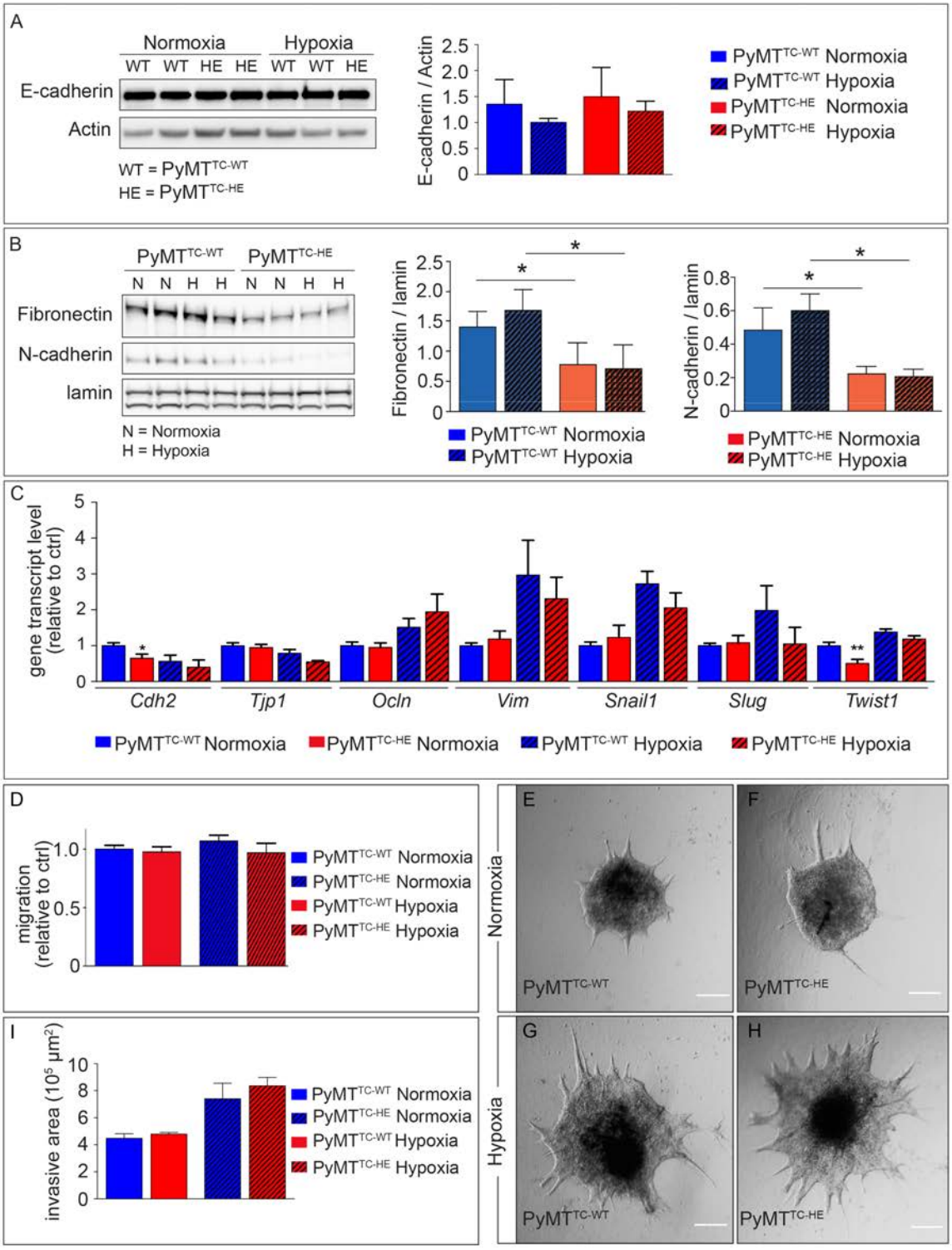

FIGURE 17: CANCER CELL PHD2 HAPLODEFICIENCY DOES NOT AFFECT INVASION

A,B, Immunoblotting and densitometric quantification of EMT protein levels (E-cadherin (A), N-cadherin (B), Fibronectin (B)) in PyMT$^{TC\text{-}WT}$ and PyMT$^{TC\text{-}HE}$ cancer cell lysates (n = 3 independent experiments; analyzed by mixed model statistics). Actin or lamin was used as loading control. **C**, RT-PCR analysis of EMT genes in PyMT$^{TC\text{-}WT}$ and PyMT$^{TC\text{-}HE}$ cancer cells (n = 3). **D**, Scratch wound assay: analysis of PyMT$^{TC\text{-}WT}$ and PyMT$^{TC\text{-}HE}$ cancer cell migration in normoxia or hypoxia (n = 4-6; p = ns). **E-I**, Cancer cell spheroid invasion assay: analysis of collective invasion of

PyMT^{TC-WT} and PyMT^{TC-HE} cancer cells into a collagen I matrix in normoxia (E,F) or hypoxia (G,H). Note that cancer cells invade collectively as sheets with emerging sprouts. Panel I shows the morphometric quantification of the area of the entire invasive spheroid (see methods) (n > 45 spheroids; p = ns). Bar: 100 µm (E-H). All quantitative data are mean ± SEM. * $p < 0.05$, ** $p < 0.01$.

REDUCED ACTIVATION OF CAFS IN PYMT^{TC-HE} TUMORS

We then characterized the expression of several markers, known to be enriched in activated CAFs: FSP1, PDGFRα, and the contractile protein αSMA in PyMT^{TC-WT} and PyMT^{TC-HE} tumors *in situ*, and morphometrically quantified the CAF marker-positive area as a percent of the total tumor area. These analyses revealed that PyMT^{TC-HE} tumors, as compared to PyMT^{TC-WT} tumors, contained substantially fewer activated CAFs (Figure 18A-I). Also, gene expression profiling confirmed that CAFs isolated from PyMT^{TC-HE} tumors expressed lower levels of these markers, such as FSP1, PDGFRα and αSMA (*Acta2*) (Figure 18J). Moreover, stromal PyMT^{TC-HE} CAFs exhibited a lower proliferation rate, as measured by [^{3}H]-thymidine incorporation into DNA (Figure 18K). Similar to PyMT$^{+/-}$ tumors, PyMT^{TC-HE} tumors contained smaller amounts of fibrillar collagen (Figure 19A-C), which was less crosslinked (Figure 19D-F). Also, CAFs isolated from PyMT^{TC-HE} tumors had impaired matrix production (Figure 19G) and remodelling capacity *in vitro* (as assessed by their invasion into collagen I matrix (Figure 19H-J), expression of *Mmp2* and *Mmp9* (Figure 19K), and contractile capacity (Figure 19L). Moreover, PyMT^{TC-HE} CAFs did not stimulate the invasive behaviour of cancer cells to the same extent as CAFs, primed by PyMT^{TC-WT} cancer cells (Figure 19M-O).

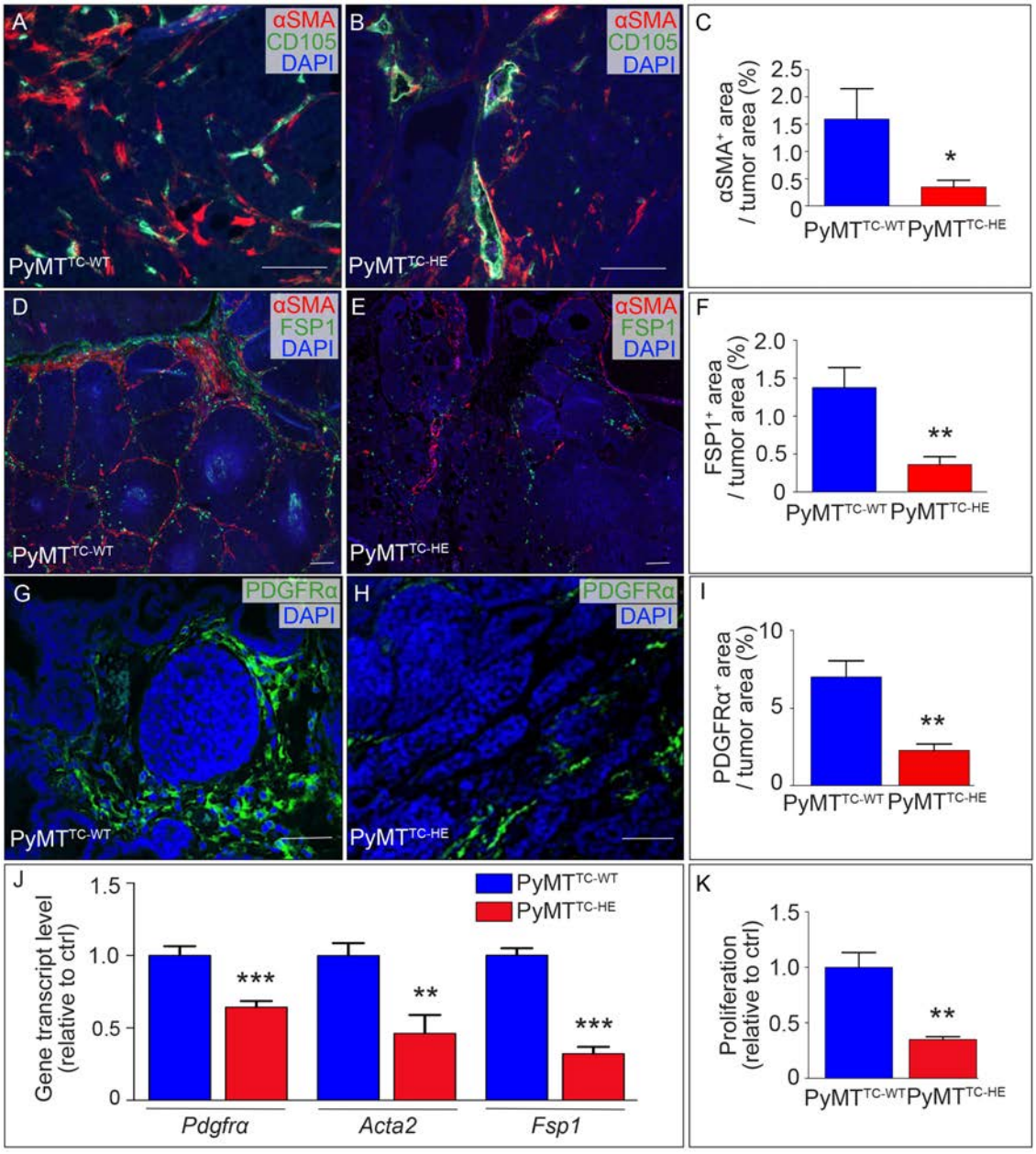

FIGURE 18: EFFECT OF CANCER CELL PHD2 HAPLODEFICIENCY ON CAF ACTIVATION

A-C, Double immunostaining of tumor sections from PyMT$^{TC\text{-}WT}$ (A) and PyMT$^{TC\text{-}HE}$ (B) mice for the CAF-enriched activation marker αSMA and the endothelial marker CD105, counterstained with DAPI. Panel C: quantification of the αSMA$^+$ area (% of tumor area) in both genotypes (n = 7). The staining of the endothelial cells was done to exclude the αSMA$^+$ perivascular smooth muscle cells. **D-F**, Double immunostaining of tumor sections from PyMT$^{TC\text{-}WT}$ (D) and PyMT$^{TC\text{-}HE}$ (E) mice for the CAF-enriched activation markers FSP1 and αSMA, counterstained with DAPI. Panel F: quantification of the FSP1$^+$ area (% of tumor area) (n = 7). The double staining for FSP1 and αSMA was done to illustrate the heterogeneity of the CAF population in the tumors. **G-I**, Staining of tumor sections from PyMT$^{TC\text{-}WT}$ (G) and PyMT$^{TC\text{-}HE}$ (H) mice for the CAF-enriched activation marker PDGFRα, counterstained with DAPI. Panel I: quantification of the PDGFRα$^+$ area (% of tumor area) in both genotypes (n = 7). **J**, RT-PCR analysis of genes associated with CAF activation (*Pdgfra, Acta2* (αSMA), *Fsp1*) in CAFs isolated from end-stage PyMT$^{TC\text{-}WT}$ and PyMT$^{TC\text{-}HE}$ tumors (n = 6-8). **K**, Proliferation ([3H]-thymidine incorporation) of CAFs isolated from

PyMT^{TC-WT} and PyMT^{TC-HE} tumors (n = 3-4). Bar: 50 µm (G,H), 100 µm (A,B,D,E). All quantitative data are mean ± SEM and statistical significance in (C,F,I) was analyzed with t-test with Welch's correction. * p < 0.05, ** p < 0.01, *** p < 0.001.

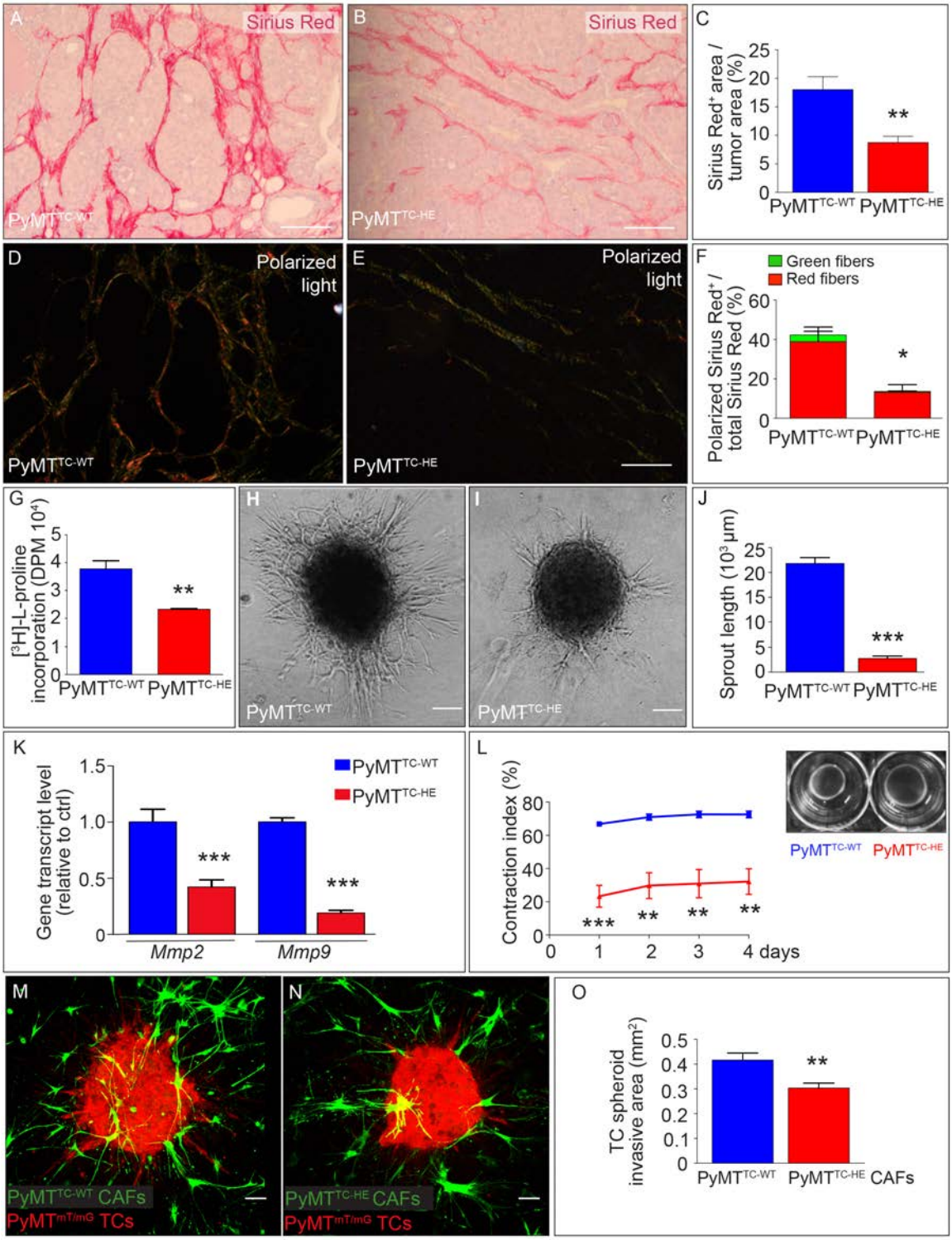

FIGURE 19: EFFECT OF CANCER CELL PHD2 HAPLODEFICIENCY ON ECM PRODUCTION AND LING BY CAFS

A-C, Picro Sirius Red staining of PyMT^{TC-WT} (A) and PyMT^{TC-HE} (B) tumor sections. Panel C:

quantification of Picro Sirius Red^{+} area (n = 7). **D-F**, Polarized light microscopy analysis of Picro Sirius Red stained PyMT$^{TC\text{-}WT}$ (D) and PyMT$^{TC\text{-}HE}$ (E) tumors to visualize thick cross-linked (red) versus thin non-cross-linked (green) collagen fibers. Panel F: quantifications of cross-linked and thin fibers (n = 7; t-test with Welch's correction). **G**, Quantification of matrix synthesis by CAFs isolated from PyMT$^{TC\text{-}WT}$ or PyMT$^{TC\text{-}HE}$ tumors as measured by an in vitro [^{3}H]-L-proline incorporation assay (n = 3); DPM, disintegrations per minute. **H-J**, CAF spheroid invasion assay using CAFs isolated from PyMT$^{TC\text{-}WT}$ (H) and PyMT$^{TC\text{-}HE}$ (I) tumors. Quantification of invasive sprout length is shown in panel J (n > 21 spheroids). **K**, RT-PCR analysis of *Mmp2* and *Mmp9* in CAFs isolated from PyMT$^{TC\text{-}WT}$ and PyMT$^{TC\text{-}HE}$ end stage tumors (n = 6-8). **L**, Collagen gel contraction assay using CAFs isolated from PyMT$^{TC\text{-}WT}$ or PyMT$^{TC\text{-}HE}$ tumors (n = 6; t-test with Welch's correction). Inset: representative pictures of contracted gel. To determine the contraction index, the area of the gel at the indicated time was substracted from the initial area of the gel at the beginning of the experiment, and this value was expressed as a percentage of the initial gel area. **M-O**, Invasion assay using spheroids of Tomato^{+} PyMT$^{mT/mG}$ tumor cells (TCs, red) in collagen gels into which GFP^{+} CAFs (green) isolated from PyMT$^{TC\text{-}WT}$ (M) or from PyMT$^{TC\text{-}HE}$ (N) tumors were homogeneously dispersed. Panel O: quantification of the area of the entire cancer cell spheroids (n > 18 spheroids). Bar: 50 µm (A,B,D,E), 100 µm (H,I,M,N). All quantitative data are mean ± SEM. * $p < 0.05$, ** $p < 0.01$, *** $p < 0.001$.

Overall, PyMT$^{TC\text{-}HE}$ CAFs were less activated, less proliferative, and had impaired capacity to remodel the ECM and, thus, did not enhance the invasive behaviour of cancer cells to the same extent as CAFs, primed by PyMT$^{TC\text{-}WT}$ cancer cells.

Although metastasis in PyMT$^{TC\text{-}HE}$ mice was reduced, the reduction was not to the same extent as in PyMT$^{+/-}$ mice, suggesting that blockade of PHD2 in both ECs and TCs is necessary to restrict metastasis more efficiently.

EDUCATION OF NORMAL FIBROBLASTS BY CANCER CELL-DERIVED TGF-ß1

To determine whether this decrease in TGF-β1 production by PyMT$^{TC\text{-}HE}$ cancer cells (Figure 16H,I) contributed to the reduced activation of CAFs, we cultured WT normal fibroblasts (NFs) with conditioned media from PyMT$^{TC\text{-}WT}$ or PyMT$^{TC\text{-}HE}$ cancer cells. Molecular and functional analysis indicated that NFs acquired the activated CAF-phenotype only when cultured in the presence of medium, conditioned by PyMT$^{TC\text{-}WT}$ but not by PyMT$^{TC\text{-}HE}$ cancer cells (Figure 20A-C). Furthermore, induction of the CAF phenotype was prevented when TGF-β1 was immuno-neutralized (Figure 20A-C), suggesting that indeed TGF-β1 is the regulator of CAF activation in the MMTV-PyMT tumor model.

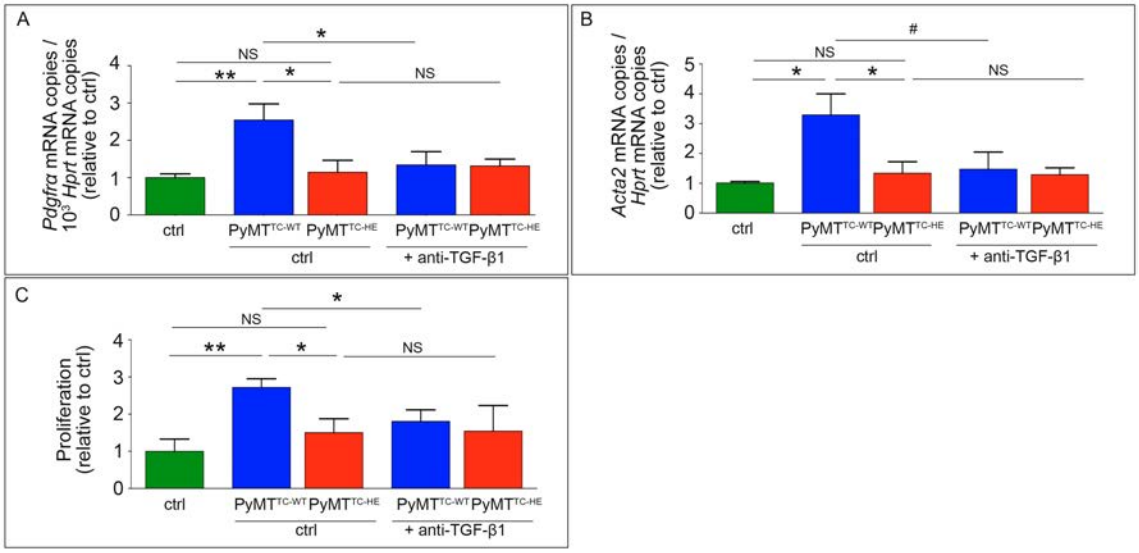

FIGURE 20: EFFECT OF CANCER CELL PHD2 HAPLODEFICIENCY ON PARACRINE TGF-β1 CROSS-TALK BETWEEN CANCER CELLS AND CAFS

A,B, RT-PCR analysis of the mRNA levels of the CAF activation markers *Pdgfra* (A) and *Acta 2* (αSMA; B) in normal fibroblasts cultured in medium conditioned by PyMT$^{TC\text{-}WT}$ or PyMT$^{TC\text{-}HE}$ cancer cells in the presence of a control or neutralizing antibody against TGF-β1 (n = 5-6). **C,** Proliferation ([^{3}H]-thymidine incorporation) of normal fibroblasts cultured in medium conditioned by PyMT$^{TC\text{-}WT}$ or PyMT$^{TC\text{-}HE}$ cancer cells in the presence of a control or neutralizing antibody against TGF-β1 (n = 3-6). All quantitative data are mean ± SEM. * $p < 0.05$, ** $p < 0.01$, $^{\#}$ $p = 0.08$, NS – not significant.

TRANSLATIONAL IMPLICATIONS

To explore whether inducible global inactivation of PHD2, initiated at the time of pre-invasive adenoma, can still prevent progression to metastatic disease, we used Rosa26:Cre^{ERT2} mice, intercrossed with MMTV-PyMT:PHD2$^{+/lox}$ mice (PyMT$^{R26\text{-}HE}$ mice). Tamoxifen treatment of PyMT$^{R26\text{-}HE}$ mice after onset (7 weeks, corresponding to 3 weeks after the first tumor nodules appeared; Figure 21A) of tumor growth failed to affect primary tumor growth but substantially reduced pulmonary metastasis (Figure 21B-D). Interestingly, homozygous deficiency of PHD2 (PyMT$^{R26\text{-}HO}$; Rosa26:Cre^{ERT2}:PHD2$^{lox/lox}$: MMTV-PyMT), not only decreased metastasis (Figure 21C,D), but also diminished primary tumor growth (Figure 21B). The underlying bases of this reduction of primary tumor growth still need to be investigated.

These results warrant further research to explore whether partial PHD2 inactivation in the neo-adjuvant setting would improve the delivery of chemotherapeutics and impair primary tumor growth by improving vessel function and decreasing interstitial fluid pressure in this spontaneously developing breast cancer model. Moreover, understanding the underlying mechanism of reduced primary tumor growth in $PyMT^{R26\text{-}HO}$ mice will be pivotal to design improved and safe breast cancer regimens of a pharmacological PHD2 blocker.

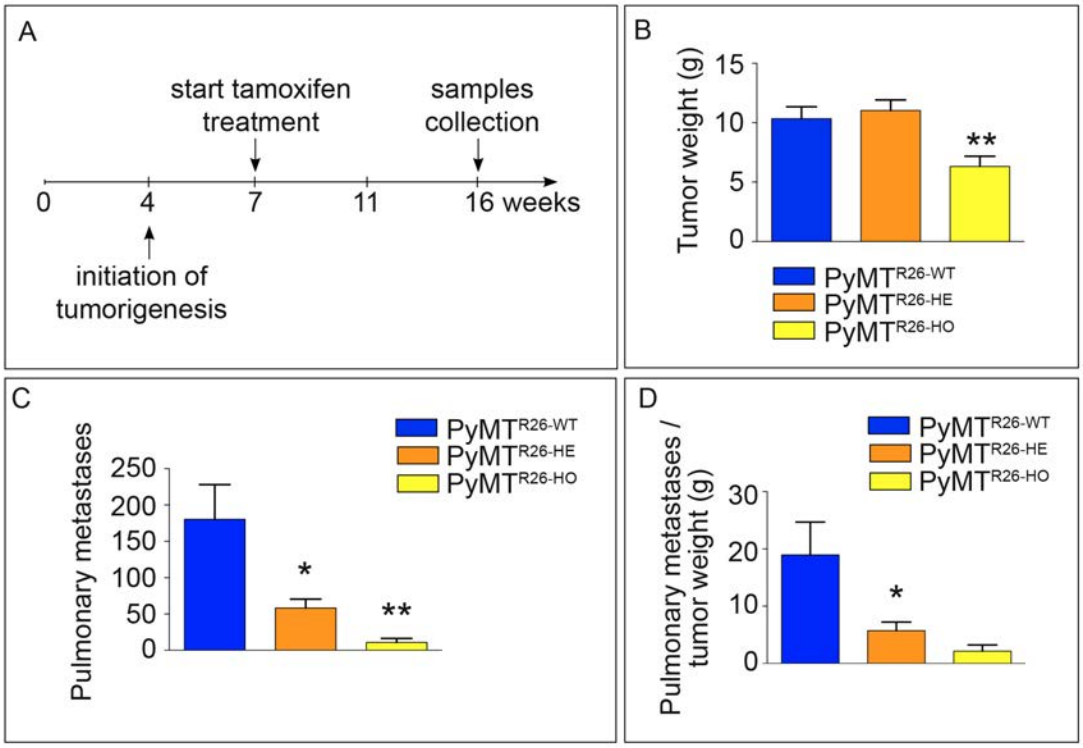

FIGURE 21: BLOCKADGE OF PHD2 AT LATER STAGES DIMINISHES PULMONARY METASTASIS
A, Scheme representing the time-course of tumor initiation, PHD2 exicision and sample collection. **B-D,** Tumor weight of tumors (B), number of pulmonary metastases (C) and metastatic index in $PyMT^{R26\text{-}WT}$, $PyMT^{R26\text{-}WT}$ and $PyMTR^{26\text{-}HO}$ mice at 16 weeks of age ($n > 5$; t-test with Welch's correction). All quantitative data are mean ± SEM. * $p < 0.05$, ** $p < 0.01$.

CHAPTER V

DISCUSSION

During the last decade, much progress has been made towards improved diagnosis and therapy. However, the treatment of metastasis remains an unmet medical challenge. The work presented in this thesis identifies the oxygen sensor PHD2 as a potential and promising target to reduce metastasis in BC. Using a spontaneously developing BC model we show that haplodeficiency of PHD2 in both cancer and stromal cells impaired pulmonary metastasis, without affecting primary tumor growth. Reduction of metastasis was mediated by two independent and distinct mechanisms: (i) tumor vessel normalization and (ii) reduced CAF activation as a result of altered paracrine crosstalk from cancer cells to stromal CAFs. In turn, primed CAFs reciprocally affected cancer cells by modulating their invasive behavior via pleiotropic effects on the extracellular matrix.

THE ROLE OF PHD2 IN CANCER

Numerous studies characterized the importance of hypoxia signaling in tumor biology, but the large majority of them focused on cancer cells (Klotzsche-von Ameln et al., 2011; Semenza, 2012; Su et al., 2012; Wottawa et al., 2012). Moreover, the role of PHD2, the key regulator of HIF1α, in tumorigenesis and metastasis remains largely unresolved. Previous studies described the role of PHD2 in regulating the behavior of cancer cells. However, divergent (even opposite) phenotypic effects have been reported. Indeed, silencing of PHD2 in cancer cells does either not affect, increases or reduces primary tumor growth (Bordoli et al., 2010; Chan et al., 2009; Klotzsche-von Ameln et al., 2011; Su et

al., 2012; Wottawa et al., 2012). These discordant results may be due to the different types of tumor models and experimental approaches used. Moreover, to date, only a single study evaluated the role of PHD2 in cancer cells on metastasis, and identified a role for PHD2 in the late steps of metastasis (Naba et al., 2014).

Moreover, the role of PHD2 in stromal cells adds an additional level of complexity. Selective PHD2 haplodeficiency in ECs reduced metastasis without affecting tumor growth, by normalizing the abnormal tumor vessels and reducing tumor cell intravasation (Mazzone et al., 2009), and deficiency of PHD2 in myeloid and T-cells decreased primary tumor growth (Mamlouk et al., 2014). These studies suggest that PHD2 could be an anti-BC drug target in stromal cells. However, it remained unclear what to expect when PHD2 is targeted in all cells of the tumor, both cancer cells and stroma, in a clinically more relevant spontaneously developing tumor model. Would primary tumor growth be increased, reduced or unchanged? What would be the effect of PHD2 blockade on metastasis?

By crossing PHD2 haplodeficient mice into the spontaneously developing breast cancer model MMTV-PyMT, closely resembling human luminal BC, we could evaluate the role of PHD2 in both cancer cells and the stroma. No effect of PHD2 haplodeficiency in cancer and stromal cells was observed on primary tumor growth in this study, but pulmonary metastasis and circulating tumor cells were significantly reduced. Moreover, further *in vitro* and *in vivo* phenotyping confirmed that there was no effect of PHD2 haplodeficiency on tumor proliferation and progression. These results support the concept of the oxygen sensor PHD2 being a potential drug target for decreasing metastatic disease and prolonging the survival of BC patients.

PHD2 HAPLODEFICIENCY IN CANCER AND STROMAL CELLS IMPROVES VESSEL STRUCTURE AND FUNCTION

Previous studies highlighted different possible effects on tumor angiogenesis (Bordoli et al., 2010; Klotzsche-von Ameln et al., 2011; Leite de Oliveira et al., 2012; Mazzone et al., 2009) or vasculogenesis (Chan et al., 2009) upon targeting of PHD2 in either ECs or in cancer cells. Development of the vasculature is necessary for tumor growth. When deprived of oxygen and nutrient supply, cancer cells stimulate the development of vessels by upregulating angiogenic factors such as VEGF, and this response is under control of PHD2 (Bordoli et al., 2010; Lee et al., 2008). However, this production of pro-angiogenic factors is often excessive in the tumor microenvironment. As a result, these growth signals turn into abnormalization factors, tilting the process of neovascularization towards unproductive angiogenesis, and leading to the formation of vessels with abnormal features (Carmeliet and Jain, 2011b). This may initiate a vicious self-sustaining cycle, in which tumor vessel abnormalities will impair tumor perfusion and increase intratumoral hypoxia, increasing abnormalization factors even more and amplifying vascular disorganization even more.

Coordinated responses of ECs and cancer cells to hypoxia regulate angiogenesis. Indeed, targeting one of these cell compartments in tumors induces a direct response on the other. Silencing PHD2 in cancer cells led to increased angiogenesis (Bordoli et al., 2010; Klotzsche-von Ameln et al., 2011) or vasculogenesis (Chan et al., 2009). On the other hand, haplodeficiency of PHD2 in ECs rendered them pre-adapted to hypoxia and favored the endothelial cell normalization responses. This lowered intratumoral hypoxia and thus decreased the invasive phenotype of cancer cells (Leite de Oliveira et al., 2012; Mazzone et al., 2009). Our analyses show that targeting PHD2 in both cancer and stromal cells did not affect vessel density. This seems surprising at first, given that PHD2 haplodeficiency in cancer cells increased HIF1α and HIF2α

levels in nuclear and cytoplasmic fractions, and thus would results in higher VEGF level. Previous studies indicated that PHD2 haplodeficient ECs are more quiescent, and their mitogenic and migratory responses to VEGF are impaired (Mazzone et al., 2009). Hence, they suggest that PHD2 haplodeficiency in ECs prevents excessive angiogenesis and maintains the same number of vessels as in WT conditions.

Further analysis confirmed that PHD2 haplodeficiency in ECs in the MMTV-PyMT spontaneous tumor model induced endothelial normalization in mice lacking PHD2 in cancer and stromal cells. Not only did vessels from $PyMT^{+/-}$ tumors have better EC lining and pericyte coverage, but their function was also improved. Consequently, intratumoral hypoxia was decreased in $PyMT^{+/-}$ tumors.

These results suggest that despite the increased pro-tumorigenic HIF1α levels in cancer cells, ECs, haplodeficient for PHD2, were able to retain their pro-quiescent phenotype and favor tumor vessel normalization. Importantly, analysis of metastatic dissemination in mice lacking one allele of PHD2 selectively in ECs revealed that the magnitude of reduction of metastasis was smaller in these $PyMT^{Tie2\text{-}HE}$ and $PyMT^{Cdh5\text{-}HE}$ mice than in $PyMT^{+/-}$ mice. This raised the question whether another cell population was also limiting the metastatic process in $PyMT^{+/-}$ mice.

PHD2-DEPENDENT REGULATION OF CANCER CELL INVASION BY CAFS

Malignant breast epithelial cells can invade tissues in different ways. When they undergo EMT and become mesenchymal in nature, they acquire invasive properties and are capable of breaching matrix-dense tissue barriers (Friedl and Wolf, 2003; Waldmeier et al., 2012). Alternatively, when they do not undergo EMT but remain epithelial in nature, they are still able to invade tissues via collective migration, especially when assisted by invasive CAFs (Calvo et al.,

2013; Friedl and Wolf, 2003). In line with previous reports (Trimboli et al., 2008; Waldmeier et al., 2012), we observed only minimal signs of EMT in this breast cancer model. Wild type cancer cells alone (i.e., without co-invading CAFs) invaded the collagen gel only minimally. PHD2 did not control these cancer cell-intrinsic invasive processes. In contrast, our data show that CAFs stimulated the invasion of cancer cells when they were co-cultured with cancer cells, a process that was under the control of PHD2 in the cancer cells.

CAFs can modulate cancer cell invasion via several complementary mechanisms. First, these stromal cells can alter cancer cell invasion by depositing bundles of cross-linked collagen, known migration "highways" for invading cancer cells (Lu et al., 2012). Our findings not only indicate that CAFs were a prominent source of matrix production in PyMT tumors, but also reveal that $PyMT^{+/-}$ and $PyMT^{TC\text{-}HE}$ CAFs deposited smaller amounts of thick bundles of cross-linked collagen. A second mechanism whereby CAFs might regulate cancer cell invasion is by remodeling the ECM via force-mediated contraction (Calvo et al., 2013). This process is part of a "mechano-reciprocal" response of CAFs to the heightened tensile forces in the tumor environment, which increases the contractility of these stromal cells (Lu et al., 2012). Contraction of the matrix induces physical movement and alignment of collagen fibers, which results in enhanced cross-linking of collagen fibers and increased matrix stiffness (Calvo et al., 2013). The importance of such matrix remodeling is highlighted by the fact that matrix stiffness promotes cancer cell invasion and dissemination (Provenzano et al., 2006). Noteworthy, since remodeling of the matrix by CAFs enhances the activation of the CAFs themselves, a self-sustaining feed-forward loop of CAF activation and matrix remodeling is initiated that progressively aggravates malignancy (Lu et al., 2012). Our findings indicate that $PyMT^{+/-}$ and

PyMT^{TC-HE} tumors not only contained fewer activated CAFs, but also that CAFs, primed by PHD2 haplodeficient cancer cells, expressed lower levels of the contractile protein αSMA, and effectively contracted the collagen gel less. Also, the amount of cross-linked collagen fibers was reduced in PyMT^{TC-HE} tumors.

A third mechanism relies on the remodeling of the tumor matrix by proteolysis. By proteolytically remodeling the ECM, CAFs can (i) physically free up space for invading cancer cells (ii) liberate matrix-bound migratory signals, or (iii) alter biochemical / structural properties of matrix components, all stimulating cancer cell migration (Cirri and Chiarugi, 2011). Our expression analysis showed that CAFs, primed by PHD2 haplodeficient cancer cells, produced less matrix-degrading metalloproteinases, providing circumstantial evidence for this mechanism.

Together, these mechanisms may provide a mechanistic explanation of how CAFs, primed by PHD2 haplodeficient cancer cells, did not enhance the invasive behavior of cancer cells to the same extent as CAFs, primed by wild type cancer cells. Since such invasive activity helps cancer cells to travel through the tumor matrix and breach the endothelial barrier during intravasation (van Zijl et al., 2011), these mechanisms can explain why metastasis was lower in PyMT^{TC-HE} and PyMT$^{+/-}$ than PyMT^{TC-WT} and PyMT$^{+/+}$ tumors.

The results from PyMT^{TC-HE} mice provided evidence of an additional mechanism through which PHD2 haplodeficiency in cancer and stromal cells reduces metastasis.

CAF ACTIVATION IS NOT DEPENDENT ON PHD2 LEVELS IN FIBROBLASTS

CAFs are an important stromal cell population, contributing up to 90% of the tumor mass in some tumors (Karagiannis et al., 2012). However, only a few

papers documented an involvement of hypoxia signaling in CAF behavior (Chiavarina et al., 2010; Gilkes et al., 2013; Kim et al., 2012). Not surprisingly, HIF1α in fibroblasts functions as a tumor promoter (Chiavarina et al., 2010). It is also a critical regulator of ECM remodeling by fibroblasts (Gilkes et al., 2013) and critical component of tumor vasculature (Kim et al., 2012). In line with these findings, transplantation of fibroblasts, silenced for PHD2 by 87.5%, in close proximity of a wound accelerated the wound healing process, by increasing fibroblast proliferation and angiogenesis at the wound site (Zhang et al., 2013). As PHD2 haplodeficiency in fibroblasts would result in increased HIF signaling, it might promote pro-tumorigenic effects, rather than contribute to a reduction in metastasis. Interestingly, haplodeficiency of PHD2 in fibroblasts did not affect tumor progression and metastatic dissemination, as compared to mice having wild type fibroblasts. Their characteristics were also unchanged *in vitro*, suggesting that PHD2 haplodeficiency in fibroblasts does not affect their intrinsic properties and thus does not contribute to the reduction of pulmonary metastasis in global PHD2 haplodeficient mice.

PHD2-DEPENDENT REGULATION OF TGF-β1 CROSSTALK

Silencing of PHD2 in a breast cancer cell line and in keratinocytes reduces TGF-β1 secretion (Kalucka et al., 2013; Wottawa et al., 2012). In agreement with these findings, PHD2 haplodeficiency in PyMT cancer cells also lowered the release of TGF-β1 from these malignant cells. Since TGF-β1 is an established inducer of the differentiation of normal fibroblasts to activated CAFs (Calon et al., 2014; Evans et al., 2003), the reduced release of TGF-β1 by $PyMT^{+/-}$ cancer cells could thus explain the reduced activation of $PyMT^{+/-}$ CAFs. Additionally, mRNA levels of *Sdf-1α* and *Tgf-β1* were lower in $PyMT^{+/-}$ than $PyMT^{+/+}$ CAFs. Since

these cytokines are released by activated CAFs as autocrine signals to maintain an activated state (Kojima et al., 2010), their reduced expression could further contribute to the decreased activation of $PyMT^{+/-}$ CAFs. Together, these data suggest a model where PHD2 haplodeficient cancer cells initially reduce the activation of CAFs releasing less paracrine TGF-β1 to the CAFs. Secondly, these hypo-activated CAFs in turn maintain their reduced activation status by expressing lower levels of the autocrine activation signals SDF-1α and TGF-β1, resulting in a self-sustaining loop.

TGF-β1 is the most potent factor inducing myofibroblast differentiation (Desmouliere et al., 1993; Ronnov-Jessen and Petersen, 1993) and one of the strongest cytokines regulating pro-fibrotic reactions (Branton and Kopp, 1999). It is also known that TGF-β signaling regulates cell-intrinsic responses in epithelial cells, normal fibroblasts and their transformed counterparts. The importance of TGF-β signaling in non-transformed epithelial cells has been well characterized. In healthy tissue, TGF-β1 inhibits epithelial cell proliferation, but stimulates the proliferation of fibroblasts (Giannouli and Kletsas, 2006; Strutz et al., 2001). However, cancer cells become insensitive to the growth arresting activity of TGF-β1 (Bierie and Moses, 2006; Siegel and Massague, 2003). In the same context, transdifferentiation of fibroblasts to myofibroblasts upon TGF-β1 stimulation has been associated with carcinoma progression by increased myofibroblast-derived production of HGF (De Wever et al., 2004; Lewis et al., 2004). However, when TGF-β signaling was lost in FSP-1 expressing fibroblasts (by conditional deletion of exon 2 from *Tgf-βR2* in the FSP1-expressing fibroblast population), carcinoma initiation, progression and metastasis were enhanced by the release of the tumor-promoting paracrine signals TGF-α, Mst-1 and HGF (Bhowmick et al., 2004; Cheng et al., 2005). Additionally, heterozygous deletion of *Tgf-βR2* in

FSP1^{+} fibroblasts does not significantly affect tumor growth, but increases pulmonary metastasis (Fang et al., 2011). This highlights the differential role of TGF-β signaling in non-transformed fibroblasts, where TGF-β can suppress HGF expression. However, once fibroblasts are transdifferentiated into myofibroblast, they can promote HGF signaling. Moreover, TGF-β derived from CAFs can regulate tumor progression by increasing the expression of CXCR-4 on cancer cells and thereby enhancing their response to SDF-1, abundantly produced by CAFs (Ao et al., 2007). Our results show that cancer cell-secreted TGF-β1 regulated the transdifferentiation of myofibroblast in PyMT$^{+/+}$ and PyMT$^{TC\text{-}WT}$ tumors. This activation of CAFs was impaired in PyMT$^{+/-}$ and PyMT$^{TC\text{-}HE}$ mice. As a consequence, PyMT$^{+/-}$ and PyMT$^{TC\text{-}HE}$ CAFs had diminished, but not completely ablated, *Tgf-β1* and *Sdf-1* mRNA levels, but *Tgf-βR2* mRNA levels were not changed. These results suggest that PyMT$^{+/-}$ and PyMT$^{TC\text{-}HE}$ CAFs are still able to respond to surrounding TGF-β ligands and thus this might prevent the production of tumor-promoting paracrine signals. Additionally, conditional deletion of PHD2 in fibroblasts did not alter tumor growth and metastasis, suggesting that TGF-β signaling might not have been impaired in this cell type.

Overall, these diverse and opposing biological functions of TGF-β signaling in cancer at different stages of tumor development and progression make it a challenging target for cancer therapy. Potentially, partial blockade of TGF-β signaling, by upstream targeting at cell-specific site, might be a strategy to inhibit the pro-tumorigenic axis of this pathway.

POSSIBLE TRANSLATIONAL IMPLICATIONS

Finally, our genetic data might have translational implications, as they identify PHD2 as pro-metastatic factor. We have not only observed that PHD2

haplodeficiency normalizes tumor blood vessels, but also that it impaired CAF activation.

From a conceptual perspective, it is puzzling that inactivation of PHD2 by hypoxia in the tumor microenvironment suppresses the pro-metastatic activity of CAFs, given the vast literature that hypoxia promotes metastasis (De Bock et al., 2011; Semenza, 2012). The precise pathophysiological purpose of this phenomenon remains to be elucidated. Regardless however, from a therapeutic perspective, blocking this CAF-dependent pro-metastatic activity of PHD2 might offer novel opportunities to suppress cancer cell dissemination. In fact, the results of this study highlight the importance of CAFs in promoting metastasis, and illustrate that even in the absence of prominent alterations in the intrinsic invasive behavior of cancer cells (migration, EMT, etc), a change in CAF behavior suffices to impair metastasis. Moreover, we provide genetic evidence that global PHD2 haplodeficiency from the start of tumorigenesis is not only well tolerated, but also reduces metastatic disease. Intrestingly, PHD2 blockadge seems sufficient to reduce metastasis when initiated at the later stages, when invasive adenoma is already present. This implies that administration of a pharmacological PHD2 blocker, which would inhibit PHD2 in both cancer and stromal cells, might be therapeutically considered to prevent / minimize metastatic disease.

CHAPTER VI

CONCLUSION AND FUTURE PROSPECTS

This work provides evidence that blocking PHD2 in cancer and stromal cells of the spontaneously developing BC model, MMTV-PyMT, did not affect primary tumor growth but resulted in a substantial reduction of pulmonary metastasis. We revealed that reduced metastasis was related to both tumor vessel normalization and impaired paracrine cross-talk between cancer cells and fibroblasts. TGF-β1 secretion was reduced in PHD2 haplodeficient cancer cells, which subsequently led to reduced fibroblast transdifferentiation into CAFs. While cancer cells activate fibroblasts in the tumor stroma, CAFs modulate the local microenvironment (by remodelling and contracting the ECM) for cancer cells to enable their invasion and dissemination to distant organs. The diminished CAF activation in $PyMT^{+/-}$ and $PyMT^{TC\text{-}HE}$ tumors reduced CAF-mediated cancer cell invasion.

These results suggest that blocking PHD2 in cancer cells could be beneficial to restrain metastatic dissemination in BC patients, and could thus be considered as a potential target for novel anti-metastatic drugs. We do not exclude the possibility that blocking PHD2 might impair metastasis via additional complemantary mechanisms. For instance, effects on the pre-metastatic niche and outgrowth from micro- to macro-metastasis, as it has been recently reported (Naba et al., 2014), should be further evaluated in a spontaneously arising tumor model.

REFERENCES

Aguirre-Ghiso, J. A. (2007). Models, mechanisms and clinical evidence for cancer dormancy. Nat Rev Cancer *7*, 834-846.

Ao, M., Franco, O. E., Park, D., Raman, D., Williams, K., and Hayward, S. W. (2007). Cross-talk between paracrine-acting cytokine and chemokine pathways promotes malignancy in benign human prostatic epithelium. Cancer Res *67*, 4244-4253.

Aragones, J., Schneider, M., Van Geyte, K., Fraisl, P., Dresselaers, T., Mazzone, M., Dirkx, R., Zacchigna, S., Lemieux, H., Jeoung, N. H*., et al.* (2008). Deficiency or inhibition of oxygen sensor Phd1 induces hypoxia tolerance by reprogramming basal metabolism. Nat Genet *40*, 170-180.

Augsten, M. (2014). Cancer-associated fibroblasts as another polarized cell type of the tumor microenvironment. Frontiers in oncology *4*, 62.

Baish, J. W., Gazit, Y., Berk, D. A., Nozue, M., Baxter, L. T., and Jain, R. K. (1996). Role of tumor vascular architecture in nutrient and drug delivery: an invasion percolation-based network model. Microvasc Res *51*, 327-346.

Barkan, D., Green, J. E., and Chambers, A. F. (2010). Extracellular matrix: a gatekeeper in the transition from dormancy to metastatic growth. Eur J Cancer *46*, 1181-1188.

Bellini, A., and Mattoli, S. (2007). The role of the fibrocyte, a bone marrow-derived mesenchymal progenitor, in reactive and reparative fibroses. Lab Invest *87*, 858-870.

Benedito, R., Rocha, S. F., Woeste, M., Zamykal, M., Radtke, F., Casanovas, O., Duarte, A., Pytowski, B., and Adams, R. H. (2012). Notch-dependent VEGFR3 upregulation allows angiogenesis without VEGF-VEGFR2 signalling. Nature *484*, 110-114.

Bergers, G., and Benjamin, L. E. (2003). Tumorigenesis and the angiogenic switch. Nat Rev Cancer *3*, 401-410.

Bergers, G., and Hanahan, D. (2008). Modes of resistance to anti-angiogenic therapy. Nat Rev Cancer *8*, 592-603.

Berra, E., Benizri, E., Ginouves, A., Volmat, V., Roux, D., and Pouyssegur, J. (2003). HIF prolyl-hydroxylase 2 is the key oxygen sensor setting low steady-state levels of HIF-1alpha in normoxia. Embo J *22*, 4082-4090.

Bertout, J. A., Patel, S. A., and Simon, M. C. (2008). The impact of O2 availability on human cancer. Nat Rev Cancer *8*, 967-975.

Bhowmick, N. A., Chytil, A., Plieth, D., Gorska, A. E., Dumont, N., Shappell, S., Washington, M. K., Neilson, E. G., and Moses, H. L. (2004). TGF-beta signaling in fibroblasts modulates the oncogenic potential of adjacent epithelia. Science *303*, 848-851.

Bierie, B., and Moses, H. L. (2006). Tumour microenvironment: TGFbeta: the molecular Jekyll and Hyde of cancer. Nat Rev Cancer *6*, 506-520.

Bishop, T., Gallagher, D., Pascual, A., Lygate, C. A., de Bono, J. P., Nicholls, L. G., Ortega-Saenz, P., Oster, H., Wijeyekoon, B., Sutherland, A. I*., et al.* (2008). Abnormal sympathoadrenal development and systemic hypotension in PHD3-/- mice. Mol Cell Biol *28*, 3386-3400.

Bordoli, M. R., Stiehl, D. P., Borsig, L., Kristiansen, G., Hausladen, S., Schraml, P., Wenger, R. H., and Camenisch, G. (2010). Prolyl-4-hydroxylase PHD2- and hypoxia-inducible factor 2-dependent regulation of amphiregulin contributes to breast tumorigenesis. Oncogene *30*, 548-560.

Boyd, N. F., Dite, G. S., Stone, J., Gunasekara, A., English, D. R., McCredie, M. R., Giles, G. G., Tritchler, D., Chiarelli, A., Yaffe, M. J., and Hopper, J. L. (2002). Heritability of mammographic density, a risk factor for breast cancer. N Engl J Med *347*, 886-894.

Branton, M. H., and Kopp, J. B. (1999). TGF-beta and fibrosis. Microbes Infect *1*, 1349-1365.

Bruick, R. K., and McKnight, S. L. (2001). A conserved family of prolyl-4-hydroxylases that modify HIF. Science *294*, 1337-1340.

Butler, T. P., and Gullino, P. M. (1975). Quantitation of cell shedding into efferent blood of mammary adenocarcinoma. Cancer Res *35*, 512-516.

Calon, A., Tauriello, D. V., and Batlle, E. (2014). TGF-beta in CAF-mediated tumor growth and metastasis. Semin Cancer Biol *25*, 15-22.

Calvo, F., Ege, N., Grande-Garcia, A., Hooper, S., Jenkins, R. P., Chaudhry, S. I., Harrington, K., Williamson, P., Moeendarbary, E., Charras, G., and Sahai, E. (2013). Mechanotransduction and YAP-dependent matrix remodelling is required for the generation and maintenance of cancer-associated fibroblasts. Nat Cell Biol *15*, 637-646.

Carmeliet, P., Ferreira, V., Breier, G., Pollefeyt, S., Kieckens, L., Gertsenstein, M., Fahrig, M., Vandenhoeck, A., Harpal, K., Eberhardt, C*., et al.* (1996). Abnormal blood vessel development and lethality in embryos lacking a single VEGF allele. Nature *380*, 435-439.

Carmeliet, P., and Jain, R. K. (2000). Angiogenesis in cancer and other diseases. Nature *407*, 249-257.

Carmeliet, P., and Jain, R. K. (2011a). Molecular mechanisms and clinical applications of angiogenesis. Nature *473*, 298-307.

Carmeliet, P., and Jain, R. K. (2011b). Principles and mechanisms of vessel normalization for cancer and other angiogenic diseases. Nat Rev Drug Discov *10*, 417-427.

Carmeliet, P., Moons, L., Luttun, A., Vincenti, V., Compernolle, V., De Mol, M., Wu, Y., Bono, F., Devy, L., Beck, H*., et al.* (2001). Synergism between vascular endothelial growth factor and placental growth factor contributes to angiogenesis and plasma extravasation in pathological conditions. Nat Med *7*, 575-583.

Chambers, A. F., Groom, A. C., and MacDonald, I. C. (2002). Dissemination and growth of cancer cells in metastatic sites. Nat Rev Cancer *2*, 563-572.

Chan, D. A., Kawahara, T. L., Sutphin, P. D., Chang, H. Y., Chi, J. T., and Giaccia, A. J. (2009). Tumor vasculature is regulated by PHD2-mediated angiogenesis and bone marrow-derived cell recruitment. Cancer Cell *15*, 527-538.

Chen, N., Rinner, O., Czernik, D., Nytko, K. J., Zheng, D., Stiehl, D. P., Zamboni, N., Gstaiger, M., and Frei, C. (2011). The oxygen sensor PHD3 limits glycolysis under hypoxia via direct binding to pyruvate kinase. Cell Res *21*, 983-986.

Cheng, N., Bhowmick, N. A., Chytil, A., Gorksa, A. E., Brown, K. A., Muraoka, R., Arteaga, C. L., Neilson, E. G., Hayward, S. W., and Moses, H. L. (2005). Loss of TGF-beta type II receptor in fibroblasts promotes mammary carcinoma growth and invasion through upregulation of TGF-alpha-, MSP- and HGF-mediated signaling networks. Oncogene *24*, 5053-5068.

Chiavarina, B., Whitaker-Menezes, D., Migneco, G., Martinez-Outschoorn, U. E., Pavlides, S., Howell, A., Tanowitz, H. B., Casimiro, M. C., Wang, C., Pestell, R. G*., et al.* (2010). HIF1-alpha functions as a tumor promoter in cancer associated fibroblasts, and as a tumor suppressor in breast cancer cells: Autophagy drives compartment-specific oncogenesis. Cell Cycle *9*, 3534-3551.

Cirri, P., and Chiarugi, P. (2011). Cancer associated fibroblasts: the dark side of the coin. Am J Cancer Res *1*, 482-497.

Condeelis, J., and Segall, J. E. (2003). Intravital imaging of cell movement in tumours. Nat Rev Cancer *3*, 921-930.

Conklin, M. W., Eickhoff, J. C., Riching, K. M., Pehlke, C. A., Eliceiri, K. W., Provenzano, P. P., Friedl, A., and Keely, P. J. (2011). Aligned collagen is a prognostic signature for survival in human breast carcinoma. Am J Pathol *178*, 1221-1232.

Couvelard, A., Deschamps, L., Rebours, V., Sauvanet, A., Gatter, K., Pezzella, F., Ruszniewski, P., and Bedossa, P. (2008). Overexpression of the oxygen sensors PHD-1, PHD-2, PHD-3, and FIH Is associated with tumor aggressiveness in pancreatic endocrine tumors. Clin Cancer Res *14*, 6634-6639.

Cummins, E. P., Berra, E., Comerford, K. M., Ginouves, A., Fitzgerald, K. T., Seeballuck, F., Godson, C., Nielsen, J. E., Moynagh, P., Pouyssegur, J., and Taylor, C. T. (2006). Prolyl hydroxylase-1 negatively regulates IkappaB kinase-beta, giving insight into hypoxia-induced NFkappaB activity. Proc Natl Acad Sci U S A *103*, 18154-18159.

Cummins, E. P., and Taylor, C. T. (2005). Hypoxia-responsive transcription factors. Pflugers Arch *450*, 363-371.

Dang, L., White, D. W., Gross, S., Bennett, B. D., Bittinger, M. A., Driggers, E. M., Fantin, V. R., Jang, H. G., Jin, S., Keenan, M. C.*, et al.* (2009). Cancer-associated IDH1 mutations produce 2-hydroxyglutarate. Nature *462*, 739-744.

Dankort, D. L., and Muller, W. J. (2000). Signal transduction in mammary tumorigenesis: a transgenic perspective. Oncogene *19*, 1038-1044.

De Bock, K., Georgiadou, M., Schoors, S., Kuchnio, A., Wong, B. W., Cantelmo, A. R., Quaegebeur, A., Ghesquiere, B., Cauwenberghs, S., Eelen, G.*, et al.* (2013). Role of PFKFB3-driven glycolysis in vessel sprouting. Cell *154*, 651-663.

De Bock, K., Mazzone, M., and Carmeliet, P. (2011). Antiangiogenic therapy, hypoxia, and metastasis: risky liaisons, or not? Nature reviews Clinical oncology *8*, 393-404.

De Smet, F., Segura, I., De Bock, K., Hohensinner, P. J., and Carmeliet, P. (2009). Mechanisms of vessel branching: filopodia on endothelial tip cells lead the way. Arterioscler Thromb Vasc Biol *29*, 639-649.

De Wever, O., Nguyen, Q. D., Van Hoorde, L., Bracke, M., Bruyneel, E., Gespach, C., and Mareel, M. (2004). Tenascin-C and SF/HGF produced by myofibroblasts in vitro provide convergent pro-invasive signals to human colon cancer cells through RhoA and Rac. Faseb J *18*, 1016-1018.

Desmouliere, A., Geinoz, A., Gabbiani, F., and Gabbiani, G. (1993). Transforming growth factor-beta 1 induces alpha-smooth muscle actin expression in granulation tissue myofibroblasts and in quiescent and growing cultured fibroblasts. J Cell Biol *122*, 103-111.

Duda, D. G., Duyverman, A. M., Kohno, M., Snuderl, M., Steller, E. J., Fukumura, D., and Jain, R. K. (2010). Malignant cells facilitate lung metastasis by bringing their own soil. Proc Natl Acad Sci U S A *107*, 21677-21682.

Dvorak, H. F., Nagy, J. A., Feng, D., Brown, L. F., and Dvorak, A. M. (1999). Vascular permeability factor/vascular endothelial growth factor and the significance of microvascular hyperpermeability in angiogenesis. Curr Top Microbiol Immunol *237*, 97-132.

Ebos, J. M., Lee, C. R., Cruz-Munoz, W., Bjarnason, G. A., Christensen, J. G., and Kerbel, R. S. (2009). Accelerated metastasis after short-term treatment with a potent inhibitor of tumor angiogenesis. Cancer Cell *15*, 232-239.

Egeblad, M., Ewald, A. J., Askautrud, H. A., Truitt, M. L., Welm, B. E., Bainbridge, E., Peeters, G., Krummel, M. F., and Werb, Z. (2008). Visualizing stromal cell dynamics in different tumor

microenvironments by spinning disk confocal microscopy. Dis Model Mech *1*, 155-167; discussion 165.

Ehrismann, D., Flashman, E., Genn, D. N., Mathioudakis, N., Hewitson, K. S., Ratcliffe, P. J., and Schofield, C. J. (2007). Studies on the activity of the hypoxia-inducible-factor hydroxylases using an oxygen consumption assay. Biochem J *401*, 227-234.

Epstein, A. C., Gleadle, J. M., McNeill, L. A., Hewitson, K. S., O'Rourke, J., Mole, D. R., Mukherji, M., Metzen, E., Wilson, M. I., Dhanda, A.*, et al.* (2001). C. elegans EGL-9 and mammalian homologs define a family of dioxygenases that regulate HIF by prolyl hydroxylation. Cell *107*, 43-54.

Erler, J. T., Bennewith, K. L., Cox, T. R., Lang, G., Bird, D., Koong, A., Le, Q. T., and Giaccia, A. J. (2009). Hypoxia-induced lysyl oxidase is a critical mediator of bone marrow cell recruitment to form the premetastatic niche. Cancer Cell *15*, 35-44.

Erler, J. T., Bennewith, K. L., Nicolau, M., Dornhofer, N., Kong, C., Le, Q. T., Chi, J. T., Jeffrey, S. S., and Giaccia, A. J. (2006). Lysyl oxidase is essential for hypoxia-induced metastasis. Nature *440*, 1222-1226.

Evans, R. A., Tian, Y. C., Steadman, R., and Phillips, A. O. (2003). TGF-beta1-mediated fibroblast-myofibroblast terminal differentiation-the role of Smad proteins. Exp Cell Res *282*, 90-100.

Falanga, V., Qian, S. W., Danielpour, D., Katz, M. H., Roberts, A. B., and Sporn, M. B. (1991). Hypoxia upregulates the synthesis of TGF-beta 1 by human dermal fibroblasts. J Invest Dermatol *97*, 634-637.

Falcon, B. L., Hashizume, H., Koumoutsakos, P., Chou, J., Bready, J. V., Coxon, A., Oliner, J. D., and McDonald, D. M. (2009). Contrasting actions of selective inhibitors of angiopoietin-1 and angiopoietin-2 on the normalization of tumor blood vessels. Am J Pathol *175*, 2159-2170.

Fang, W. B., Jokar, I., Chytil, A., Moses, H. L., Abel, T., and Cheng, N. (2011). Loss of one Tgfbr2 allele in fibroblasts promotes metastasis in MMTV: polyoma middle T transgenic and transplant mouse models of mammary tumor progression. Clin Exp Metastasis *28*, 351-366.

Ferlay, J., Soerjomataram, I., Dikshit, R., Eser, S., Mathers, C., Rebelo, M., Parkin, D. M., Forman, D., and Bray, F. (2015). Cancer incidence and mortality worldwide: Sources, methods and major patterns in GLOBOCAN 2012. Int J Cancer *136*, E359-386.

Ferrara, N., Carver-Moore, K., Chen, H., Dowd, M., Lu, L., O'Shea, K. S., Powell-Braxton, L., Hillan, K. J., and Moore, M. W. (1996). Heterozygous embryonic lethality induced by targeted inactivation of the VEGF gene. Nature *380*, 439-442.

Fischer, C., Jonckx, B., Mazzone, M., Zacchigna, S., Loges, S., Pattarini, L., Chorianopoulos, E., Liesenborghs, L., Koch, M., De Mol, M.*, et al.* (2007). Anti-PlGF inhibits growth of VEGF(R)-inhibitor-resistant tumors without affecting healthy vessels. Cell *131*, 463-475.

Folkman, J. (1971). Tumor angiogenesis: therapeutic implications. N Engl J Med *285*, 1182-1186.

Fraisl, P., Aragones, J., and Carmeliet, P. (2009). Inhibition of oxygen sensors as a therapeutic strategy for ischaemic and inflammatory disease. Nature reviews Drug discovery *8*, 139-152.

Friedl, P., and Alexander, S. (2011). Cancer invasion and the microenvironment: plasticity and reciprocity. Cell *147*, 992-1009.

Friedl, P., and Gilmour, D. (2009). Collective cell migration in morphogenesis, regeneration and cancer. Nat Rev Mol Cell Biol *10*, 445-457.

Friedl, P., and Wolf, K. (2003). Tumour-cell invasion and migration: diversity and escape mechanisms. Nat Rev Cancer *3*, 362-374.

Frisch, S. M., and Francis, H. (1994). Disruption of epithelial cell-matrix interactions induces apoptosis. J Cell Biol *124*, 619-626.

Fu, J., and Taubman, M. B. (2010). Prolyl hydroxylase EGLN3 regulates skeletal myoblast differentiation through an NF-kappaB-dependent pathway. J Biol Chem *285*, 8927-8935.

Fu, J., and Taubman, M. B. (2013). EGLN3 inhibition of NF-kappaB is mediated by prolyl hydroxylase-independent inhibition of IkappaB kinase gamma ubiquitination. Mol Cell Biol *33*, 3050-3061.

Fyles, A., Milosevic, M., Hedley, D., Pintilie, M., Levin, W., Manchul, L., and Hill, R. P. (2002). Tumor hypoxia has independent predictor impact only in patients with node-negative cervix cancer. J Clin Oncol *20*, 680-687.

Gaggioli, C., Hooper, S., Hidalgo-Carcedo, C., Grosse, R., Marshall, J. F., Harrington, K., and Sahai, E. (2007). Fibroblast-led collective invasion of carcinoma cells with differing roles for RhoGTPases in leading and following cells. Nat Cell Biol *9*, 1392-1400.

Galaup, A., Cazes, A., Le Jan, S., Philippe, J., Connault, E., Le Coz, E., Mekid, H., Mir, L. M., Opolon, P., Corvol, P.*, et al.* (2006). Angiopoietin-like 4 prevents metastasis through inhibition of vascular permeability and tumor cell motility and invasiveness. Proc Natl Acad Sci U S A *103*, 18721-18726.

Gao, D., Nolan, D. J., Mellick, A. S., Bambino, K., McDonnell, K., and Mittal, V. (2008). Endothelial progenitor cells control the angiogenic switch in mouse lung metastasis. Science *319*, 195-198.

Garvalov, B. K., Foss, F., Henze, A. T., Bethani, I., Graf-Hochst, S., Singh, D., Filatova, A., Dopeso, H., Seidel, S., Damm, M.*, et al.* (2014). PHD3 regulates EGFR internalization and signalling in tumours. Nat Commun *5*, 5577.

Geiger, B., Bershadsky, A., Pankov, R., and Yamada, K. M. (2001). Transmembrane crosstalk between the extracellular matrix--cytoskeleton crosstalk. Nat Rev Mol Cell Biol *2*, 793-805.

Ghajar, C. M., Peinado, H., Mori, H., Matei, I. R., Evason, K. J., Brazier, H., Almeida, D., Koller, A., Hajjar, K. A., Stainier, D. Y.*, et al.* (2013). The perivascular niche regulates breast tumour dormancy. Nat Cell Biol *15*, 807-817.

Giaccia, A. J., and Schipani, E. (2010). Role of carcinoma-associated fibroblasts and hypoxia in tumor progression. Curr Top Microbiol Immunol *345*, 31-45.

Giancotti, F. G. (2013). Mechanisms governing metastatic dormancy and reactivation. Cell *155*, 750-764.

Giannouli, C. C., and Kletsas, D. (2006). TGF-beta regulates differentially the proliferation of fetal and adult human skin fibroblasts via the activation of PKA and the autocrine action of FGF-2. Cell Signal *18*, 1417-1429.

Gilkes, D. M., Bajpai, S., Chaturvedi, P., Wirtz, D., and Semenza, G. L. (2013). Hypoxia-inducible factor 1 (HIF-1) promotes extracellular matrix remodeling under hypoxic conditions by inducing P4HA1, P4HA2, and PLOD2 expression in fibroblasts. J Biol Chem *288*, 10819-10829.

Goel, S., Duda, D. G., Xu, L., Munn, L. L., Boucher, Y., Fukumura, D., and Jain, R. K. (2011). Normalization of the vasculature for treatment of cancer and other diseases. Physiol Rev *91*, 1071-1121.

Goetz, J. G., Minguet, S., Navarro-Lerida, I., Lazcano, J. J., Samaniego, R., Calvo, E., Tello, M., Osteso-Ibanez, T., Pellinen, T., Echarri, A.*, et al.* (2011). Biomechanical remodeling of the microenvironment by stromal caveolin-1 favors tumor invasion and metastasis. Cell *146*, 148-163.

Goss, P. E., and Chambers, A. F. (2010). Does tumour dormancy offer a therapeutic target? Nat Rev Cancer *10*, 871-877.

Goswami, S., Sahai, E., Wyckoff, J. B., Cammer, M., Cox, D., Pixley, F. J., Stanley, E. R., Segall, J. E., and Condeelis, J. S. (2005). Macrophages promote the invasion of breast carcinoma cells via a colony-stimulating factor-1/epidermal growth factor paracrine loop. Cancer Res *65*, 5278-5283.

Guadamillas, M. C., Cerezo, A., and Del Pozo, M. A. (2011). Overcoming anoikis--pathways to anchorage-independent growth in cancer. J Cell Sci *124*, 3189-3197.

Gupta, G. P., and Massague, J. (2006). Cancer metastasis: building a framework. Cell *127*, 679-695.

Guy, C. T., Cardiff, R. D., and Muller, W. J. (1992). Induction of mammary tumors by expression of polyomavirus middle T oncogene: a transgenic mouse model for metastatic disease. Mol Cell Biol *12*, 954-961.

Haeger, A., Krause, M., Wolf, K., and Friedl, P. (2014). Cell jamming: collective invasion of mesenchymal tumor cells imposed by tissue confinement. Biochim Biophys Acta *1840*, 2386-2395.

Halim, H., Luanpitpong, S., and Chanvorachote, P. (2012). Acquisition of anoikis resistance up-regulates caveolin-1 expression in human non-small cell lung cancer cells. Anticancer Res *32*, 1649-1658.

Hanahan, D., and Weinberg, R. A. (2000). The hallmarks of cancer. Cell *100*, 57-70.

Hanahan, D., and Weinberg, R. A. (2011). Hallmarks of cancer: the next generation. Cell *144*, 646-674.

Hedley, B. D., and Chambers, A. F. (2009). Tumor dormancy and metastasis. Adv Cancer Res *102*, 67-101.

Heikkila, M., Pasanen, A., Kivirikko, K. I., and Myllyharju, J. (2011). Roles of the human hypoxia-inducible factor (HIF)-3alpha variants in the hypoxia response. Cell Mol Life Sci *68*, 3885-3901.

Henze, A. T., Garvalov, B. K., Seidel, S., Cuesta, A. M., Ritter, M., Filatova, A., Foss, F., Dopeso, H., Essmann, C. L., Maxwell, P. H.*, et al.* (2014). Loss of PHD3 allows tumours to overcome hypoxic growth inhibition and sustain proliferation through EGFR. Nat Commun *5*, 5582.

Henze, A. T., Riedel, J., Diem, T., Wenner, J., Flamme, I., Pouyseggur, J., Plate, K. H., and Acker, T. (2010). Prolyl hydroxylases 2 and 3 act in gliomas as protective negative feedback regulators of hypoxia-inducible factors. Cancer Res *70*, 357-366.

Hewitson, K. S., Lienard, B. M., McDonough, M. A., Clifton, I. J., Butler, D., Soares, A. S., Oldham, N. J., McNeill, L. A., and Schofield, C. J. (2007). Structural and mechanistic studies on the inhibition of the hypoxia-inducible transcription factor hydroxylases by tricarboxylic acid cycle intermediates. J Biol Chem *282*, 3293-3301.

Higgins, D. F., Kimura, K., Iwano, M., and Haase, V. H. (2008). Hypoxia-inducible factor signaling in the development of tissue fibrosis. Cell Cycle *7*, 1128-1132.

Hiratsuka, S., Goel, S., Kamoun, W. S., Maru, Y., Fukumura, D., Duda, D. G., and Jain, R. K. (2011). Endothelial focal adhesion kinase mediates cancer cell homing to discrete regions of the lungs via E-selectin up-regulation. Proc Natl Acad Sci U S A *108*, 3725-3730.

Hiratsuka, S., Nakamura, K., Iwai, S., Murakami, M., Itoh, T., Kijima, H., Shipley, J. M., Senior, R. M., and Shibuya, M. (2002). MMP9 induction by vascular endothelial growth factor receptor-1 is involved in lung-specific metastasis. Cancer Cell *2*, 289-300.

Hiratsuka, S., Watanabe, A., Aburatani, H., and Maru, Y. (2006). Tumour-mediated upregulation of chemoattractants and recruitment of myeloid cells predetermines lung metastasis. Nat Cell Biol *8*, 1369-1375.

Hiratsuka, S., Watanabe, A., Sakurai, Y., Akashi-Takamura, S., Ishibashi, S., Miyake, K., Shibuya, M., Akira, S., Aburatani, H., and Maru, Y. (2008). The S100A8-serum amyloid A3-TLR4 paracrine cascade establishes a pre-metastatic phase. Nat Cell Biol *10*, 1349-1355.

Hirsila, M., Koivunen, P., Gunzler, V., Kivirikko, K. I., and Myllyharju, J. (2003). Characterization of the human prolyl 4-hydroxylases that modify the hypoxia-inducible factor. J Biol Chem *278*, 30772-30780.

Hockel, M., Schlenger, K., Aral, B., Mitze, M., Schaffer, U., and Vaupel, P. (1996a). Association between tumor hypoxia and malignant progression in advanced cancer of the uterine cervix. Cancer Res *56*, 4509-4515.

Hockel, M., Schlenger, K., Mitze, M., Schaffer, U., and Vaupel, P. (1996b). Hypoxia and Radiation Response in Human Tumors. Semin Radiat Oncol *6*, 3-9.

Holscher, M., Silter, M., Krull, S., von Ahlen, M., Hesse, A., Schwartz, P., Wielockx, B., Breier, G., Katschinski, D. M., and Zieseniss, A. (2011). Cardiomyocyte-specific prolyl-4-hydroxylase domain 2 knock out protects from acute myocardial ischemic injury. J Biol Chem *286*, 11185-11194.

Huang, Y., Song, N., Ding, Y., Yuan, S., Li, X., Cai, H., Shi, H., and Luo, Y. (2009). Pulmonary vascular destabilization in the premetastatic phase facilitates lung metastasis. Cancer Res *69*, 7529-7537.

Huo, Z., Ye, J. C., Chen, J., Lin, X., Zhou, Z. N., Xu, X. R., Li, C. M., Qi, M., Liang, D., Liu, Y., and Li, J. (2012). Prolyl hydroxylase domain protein 2 regulates the intracellular cyclic AMP level in cardiomyocytes through its interaction with phosphodiesterase 4D. Biochem Biophys Res Commun *427*, 73-79.

Hyvarinen, J., Hassinen, I. E., Sormunen, R., Maki, J. M., Kivirikko, K. I., Koivunen, P., and Myllyharju, J. (2010). Hearts of hypoxia-inducible factor prolyl 4-hydroxylase-2 hypomorphic mice show protection against acute ischemia-reperfusion injury. J Biol Chem *285*, 13646-13657.

Ito, Y., Oike, Y., Yasunaga, K., Hamada, K., Miyata, K., Matsumoto, S., Sugano, S., Tanihara, H., Masuho, Y., and Suda, T. (2003). Inhibition of angiogenesis and vascular leakiness by angiopoietin-related protein 4. Cancer Res *63*, 6651-6657.

Ivan, M., Kondo, K., Yang, H., Kim, W., Valiando, J., Ohh, M., Salic, A., Asara, J. M., Lane, W. S., and Kaelin, W. G., Jr. (2001). HIFalpha targeted for VHL-mediated destruction by proline hydroxylation: implications for O2 sensing. Science *292*, 464-468.

Izumi, Y., Xu, L., di Tomaso, E., Fukumura, D., and Jain, R. K. (2002). Tumour biology: herceptin acts as an anti-angiogenic cocktail. Nature *416*, 279-280.

Jaakkola, P., Mole, D. R., Tian, Y. M., Wilson, M. I., Gielbert, J., Gaskell, S. J., von Kriegsheim, A., Hebestreit, H. F., Mukherji, M., Schofield, C. J.*, et al.* (2001). Targeting of HIF-alpha to the von Hippel-Lindau ubiquitylation complex by O2-regulated prolyl hydroxylation. Science *292*, 468-472.

Jain, R. K. (2001). Normalizing tumor vasculature with anti-angiogenic therapy: a new paradigm for combination therapy. Nat Med *7*, 987-989.

Jain, R. K. (2014). Antiangiogenesis Strategies Revisited: From Starving Tumors to Alleviating Hypoxia. Cancer Cell *26*, 605-622.

Jean, C., Gravelle, P., Fournie, J. J., and Laurent, G. (2011). Influence of stress on extracellular matrix and integrin biology. Oncogene *30*, 2697-2706.

Jin, F., Brockmeier, U., Otterbach, F., and Metzen, E. (2012). New insight into the SDF-1/CXCR4 axis in a breast carcinoma model: hypoxia-induced endothelial SDF-1 and tumor cell CXCR4 are required for tumor cell intravasation. Mol Cancer Res *10*, 1021-1031.

Josson, S., Matsuoka, Y., Chung, L. W., Zhau, H. E., and Wang, R. (2010). Tumor-stroma co-evolution in prostate cancer progression and metastasis. Semin Cell Dev Biol *21*, 26-32.

Joyce, J. A., and Pollard, J. W. (2009). Microenvironmental regulation of metastasis. Nat Rev Cancer *9*, 239-252.

Jubb, A. M., Buffa, F. M., and Harris, A. L. (2010). Assessment of tumour hypoxia for prediction of response to therapy and cancer prognosis. J Cell Mol Med *14*, 18-29.

Jurasz, P., Alonso-Escolano, D., and Radomski, M. W. (2004). Platelet--cancer interactions: mechanisms and pharmacology of tumour cell-induced platelet aggregation. Br J Pharmacol *143*, 819-826.

Kaelin, W. G., Jr. (2011). Cancer and altered metabolism: potential importance of hypoxia-inducible factor and 2-oxoglutarate-dependent dioxygenases. Cold Spring Harb Symp Quant Biol *76*, 335-345.

Kaelin, W. G., Jr., and Ratcliffe, P. J. (2008). Oxygen sensing by metazoans: the central role of the HIF hydroxylase pathway. Mol Cell *30*, 393-402.

Kalluri, R., and Weinberg, R. A. (2009). The basics of epithelial-mesenchymal transition. J Clin Invest *119*, 1420-1428.

Kalluri, R., and Zeisberg, M. (2006). Fibroblasts in cancer. Nat Rev Cancer *6*, 392-401.

Kalucka, J., Ettinger, A., Franke, K., Mamlouk, S., Singh, R. P., Farhat, K., Muschter, A., Olbrich, S., Breier, G., Katschinski, D. M.*, et al.* (2013). Loss of epithelial hypoxia-inducible factor prolyl hydroxylase 2 accelerates skin wound healing in mice. Mol Cell Biol *33*, 3426-3438.

Kaplan, R. N., Riba, R. D., Zacharoulis, S., Bramley, A. H., Vincent, L., Costa, C., MacDonald, D. D., Jin, D. K., Shido, K., Kerns, S. A.*, et al.* (2005). VEGFR1-positive haematopoietic bone marrow progenitors initiate the pre-metastatic niche. Nature *438*, 820-827.

Karagiannis, G. S., Poutahidis, T., Erdman, S. E., Kirsch, R., Riddell, R. H., and Diamandis, E. P. (2012). Cancer-associated fibroblasts drive the progression of metastasis through both paracrine and mechanical pressure on cancer tissue. Mol Cancer Res *10*, 1403-1418.

Karnoub, A. E., Dash, A. B., Vo, A. P., Sullivan, A., Brooks, M. W., Bell, G. W., Richardson, A. L., Polyak, K., Tubo, R., and Weinberg, R. A. (2007). Mesenchymal stem cells within tumour stroma promote breast cancer metastasis. Nature *449*, 557-563.

Kasashima, H., Yashiro, M., Kinoshita, H., Fukuoka, T., Morisaki, T., Masuda, G., Sakurai, K., Kubo, N., Ohira, M., and Hirakawa, K. (2014). Lysyl oxidase-like 2 (LOXL2) from stromal fibroblasts stimulates the progression of gastric cancer. Cancer Lett *354*, 438-446.

Kerbel, R. S. (2008). Tumor angiogenesis. N Engl J Med *358*, 2039-2049.

Kim, J. W., Evans, C., Weidemann, A., Takeda, N., Lee, Y. S., Stockmann, C., Branco-Price, C., Brandberg, F., Leone, G., Ostrowski, M. C., and Johnson, R. S. (2012). Loss of fibroblast HIF-1alpha accelerates tumorigenesis. Cancer Res *72*, 3187-3195.

Kim, S., Takahashi, H., Lin, W. W., Descargues, P., Grivennikov, S., Kim, Y., Luo, J. L., and Karin, M. (2009). Carcinoma-produced factors activate myeloid cells through TLR2 to stimulate metastasis. Nature *457*, 102-106.

Kisanuki, Y. Y., Hammer, R. E., Miyazaki, J., Williams, S. C., Richardson, J. A., and Yanagisawa, M. (2001). Tie2-Cre transgenic mice: a new model for endothelial cell-lineage analysis in vivo. Dev Biol *230*, 230-242.

Klotzsche-von Ameln, A., Muschter, A., Mamlouk, S., Kalucka, J., Prade, I., Franke, K., Rezaei, M., Poitz, D. M., Breier, G., and Wielockx, B. (2011). Inhibition of HIF prolyl hydroxylase-2 blocks tumor growth in mice through the antiproliferative activity of TGFbeta. Cancer Res *71*, 3306-3316.

Koike, T., Kimura, N., Miyazaki, K., Yabuta, T., Kumamoto, K., Takenoshita, S., Chen, J., Kobayashi, M., Hosokawa, M., Taniguchi, A.*, et al.* (2004). Hypoxia induces adhesion molecules

on cancer cells: A missing link between Warburg effect and induction of selectin-ligand carbohydrates. Proc Natl Acad Sci U S A *101*, 8132-8137.

Koivunen, P., Hirsila, M., Gunzler, V., Kivirikko, K. I., and Myllyharju, J. (2004). Catalytic properties of the asparaginyl hydroxylase (FIH) in the oxygen sensing pathway are distinct from those of its prolyl 4-hydroxylases. J Biol Chem *279*, 9899-9904.

Koivunen, P., Hirsila, M., Kivirikko, K. I., and Myllyharju, J. (2006). The length of peptide substrates has a marked effect on hydroxylation by the hypoxia-inducible factor prolyl 4-hydroxylases. J Biol Chem *281*, 28712-28720.

Koivunen, P., Lee, S., Duncan, C. G., Lopez, G., Lu, G., Ramkissoon, S., Losman, J. A., Joensuu, P., Bergmann, U., Gross, S.*, et al.* (2012). Transformation by the (R)-enantiomer of 2-hydroxyglutarate linked to EGLN activation. Nature *483*, 484-488.

Kojima, Y., Acar, A., Eaton, E. N., Mellody, K. T., Scheel, C., Ben-Porath, I., Onder, T. T., Wang, Z. C., Richardson, A. L., Weinberg, R. A., and Orimo, A. (2010). Autocrine TGF-beta and stromal cell-derived factor-1 (SDF-1) signaling drives the evolution of tumor-promoting mammary stromal myofibroblasts. Proc Natl Acad Sci U S A *107*, 20009-20014.

Konstantopoulos, K., and Thomas, S. N. (2009). Cancer cells in transit: the vascular interactions of tumor cells. Annu Rev Biomed Eng *11*, 177-202.

Korff, T., Krauss, T., and Augustin, H. G. (2004). Three-dimensional spheroidal culture of cytotrophoblast cells mimics the phenotype and differentiation of cytotrophoblasts from normal and preeclamptic pregnancies. Exp Cell Res *297*, 415-423.

Kumar, S., and Weaver, V. M. (2009). Mechanics, malignancy, and metastasis: the force journey of a tumor cell. Cancer Metastasis Rev *28*, 113-127.

Le Jan, S., Amy, C., Cazes, A., Monnot, C., Lamande, N., Favier, J., Philippe, J., Sibony, M., Gasc, J. M., Corvol, P., and Germain, S. (2003). Angiopoietin-like 4 is a proangiogenic factor produced during ischemia and in conventional renal cell carcinoma. Am J Pathol *162*, 1521-1528.

Lee, K. A., Lynd, J. D., O'Reilly, S., Kiupel, M., McCormick, J. J., and LaPres, J. J. (2008). The biphasic role of the hypoxia-inducible factor prolyl-4-hydroxylase, PHD2, in modulating tumor-forming potential. Mol Cancer Res *6*, 829-842.

Lehr, J. E., and Pienta, K. J. (1998). Preferential adhesion of prostate cancer cells to a human bone marrow endothelial cell line. J Natl Cancer Inst *90*, 118-123.

Leite de Oliveira, R., Deschoemaeker, S., Henze, A. T., Debackere, K., Finisguerra, V., Takeda, Y., Roncal, C., Dettori, D., Tack, E., Jonsson, Y.*, et al.* (2012). Gene-targeting of Phd2 improves tumor response to chemotherapy and prevents side-toxicity. Cancer Cell *22*, 263-277.

Levental, K. R., Yu, H., Kass, L., Lakins, J. N., Egeblad, M., Erler, J. T., Fong, S. F., Csiszar, K., Giaccia, A., Weninger, W.*, et al.* (2009). Matrix crosslinking forces tumor progression by enhancing integrin signaling. Cell *139*, 891-906.

Lewis, M. P., Lygoe, K. A., Nystrom, M. L., Anderson, W. P., Speight, P. M., Marshall, J. F., and Thomas, G. J. (2004). Tumour-derived TGF-beta1 modulates myofibroblast differentiation and promotes HGF/SF-dependent invasion of squamous carcinoma cells. Br J Cancer *90*, 822-832.

Li, K. Q., Li, W. L., Peng, S. Y., Shi, X. Y., Tang, H. L., and Liu, Y. B. (2004). Anti-tumor effect of recombinant retroviral vector-mediated human ANGPTL4 gene transfection. Chin Med J (Engl) *117*, 1364-1369.

Lin, E. Y., Jones, J. G., Li, P., Zhu, L., Whitney, K. D., Muller, W. J., and Pollard, J. W. (2003). Progression to malignancy in the polyoma middle T oncoprotein mouse breast cancer model provides a reliable model for human diseases. Am J Pathol *163*, 2113-2126.

Liu, M., Xu, J., and Deng, H. (2011). Tangled fibroblasts in tumor-stroma interactions. Int J Cancer.

Lu, P., Weaver, V. M., and Werb, Z. (2012). The extracellular matrix: a dynamic niche in cancer progression. J Cell Biol *196*, 395-406.

Luo, W., Hu, H., Chang, R., Zhong, J., Knabel, M., O'Meally, R., Cole, R. N., Pandey, A., and Semenza, G. L. (2011). Pyruvate kinase M2 is a PHD3-stimulated coactivator for hypoxia-inducible factor 1. Cell *145*, 732-744.

Luzzi, K. J., MacDonald, I. C., Schmidt, E. E., Kerkvliet, N., Morris, V. L., Chambers, A. F., and Groom, A. C. (1998). Multistep nature of metastatic inefficiency: dormancy of solitary cells after successful extravasation and limited survival of early micrometastases. Am J Pathol *153*, 865-873.

MacKenzie, E. D., Selak, M. A., Tennant, D. A., Payne, L. J., Crosby, S., Frederiksen, C. M., Watson, D. G., and Gottlieb, E. (2007). Cell-permeating alpha-ketoglutarate derivatives alleviate pseudohypoxia in succinate dehydrogenase-deficient cells. Mol Cell Biol *27*, 3282-3289.

Maes, H., Kuchnio, A., Peric, A., Moens, S., Nys, K., De Bock, K., Quaegebeur, A., Schoors, S., Georgiadou, M., Wouters, J*., et al.* (2014). Tumor vessel normalization by chloroquine independent of autophagy. Cancer Cell *26*, 190-206.

Mahon, P. C., Hirota, K., and Semenza, G. L. (2001). FIH-1: a novel protein that interacts with HIF-1alpha and VHL to mediate repression of HIF-1 transcriptional activity. Genes Dev *15*, 2675-2686.

Majmundar, A. J., Wong, W. J., and Simon, M. C. (2010). Hypoxia-inducible factors and the response to hypoxic stress. Mol Cell *40*, 294-309.

Malanchi, I., Santamaria-Martinez, A., Susanto, E., Peng, H., Lehr, H. A., Delaloye, J. F., and Huelsken, J. (2012). Interactions between cancer stem cells and their niche govern metastatic colonization. Nature *481*, 85-89.

Maller, O., DuFort, C. C., and Weaver, V. M. (2013). YAP forces fibroblasts to feel the tension. Nat Cell Biol *15*, 570-572.

Mamlouk, S., Kalucka, J., Singh, R. P., Franke, K., Muschter, A., Langer, A., Jakob, C., Gassmann, M., Baretton, G. B., and Wielockx, B. (2014). Loss of prolyl hydroxylase-2 in myeloid cells and T-lymphocytes impairs tumor development. Int J Cancer *134*, 849-858.

Mantovani, A., Allavena, P., Sica, A., and Balkwill, F. (2008). Cancer-related inflammation. Nature *454*, 436-444.

Mao, Y., Keller, E. T., Garfield, D. H., Shen, K., and Wang, J. (2012). Stromal cells in tumor microenvironment and breast cancer. Cancer Metastasis Rev.

Maxwell, P. H., Wiesener, M. S., Chang, G. W., Clifford, S. C., Vaux, E. C., Cockman, M. E., Wykoff, C. C., Pugh, C. W., Maher, E. R., and Ratcliffe, P. J. (1999). The tumour suppressor protein VHL targets hypoxia-inducible factors for oxygen-dependent proteolysis. Nature *399*, 271-275.

Mazzone, M., Dettori, D., Leite de Oliveira, R., Loges, S., Schmidt, T., Jonckx, B., Tian, Y. M., Lanahan, A. A., Pollard, P., Ruiz de Almodovar, C*., et al.* (2009). Heterozygous deficiency of PHD2 restores tumor oxygenation and inhibits metastasis via endothelial normalization. Cell *136*, 839-851.

McNeill, L. A., Hewitson, K. S., Claridge, T. D., Seibel, J. F., Horsfall, L. E., and Schofield, C. J. (2002). Hypoxia-inducible factor asparaginyl hydroxylase (FIH-1) catalyses hydroxylation at the beta-carbon of asparagine-803. Biochem J *367*, 571-575.

Micke, P., and Ostman, A. (2005). Exploring the tumour environment: cancer-associated fibroblasts as targets in cancer therapy. Expert Opin Ther Targets *9*, 1217-1233.

Minamishima, Y. A., Moslehi, J., Bardeesy, N., Cullen, D., Bronson, R. T., and Kaelin, W. G., Jr. (2008). Somatic inactivation of the PHD2 prolyl hydroxylase causes polycythemia and congestive heart failure. Blood *111*, 3236-3244.

Minamishima, Y. A., Moslehi, J., Padera, R. F., Bronson, R. T., Liao, R., and Kaelin, W. G., Jr. (2009). A feedback loop involving the Phd3 prolyl hydroxylase tunes the mammalian hypoxic response in vivo. Mol Cell Biol *29*, 5729-5741.

Miquerol, L., Langille, B. L., and Nagy, A. (2000). Embryonic development is disrupted by modest increases in vascular endothelial growth factor gene expression. Development *127*, 3941-3946.

Moens, S., Goveia, J., Stapor, P. C., Cantelmo, A. R., and Carmeliet, P. (2014). The multifaceted activity of VEGF in angiogenesis - Implications for therapy responses. Cytokine Growth Factor Rev *25*, 473-482.

Morris, V. L., Koop, S., MacDonald, I. C., Schmidt, E. E., Grattan, M., Percy, D., Chambers, A. F., and Groom, A. C. (1994). Mammary carcinoma cell lines of high and low metastatic potential differ not in extravasation but in subsequent migration and growth. Clin Exp Metastasis *12*, 357-367.

Munoz-Najar, U. M., Neurath, K. M., Vumbaca, F., and Claffey, K. P. (2006). Hypoxia stimulates breast carcinoma cell invasion through MT1-MMP and MMP-2 activation. Oncogene *25*, 2379-2392.

Muzumdar, M. D., Tasic, B., Miyamichi, K., Li, L., and Luo, L. (2007). A global double-fluorescent Cre reporter mouse. Genesis *45*, 593-605.

Naba, A., Clauser, K. R., Lamar, J. M., Carr, S. A., and Hynes, R. O. (2014). Extracellular matrix signatures of human mammary carcinoma identify novel metastasis promoters. Elife *3*, e01308.

Nakayama, T., Hirakawa, H., Shibata, K., Abe, K., Nagayasu, T., and Taguchi, T. (2010). Expression of angiopoietin-like 4 in human gastric cancer: ANGPTL4 promotes venous invasion. Oncol Rep *24*, 599-606.

Nash, G. F., Turner, L. F., Scully, M. F., and Kakkar, A. K. (2002). Platelets and cancer. Lancet Oncol *3*, 425-430.

Naumov, G. N., MacDonald, I. C., Weinmeister, P. M., Kerkvliet, N., Nadkarni, K. V., Wilson, S. M., Morris, V. L., Groom, A. C., and Chambers, A. F. (2002). Persistence of solitary mammary carcinoma cells in a secondary site: a possible contributor to dormancy. Cancer Res *62*, 2162-2168.

Naumov, G. N., Townson, J. L., MacDonald, I. C., Wilson, S. M., Bramwell, V. H., Groom, A. C., and Chambers, A. F. (2003). Ineffectiveness of doxorubicin treatment on solitary dormant mammary carcinoma cells or late-developing metastases. Breast Cancer Res Treat *82*, 199-206.

Nguyen, D. X., Bos, P. D., and Massague, J. (2009). Metastasis: from dissemination to organ-specific colonization. Nat Rev Cancer *9*, 274-284.

Nieswandt, B., Hafner, M., Echtenacher, B., and Mannel, D. N. (1999). Lysis of tumor cells by natural killer cells in mice is impeded by platelets. Cancer Res *59*, 1295-1300.

Okochi-Takada, E., Hattori, N., Tsukamoto, T., Miyamoto, K., Ando, T., Ito, S., Yamamura, Y., Wakabayashi, M., Nobeyama, Y., and Ushijima, T. (2014). ANGPTL4 is a secreted tumor suppressor that inhibits angiogenesis. Oncogene *33*, 2273-2278.

Olsson, A. K., Dimberg, A., Kreuger, J., and Claesson-Welsh, L. (2006). VEGF receptor signalling - in control of vascular function. Nat Rev Mol Cell Biol *7*, 359-371.

Orimo, A., Gupta, P. B., Sgroi, D. C., Arenzana-Seisdedos, F., Delaunay, T., Naeem, R., Carey, V. J., Richardson, A. L., and Weinberg, R. A. (2005). Stromal fibroblasts present in invasive human breast carcinomas promote tumor growth and angiogenesis through elevated SDF-1/CXCL12 secretion. Cell *121*, 335-348.

Ostman, A. (2012). The tumor microenvironment controls drug sensitivity. Nat Med *18*, 1332-1334.

Ozdemir, B. C., Pentcheva-Hoang, T., Carstens, J. L., Zheng, X., Wu, C. C., Simpson, T. R., Laklai, H., Sugimoto, H., Kahlert, C., Novitskiy, S. V.*, et al.* (2014). Depletion of carcinoma-associated fibroblasts and fibrosis induces immunosuppression and accelerates pancreas cancer with reduced survival. Cancer Cell *25*, 719-734.

Ozer, A., and Bruick, R. K. (2005). Regulation of HIF by prolyl hydroxylases: recruitment of the candidate tumor suppressor protein ING4. Cell Cycle *4*, 1153-1156.

Ozer, A., Wu, L. C., and Bruick, R. K. (2005). The candidate tumor suppressor ING4 represses activation of the hypoxia inducible factor (HIF). Proc Natl Acad Sci U S A *102*, 7481-7486.

Padua, D., Zhang, X. H., Wang, Q., Nadal, C., Gerald, W. L., Gomis, R. R., and Massague, J. (2008). TGFbeta primes breast tumors for lung metastasis seeding through angiopoietin-like 4. Cell *133*, 66-77.

Paez-Ribes, M., Allen, E., Hudock, J., Takeda, T., Okuyama, H., Vinals, F., Inoue, M., Bergers, G., Hanahan, D., and Casanovas, O. (2009). Antiangiogenic therapy elicits malignant progression of tumors to increased local invasion and distant metastasis. Cancer Cell *15*, 220-231.

Paget, S. (1889). The distribution of secondary growths in cancer of the breast. 1889. Cancer Metastasis Rev *8*, 98-101.

Palumbo, J. S., Talmage, K. E., Massari, J. V., La Jeunesse, C. M., Flick, M. J., Kombrinck, K. W., Hu, Z., Barney, K. A., and Degen, J. L. (2007). Tumor cell-associated tissue factor and circulating hemostatic factors cooperate to increase metastatic potential through natural killer cell-dependent and-independent mechanisms. Blood *110*, 133-141.

Perkins, N. D. (2007). Integrating cell-signalling pathways with NF-kappaB and IKK function. Nat Rev Mol Cell Biol *8*, 49-62.

Pietras, K., and Ostman, A. (2010). Hallmarks of cancer: interactions with the tumor stroma. Exp Cell Res *316*, 1324-1331.

Place, T. L., Fitzgerald, M. P., Venkataraman, S., Vorrink, S. U., Case, A. J., Teoh, M. L., and Domann, F. E. (2011). Aberrant promoter CpG methylation is a mechanism for impaired PHD3 expression in a diverse set of malignant cells. PLoS One *6*, e14617.

Prensner, J. R., and Chinnaiyan, A. M. (2011). Metabolism unhinged: IDH mutations in cancer. Nat Med *17*, 291-293.

Pries, A. R., and Secomb, T. W. (2014). Making microvascular networks work: angiogenesis, remodeling, and pruning. Physiology (Bethesda) *29*, 446-455.

Proia, D. A., and Kuperwasser, C. (2005). Stroma: tumor agonist or antagonist. Cell Cycle *4*, 1022-1025.

Provenzano, P. P., Eliceiri, K. W., Campbell, J. M., Inman, D. R., White, J. G., and Keely, P. J. (2006). Collagen reorganization at the tumor-stromal interface facilitates local invasion. BMC Med *4*, 38.

Provenzano, P. P., Inman, D. R., Eliceiri, K. W., Trier, S. M., and Keely, P. J. (2008). Contact guidance mediated three-dimensional cell migration is regulated by Rho/ROCK-dependent matrix reorganization. Biophys J *95*, 5374-5384.

Psaila, B., and Lyden, D. (2009). The metastatic niche: adapting the foreign soil. Nat Rev Cancer *9*, 285-293.

Qiu, T. H., Chandramouli, G. V., Hunter, K. W., Alkharouf, N. W., Green, J. E., and Liu, E. T. (2004). Global expression profiling identifies signatures of tumor virulence in MMTV-PyMT-transgenic mice: correlation to human disease. Cancer Res *64*, 5973-5981.

Quail, D. F., and Joyce, J. A. (2013). Microenvironmental regulation of tumor progression and metastasis. Nat Med *19*, 1423-1437.

Reese, D. M., and Slamon, D. J. (1997). HER-2/neu signal transduction in human breast and ovarian cancer. Stem Cells *15*, 1-8.

Rivers, L. E., Young, K. M., Rizzi, M., Jamen, F., Psachoulia, K., Wade, A., Kessaris, N., and Richardson, W. D. (2008). PDGFRA/NG2 glia generate myelinating oligodendrocytes and piriform projection neurons in adult mice. Nat Neurosci *11*, 1392-1401.

Rogers, M. S., Novak, K., Zurakowski, D., Cryan, L. M., Blois, A., Lifshits, E., Bo, T. H., Oyan, A. M., Bender, E. R., Lampa, M.*, et al.* (2014). Spontaneous reversion of the angiogenic phenotype to a nonangiogenic and dormant state in human tumors. Mol Cancer Res *12*, 754-764.

Rohwer, N., Welzel, M., Daskalow, K., Pfander, D., Wiedenmann, B., Detjen, K., and Cramer, T. (2008). Hypoxia-inducible factor 1alpha mediates anoikis resistance via suppression of alpha5 integrin. Cancer Res *68*, 10113-10120.

Ronnov-Jessen, L., and Petersen, O. W. (1993). Induction of alpha-smooth muscle actin by transforming growth factor-beta 1 in quiescent human breast gland fibroblasts. Implications for myofibroblast generation in breast neoplasia. Lab Invest *68*, 696-707.

Roussos, E. T., Balsamo, M., Alford, S. K., Wyckoff, J. B., Gligorijevic, B., Wang, Y., Pozzuto, M., Stobezki, R., Goswami, S., Segall, J. E.*, et al.* (2011). Mena invasive (MenaINV) promotes multicellular streaming motility and transendothelial migration in a mouse model of breast cancer. J Cell Sci *124*, 2120-2131.

Schiller, M., Dennler, S., Anderegg, U., Kokot, A., Simon, J. C., Luger, T. A., Mauviel, A., and Bohm, M. (2010). Increased cAMP levels modulate transforming growth factor-beta/Smad-induced expression of extracellular matrix components and other key fibroblast effector functions. J Biol Chem *285*, 409-421.

Schneider, M., Van Geyte, K., Fraisl, P., Kiss, J., Aragones, J., Mazzone, M., Mairbaurl, H., De Bock, K., Jeoung, N. H., Mollenhauer, M.*, et al.* (2010). Loss or silencing of the PHD1 prolyl hydroxylase protects livers of mice against ischemia/reperfusion injury. Gastroenterology *138*, 1143-1154 e1141-1142.

Schofield, C. J., and Ratcliffe, P. J. (2004). Oxygen sensing by HIF hydroxylases. Nat Rev Mol Cell Biol *5*, 343-354.

Schwab, L. P., Peacock, D. L., Majumdar, D., Ingels, J. F., Jensen, L. C., Smith, K. D., Cushing, R. C., and Seagroves, T. N. (2012). Hypoxia-inducible factor 1alpha promotes primary tumor growth and tumor-initiating cell activity in breast cancer. Breast Cancer Res *14*, R6.

Scott, L. J., Clarke, N. W., George, N. J., Shanks, J. H., Testa, N. G., and Lang, S. H. (2001). Interactions of human prostatic epithelial cells with bone marrow endothelium: binding and invasion. Br J Cancer *84*, 1417-1423.

Selak, M. A., Armour, S. M., MacKenzie, E. D., Boulahbel, H., Watson, D. G., Mansfield, K. D., Pan, Y., Simon, M. C., Thompson, C. B., and Gottlieb, E. (2005). Succinate links TCA cycle dysfunction to oncogenesis by inhibiting HIF-alpha prolyl hydroxylase. Cancer Cell *7*, 77-85.

Semenza, G. L. (2007). Life with oxygen. Science *318*, 62-64.

Semenza, G. L. (2012). Molecular mechanisms mediating metastasis of hypoxic breast cancer cells. Trends Mol Med *18*, 534-543.

Siegel, P. M., and Massague, J. (2003). Cytostatic and apoptotic actions of TGF-beta in homeostasis and cancer. Nat Rev Cancer *3*, 807-821.

Singh, R. P., Franke, K., Kalucka, J., Mamlouk, S., Muschter, A., Gembarska, A., Grinenko, T., Willam, C., Naumann, R., Anastassiadis, K.*, et al.* (2013). HIF prolyl hydroxylase 2 (PHD2) is a critical regulator of hematopoietic stem cell maintenance during steady-state and stress. Blood *121*, 5158-5166.

Spano, D., Heck, C., De Antonellis, P., Christofori, G., and Zollo, M. (2012). Molecular networks that regulate cancer metastasis. Semin Cancer Biol *22*, 234-249.

Stacker, S. A., Achen, M. G., Jussila, L., Baldwin, M. E., and Alitalo, K. (2002). Lymphangiogenesis and cancer metastasis. Nat Rev Cancer *2*, 573-583.

Strutz, F., Zeisberg, M., Renziehausen, A., Raschke, B., Becker, V., van Kooten, C., and Muller, G. (2001). TGF-beta 1 induces proliferation in human renal fibroblasts via induction of basic fibroblast growth factor (FGF-2). Kidney Int *59*, 579-592.

Stylianopoulos, T., and Jain, R. K. (2013). Combining two strategies to improve perfusion and drug delivery in solid tumors. Proc Natl Acad Sci U S A *110*, 18632-18637.

Su, Y., Loos, M., Giese, N., Metzen, E., Buchler, M. W., Friess, H., Kornberg, A., and Buchler, P. (2012). Prolyl hydroxylase-2 (PHD2) exerts tumor-suppressive activity in pancreatic cancer. Cancer *118*, 960-972.

Sung, S. Y., Hsieh, C. L., Law, A., Zhau, H. E., Pathak, S., Multani, A. S., Lim, S., Coleman, I. M., Wu, L. C., Figg, W. D.*, et al.* (2008). Coevolution of prostate cancer and bone stroma in three-dimensional coculture: implications for cancer growth and metastasis. Cancer Res *68*, 9996-10003.

Takebe Naoko, P. I., Wiliam Timmer, Nadia Khan, Timothy Schulz, Pamela Jo Harris (2013). Review of Cancer – Associated Fibroblasts and Therapies that Interfere with Their Activity. VERSITA Emerging Science *1*, 19-36.

Takeda, K., Aguila, H. L., Parikh, N. S., Li, X., Lamothe, K., Duan, L. J., Takeda, H., Lee, F. S., and Fong, G. H. (2008). Regulation of adult erythropoiesis by prolyl hydroxylase domain proteins. Blood *111*, 3229-3235.

Takeda, K., Cowan, A., and Fong, G. H. (2007). Essential role for prolyl hydroxylase domain protein 2 in oxygen homeostasis of the adult vascular system. Circulation *116*, 774-781.

Takeda, K., Ho, V. C., Takeda, H., Duan, L. J., Nagy, A., and Fong, G. H. (2006). Placental but not heart defects are associated with elevated hypoxia-inducible factor alpha levels in mice lacking prolyl hydroxylase domain protein 2. Mol Cell Biol *26*, 8336-8346.

Takeda, Y., Costa, S., Delamarre, E., Roncal, C., Leite de Oliveira, R., Squadrito, M. L., Finisguerra, V., Deschoemaeker, S., Bruyere, F., Wenes, M.*, et al.* (2011). Macrophage skewing by Phd2 haplodeficiency prevents ischaemia by inducing arteriogenesis. Nature *479*, 122-126.

Taylor, C. T. (2008). Interdependent roles for hypoxia inducible factor and nuclear factor-kappaB in hypoxic inflammation. J Physiol *586*, 4055-4059.

Tiwari, N., Gheldof, A., Tatari, M., and Christofori, G. (2012). EMT as the ultimate survival mechanism of cancer cells. Semin Cancer Biol *22*, 194-207.

Tomasek, J. J., Haaksma, C. J., Eddy, R. J., and Vaughan, M. B. (1992). Fibroblast contraction occurs on release of tension in attached collagen lattices: dependency on an organized actin cytoskeleton and serum. Anat Rec *232*, 359-368.

Tong, R. T., Boucher, Y., Kozin, S. V., Winkler, F., Hicklin, D. J., and Jain, R. K. (2004). Vascular normalization by vascular endothelial growth factor receptor 2 blockade induces a pressure gradient across the vasculature and improves drug penetration in tumors. Cancer Res *64*, 3731-3736.

Townson, J. L., Ramadan, S. S., Simedrea, C., Rutt, B. K., MacDonald, I. C., Foster, P. J., and Chambers, A. F. (2009). Three-dimensional imaging and quantification of both solitary cells and metastases in whole mouse liver by magnetic resonance imaging. Cancer Res *69*, 8326-8331.

Trimboli, A. J., Fukino, K., de Bruin, A., Wei, G., Shen, L., Tanner, S. M., Creasap, N., Rosol, T. J., Robinson, M. L., Eng, C.*, et al.* (2008). Direct evidence for epithelial-mesenchymal transitions in breast cancer. Cancer Res *68*, 937-945.

van Zijl, F., Krupitza, G., and Mikulits, W. (2011). Initial steps of metastasis: cell invasion and endothelial transmigration. Mutat Res *728*, 23-34.

Vaupel, P., Schlenger, K., Knoop, C., and Hockel, M. (1991). Oxygenation of human tumors: evaluation of tissue oxygen distribution in breast cancers by computerized O2 tension measurements. Cancer Res *51*, 3316-3322.

Wagner, K. U., Wall, R. J., St-Onge, L., Gruss, P., Wynshaw-Boris, A., Garrett, L., Li, M., Furth, P. A., and Hennighausen, L. (1997). Cre-mediated gene deletion in the mammary gland. Nucleic Acids Res *25*, 4323-4330.

Waldmeier, L., Meyer-Schaller, N., Diepenbruck, M., and Christofori, G. (2012). Py2T murine breast cancer cells, a versatile model of TGFbeta-induced EMT in vitro and in vivo. PLoS One *7*, e48651.

Wallace, J. A., Li, F., Leone, G., and Ostrowski, M. C. (2011). Pten in the breast tumor microenvironment: modeling tumor-stroma coevolution. Cancer Res *71*, 1203-1207.

Wang, W., Wyckoff, J. B., Frohlich, V. C., Oleynikov, Y., Huttelmaier, S., Zavadil, J., Cermak, L., Bottinger, E. P., Singer, R. H., White, J. G.*, et al.* (2002). Single cell behavior in metastatic primary mammary tumors correlated with gene expression patterns revealed by molecular profiling. Cancer Res *62*, 6278-6288.

Weinberg, R. A. (2008). Coevolution in the tumor microenvironment. Nat Genet *40*, 494-495.

Whelan, K. A., Caldwell, S. A., Shahriari, K. S., Jackson, S. R., Franchetti, L. D., Johannes, G. J., and Reginato, M. J. (2010). Hypoxia suppression of Bim and Bmf blocks anoikis and luminal clearing during mammary morphogenesis. Mol Biol Cell *21*, 3829-3837.

Winkler, F., Kozin, S. V., Tong, R. T., Chae, S. S., Booth, M. F., Garkavtsev, I., Xu, L., Hicklin, D. J., Fukumura, D., di Tomaso, E.*, et al.* (2004). Kinetics of vascular normalization by VEGFR2 blockade governs brain tumor response to radiation: role of oxygenation, angiopoietin-1, and matrix metalloproteinases. Cancer Cell *6*, 553-563.

Wong, B. W., Kuchnio, A., Bruning, U., and Carmeliet, P. (2013). Emerging novel functions of the oxygen-sensing prolyl hydroxylase domain enzymes. Trends Biochem Sci *38*, 3-11.

Wong, S. Y., and Hynes, R. O. (2006). Lymphatic or hematogenous dissemination: how does a metastatic tumor cell decide? Cell Cycle *5*, 812-817.

Wottawa, M., Leisering, P., Ahlen, M. V., Schnelle, M., Vogel, S., Malz, C., Bordoli, M. R., Camenisch, G., Hesse, A., Napp, J.*, et al.* (2012). Knockdown of prolyl-4-hydroxylase domain 2 inhibits tumor growth of human breast cancer MDA-MB-231 cells by affecting TGF-beta1 processing. Int J Cancer.

Wyckoff, J., Wang, W., Lin, E. Y., Wang, Y., Pixley, F., Stanley, E. R., Graf, T., Pollard, J. W., Segall, J., and Condeelis, J. (2004). A paracrine loop between tumor cells and macrophages is required for tumor cell migration in mammary tumors. Cancer Res *64*, 7022-7029.

Wyckoff, J. B., Wang, Y., Lin, E. Y., Li, J. F., Goswami, S., Stanley, E. R., Segall, J. E., Pollard, J. W., and Condeelis, J. (2007). Direct visualization of macrophage-assisted tumor cell intravasation in mammary tumors. Cancer Res *67*, 2649-2656.

Xie, L., Pi, X., Mishra, A., Fong, G., Peng, J., and Patterson, C. (2012). PHD3-dependent hydroxylation of HCLK2 promotes the DNA damage response. J Clin Invest *122*, 2827-2836.

Xue, J., Li, X., Jiao, S., Wei, Y., Wu, G., and Fang, J. (2010). Prolyl hydroxylase-3 is down-regulated in colorectal cancer cells and inhibits IKKbeta independent of hydroxylase activity. Gastroenterology *138*, 606-615.

Yilmaz, M., and Christofori, G. (2010). Mechanisms of motility in metastasizing cells. Mol Cancer Res *8*, 629-642.

Yuan, F., Chen, Y., Dellian, M., Safabakhsh, N., Ferrara, N., and Jain, R. K. (1996). Time-dependent vascular regression and permeability changes in established human tumor xenografts induced by an anti-vascular endothelial growth factor/vascular permeability factor antibody. Proc Natl Acad Sci U S A *93*, 14765-14770.

Zervantonakis, I. K., Hughes-Alford, S. K., Charest, J. L., Condeelis, J. S., Gertler, F. B., and Kamm, R. D. (2012). Three-dimensional microfluidic model for tumor cell intravasation and endothelial barrier function. Proc Natl Acad Sci U S A *109*, 13515-13520.

Zhang, N., Fu, Z., Linke, S., Chicher, J., Gorman, J. J., Visk, D., Haddad, G. G., Poellinger, L., Peet, D. J., Powell, F., and Johnson, R. S. (2010). The asparaginyl hydroxylase factor inhibiting HIF-1alpha is an essential regulator of metabolism. Cell Metab *11*, 364-378.

Zhang, Q., Gu, J., Li, L., Liu, J., Luo, B., Cheung, H. W., Boehm, J. S., Ni, M., Geisen, C., Root, D. E.*, et al.* (2009). Control of cyclin D1 and breast tumorigenesis by the EglN2 prolyl hydroxylase. Cancer Cell *16*, 413-424.

Zhang, X., Yan, X., Cheng, L., Dai, J., Wang, C., Han, P., and Chai, Y. (2013). Wound healing improvement with PHD-2 silenced fibroblasts in diabetic mice. PLoS One *8*, e84548.

Zhu, P., Tan, M. J., Huang, R. L., Tan, C. K., Chong, H. C., Pal, M., Lam, C. R., Boukamp, P., Pan, J. Y., Tan, S. H.*, et al.* (2011). Angiopoietin-like 4 protein elevates the prosurvival intracellular O2(-):H2O2 ratio and confers anoikis resistance to tumors. Cancer Cell *19*, 401-415.

CURRICULUM VITAE

PERSONAL DETAILS

Family name: Kuchnio

Given names: Anna Małgorzata

Place and date of birth: Iława, 13-04-1984

Nationality: Polish

Address: Paul van Ostaijenlaan 28D2

3001 Heverlee, Belgium

E-mail: anna.kuchnio@vib-kuleuven.be

EDUCATION

Currently: PhD student in Biomedical Sciences (University of Leuven), since June 2009

2009 Master of Science in Pharmacy (Medical University of Gdańsk (Poland) (graduated with Greatest Distinction & Congratulations from the Jury)

2008 Master in Pharmacy (Ernst-Moritz-Arndt University, Greifswald (Germany) (graduated with Greatest Distinction & Congratulations from the Jury)

HONORS AND AWARDS

2008 graduated at Ernst-Moritz-Arndt University in Greifswald with Greatest Distinction and Congratulations from the Jury

2009 graduated at Medical University of Gdansk Poland with Greatest Distinction and Congratulations from the Jury

2010 FWO 4-years PhD fellowship

2012 FWO travel grant

2014 Vlaamse Liga tegen Kanker 1 year PhD fellowship

PUBLICATIONS

1. *Tumor hypoxia causes DNA epimutations by reduction TET activity*
   Thienpont B, Zhao H, D'Anna F, Steinbacher J, Ghesquière B, **Kuchnio A,** Boeckx B, Schoonjans L, Hermans E, Amant F, Kristensen VN, Peng Koh K, Mazzone M, Carmeliet P, Carell T, Lambrechts D. *Manuscript submitted to Cancer Cell,* ***IF=23.893.***

2. *Genetic dissection of PHD2's function in breast cancer and stromal cells reveals a novel role of cancer cell PHD2 in metastasis via activation of cancer-associated fibroblasts*
   Kuchnio A, Moens S, Bruning U, Kuchnio K, Broux M, Ungureanu AA, Cruys B, Leite-de-Oliveira R, Bruyère F, Hernandez-Fernaud JR, Zanivan S, Bartic C, Foidart JM, Noel A, Vinckier S, Dewerchin M, Mazzone M, Carmeliet P. *In revision for Cell Reports.* ***IF=7.2.***

3. *Chloroquine mediates its anticancer effects in an autophagy-independent manner by acting on the tumor vasculature*
   Maes H, **Kuchnio A**, Carmeliet P, Agostinis P; *Molecular & Cellular Oncology, accepted for publication.*

4. *How to teach an old dog new tricks: autophagy-independent action of chloroquine on the tumor vasculature*
   Maes H, **Kuchnio A**, Carmeliet P, Agostinis P; *Autophagy, 2014 November.* ***IF=11.423, citations: 0.***

5. *Tumor vessel normalization by the autophagy blocker chloroquine: role of endothelial Notch signaling*
   Maes H*, **Kuchnio A***, Peric A, Moens S, Nys K, De Bock K, Quaegebeur A, Schoors S, Georgiadou M, Wouters J, Ghesquière B, Vinckier S, Vankelecom H, Garmyn M, Dewerchin M, Annaert W, Agostinis P and Carmeliet P (*: equal contribution); Cancer Cell 2014;26:190-206. ***IF=23.893, citations: 3.***

6. *Stromal cell metabolism in health and disease*
   Ghesquière B, Won BW, **Kuchnio A**, Carmeliet P; Nature 2014;511:167-76.
   IF=38.597, citations: 5.

7. *Hypoxia induces VEGF-C expression in metastatic tumor cells via HIF-1α-independent translation-mediated mechanism*
   Morfoisse F, **Kuchnio A** Frainay C, Gomez-Brouchet A, Delisle MB, Pujol F, Guillermet-Guibert J, Bousquet C, Carmeliet P, Pyronnet S, Prats AC & Garmy-Susini B; Cell reports 2014;6:155-67. ***IF=7.2, citations: 5.***

8. *Partial and transient reduction of glycolysis by PFKFB3 –blockade reduces pathological angiogenesis*
   Schoors S*, De Bock K*, Cantelmo AR*, Georgiadou M*, Ghesquière B, Cauwenberghs S, **Kuchnio A,** Wong BW, Quaegebeur A, Diaz-Moralli S, Tembuyser B, Cascante M, Chesney J, Dewerchin M & Carmeliet P; Cell metabolism, 2014;19:37-48. ***IF=14.619, citations: 18.***

9. *Absence of the Fragile X Mental Retardation Protein is protective for Breast Cancer Metastases*
   Luca R*, Averna M*, Vecchi M*, Zalfa F*, La Fata G, del Nonno F, Nardacci R, Bianchi F, Bianchi M, Nuciforo P, Munck S, Parrella P, Moura R, Signori E, Alston R, **Kuchnio A**, Farace MG, Fazio VM, Piacentini M, De Strooper B, Achsel T, Neri G, Neven P, Evans DG, Carmeliet P, Mazzone M and Bagni C (*: equal contribution); EMBO Molecular Medicine 2013;5:1523-36. ***IF=7.8, citations: 8.***

10. *Role of PFKFB3-driven glycolysis in vessel sprouting*
    De Bock K*, Georgiadou M*, Schoors S, **Kuchnio A**, Wong BW, Cantelmo AR, Quaegebeur A, Ghesquière B, Cauwenberghs S, Eelen G, Phng LK, Betz I, Tembuyser B, Brepoels K, Welti J, Geudens I, Segura I, Cruys B, Bifari F, Decimo I, Blanco R, Wyns S, Vangindertael J, Rocha S, Collins R, Munck S, Daelemans D, Imamura H, Devlieger R, Rider M, Van Veldhoven P, Schuit F, Bartrons R, Hofkens J, Fraisl P, Telang S, De Berardinis R, Schoonjans L, Vinckier S, Chesney J, Gerhardt H, Dewerchin M & Carmeliet P (*: equal contribution); Cell 2013;154:651-63. ***IF=32.401, citations: 36.***

11. *Emerging novel functions of the oxygen-sensing prolyl hydroxylase domain enzymes*
    Wong, BW, **Kuchnio A,** Brüning U, Carmeliet P; Trends in Biochemical Sciences 2013;38:3-11. ***IF=11.587, citations: 8.***

12. *Effect of prolyl hydroxylase domain-2 haplodeficiency on hepatocarcinogenesis and progenitor cell activation in mice*
    Heindryckx F, **Kuchnio A**, Casteleyn C, Coulon S, Olievier K, Colle I, Geerts A, Libbrecht L, Carmeliet P and Van Vlierberghe H; Journal of Hepatology 2012;57:61-8. ***IF=9.334, citations: 7.***

13. *A vascular niche and a VEGF-Nrp1 loop regulate the initiation and stemness of skin tumours*
    Beck B, Driessens G, Goossens S, Youssef KK, **Kuchnio A**, Caauwe A, Sotiropoulou PA, Loges S, Lapouge G, Candi A, Mascre G, Drogat B, Dekoninck S, Haigh JJ, Carmeliet P and Blanpain C; Nature 2011;478:399-403. ***IF=36.101, citations: 115.***

14. *Synthesis, Cytotoxicity Testing, and Structure-Activity Relationships of Novel 6-Chloro-7-(4-phenylimino-4H-3,1-benzoxazin-2-yl)-3-(substituted)-1,4,2-benzodithiazine 1,1-dioxides*
    Pomarnacka E, Kornicka A, **Kuchnio A**, Heinrichs M, Grünert R, Gdaniec M, Bednarski PJ. Archive der Pharmazie (Weinheim) 2011;344:431-41; ***IF=1.529, citations: 0.***

15. *Synthesis of Novel Aryl(heteroaryl)sulfonyl Ureas of Possible Biological Interest*
    Sączewski F, **Kuchnio A,** Samsel M, Łobocka M, Kiedrowska A, Lisewska K, Sączewski J, Gdaniec M, Bednarski PJ; Molecules 2010; 15(3):1113-1126; ***IF=1.988, citations: 7.***